The (Mis)Allocation Channel of Climate Change

Evidence from Global Firm-level Microdata [*]

Tianzi Liu [†]
Cornell University

Zebang Xu [‡]
Cornell University

August, 2024

Click here for the latest version

Abstract

An extensive literature has documented the negative effect of global warming on TFP, but we know little about the micro origins of this relationship. This paper examines a novel channel: the impact of temperature extremes on capital misallocation. Using global firm-level microdata from 32 countries, we provide causal evidence that a day with extreme heat (>30°C) increases the dispersion of marginal revenue products of capital (MRPK) by 0.31 log points, implying a 0.11% annual aggregate TFP loss for an average region-sector. Notably, this effect is more pronounced in hotter and more economically developed regions. Our estimates, taking future adaptation and development into account, suggest a global aggregate TFP loss of 35.4% from the misallocation channel at the end of the century under the SSP3-4.5 scenario. In light of these findings, we develop a firm dynamics model with varying sensitivity to temperature across firms to examine the mechanisms behind temperature-induced misallocation. The model reveals that greater temperature forecasting errors and increased productivity volatility from extreme climates both exacerbate the dispersion in MRPK. Our results uncover the critical role of the misallocation channel and the necessity of considering firm heterogeneity in climate policies. In addition to mitigation policies, we also highlight improving mid-range weather forecast accuracy as a key adaptation policy to improve investment efficiency.

[*]We are grateful to our advisors, Ryan Chahrour, Kristoffer Nimark, Ivan Rudik, Ezra Oberfield and Mathieu Taschereau-Dumouchel for their continued guidance and support. This paper has also benefited from discussions with Levon Barseghyan, Julieta Caunedo, Luming Chen, Pablo Ottonello, Jeffrey Shrader, and seminar participants at Columbia Climate School, Cornell Macro Lunch and Cornell SEERE Seminar, and the 2024 Econometric Society NASM. First draft was circulated on February 16th, 2024.

[†]Department of Applied Economics and Management, Cornell University (email:tl567@cornell.edu).

[‡]Department of Economics, Cornell University (email:zx88@cornell.edu).

1 Introduction

Rising temperatures due to climate change have been estimated to cause sizable aggregate economic losses. A natural question then is, what are the underlying drivers of these large economic losses from temperature? Research on this question has largely focused on how temperature worsens technology, often interpreted as damages on physical productivity. At the micro level, empirical work has shown that extreme temperature conditions can affect within-firm productivity, especially labor productivity (e.g. Zhang et al. 2018; Somanathan et al. 2021). At the macro level, a mix of structural and empirical work prioritizes aggregate productivity damage as the primary effect of climate change (e.g. Barrage and Nordhaus 2023; Cruz and Rossi-Hansberg 2023; Nath 2023). These work benchmark their results in models of efficient economies, with little to no role of micro-level distortions.

Our paper adopts a different approach, in the spirit of the seminal work by Hsieh and Klenow (2009). Instead of focusing on the physical productivity losses in production due to rising temperature, we study how climate change results in aggregate TFP losses by increasing capital misallocation across firms. The misallocation channel should come as no surprise. For instance, consider a regional economy consisting of firms with varying degrees of heat sensitivity: some are heat-loving, while others are heat-sensitive. Although all firms endure the same regional heat shocks, the impact might vary significantly. Heat-loving firms tend to be less affected and remain more productive compared to heat-sensitive firms. Given that capital is generally hard to adjust in the short term, a heat shock affecting all firms would lead to dispersion in capital returns across firms, with heat-loving firms having higher marginal revenue products of capital (MRPK) than heat-sensitive ones. This is a clear case of climate-induced misallocation: aggregate productivity and output could increase if more capital was reallocated from heat-averse firms to heat-loving ones that have higher marginal products. Therefore, the *across-firm* misallocation channel of climate change could result in depressed aggregate TFP. The misallocation channel has direct implications for adaptation policy: policies should aim not only to mitigate average damage but also to work towards reducing the disparity in adaptability to climate change across firms.

Our goals in this paper are threefold: first, to causally identify the misallocation channel using temperature shocks and assess its quantitative impact in future climate change scenarios; second, to understand the drivers of climate-induced misallocation from a firm dynamics perspective; and third, to uncover the novel implications for climate mitigation and adaptation policies suggested by the misallocation channel.

We begin by developing a climate-TFP accounting framework inspired by Hsieh and Klenow (2009). Our model features heterogeneous firms with climate-driven input distortions that can unevenly affect the marginal products of factors across firms. This framework allows us to decompose the region-sector level aggregate TFP into a set of firm-level sufficient statistics, which measures the efficient frontier (i.e., technology) and losses from capital misallocation. Specifically, the cost of capital misallocation can be measured with the variance of (log) MRPK across firms in a given year at the region-sector level. We can, therefore, exploit panel variations in across-firm MRPK dispersion from exogenous temperature shocks to causally identify the extent of misallocation stemming from temperature-related distortions.

To measure the dispersion in the marginal products within individual sectors in each subnational region each year, we use firm-level data from 30 European countries extracted from the BvD Orbis dataset, as well as data from China and India obtained from government-conducted surveys. We construct historical climate variables and temperature forecasts for each region with the ERA5-Land gridded daily temperature data from the European Centre for Medium-Range Weather Forecasts (ECMWF). Our sample covers regions with a wide range of economic and climatic conditions. Our estimation reveals a U-shaped pattern: both extreme heat and cold temperatures increase measured capital misallocation. Notably, an extra hot day with a temperature above 30°C (86°F) relative to a day in the 5-10°C (41-50°F) range within a year will increase MRPK dispersion by about 0.31 log points, which translates to a 0.11% annual aggregate TFP loss. Importantly, we also estimate the heterogeneous effects of temperature on misallocation across long-run regional climates and income levels. We find the effect of heat shocks on capital misallocation is worse in hotter and more economically developed regions, suggesting limited potential for market adaptation to mitigate the aggregate misallocation losses with the economic development and warming climates over the long run.

What do our estimates imply for the misallocation cost of future climate change? We project the impact of global warming on misallocation-induced TFP loss by the end of the century using our estimates of the heterogeneous temperature-misallocation effect. Coupled with the climate projections from the CMIP6 model and income projections from the OECD Env-Growth model under the SSP3-4.5 scenario, our estimates indicate that, compared to the current income and climate levels, the global cost of climate-induced misallocation will amount to 35.4% of aggregate TFP by the end of the century. Empirically, the projected loss can be decomposed into three channels: a 3.60% contribution from the shifted daily temperature distribution, 18.74% from the income effect of projected economic development, and 13.06% from the level effect of the long-run average temperature increase. The projected losses are large and growing over time as more regions are transitioning into richer and hotter economies, and with more extreme temperature realizations. Remarkably, the magnitude of these estimates is comparable to the projected impact reported by Burke, Hsiang, and Miguel (2015) and Bilal and Känzig (2024).

The second goal of our paper is to understand the drivers of the identified climate-induced misallocation. To explain why both the shock distributions and levels of temperature are relevant for the dispersion in capital returns, we develop a firm dynamics model featuring time-to-build capital and rich temperature-productivity interactions. Specifically, we allow firms' productivity to be heterogeneous in their persistent and idiosyncratic sensitivities to temperature. The *persistent* sensitivity reflects a firm's specific characteristics and whether a firm is heat-loving or heat-averse by nature of its production (or demand). The persistent sensitivity is assumed to be known by the firm and to affect its capital investment decisions. For example, when anticipating future heat, a heat-averse firm will invest less than an average firm due to its relatively lower expected productivity. The *idiosyncratic* sensitivity, on the other hand, is randomly assigned to each firm at each period. It reflects the increased likelihood of severe disruptions at the firm level, such as plant-level fire hazards, equipment failures, or operational shutdowns, associated with temperature extremes. As the idiosyncratic sensitivity is unknown to the firm ex-ante, it does not affect the firm's capital investment decisions (to the first order). However, it does generate unexpected productivity shocks and, consequently, affects the firm's MRPK upon realization, particularly in cases of temperature extremes.

The heterogeneity in persistent and idiosyncratic sensitivities across firms shapes two channels through which temperature affects misallocation. First, any shifts in the *level* of temperature (towards extreme heat or cold), operating through idiosyncratic sensitivities, would increase the probability of extreme events across all firms. Therefore, a region that deviates from the 'optimal level' of temperature, whether too hot or too cold, would experience higher temperature-induced damage volatility across firms and, consequently, greater capital misallocation. Secondly, any unexpected *shocks* in temperature will impact investment returns differentially among firms based on their persistent sensitivities. For example, an unexpected heat shock reduces the relative MRPK for heat-averse firms but raises it for heat-loving ones. From an ex-post perspective, heat-averse firms, anticipating higher productivity than realized, overinvested in capital. Therefore, greater forecast accuracy of future temperatures could lead to more efficient capital allocation across firms and raise aggregate TFP. Overall, these two channels closely explain our reduced-form results: the *level effect* of temperature, through damage volatility, explains why a region-sector's geographical location and long-run climates matter for capital misallocation; while the *shock effect* of temperature, stemming from temperature forecast errors, explains why larger weather shocks lead to increased misallocation.

We then empirically test the mechanisms of our model by exploiting variations at both the firm and the region-sector levels. We first examine the link between heterogeneous sensitivities and differential MRPK responses to temperature shocks using firm-level panel data. As the firm-specific sensitivities are hard to measure directly, we use firm size and AC installation as proxies. This approach allows us to test how firms' MRPKs respond heterogeneously to identical heat shocks within a region-sector. Our estimates reveal that heat shocks significantly lower the MRPK for smaller firms and firms without AC, but have minimal impact on the MRPK for larger firms and AC-installed firms, as they are less sensitive to temperature. Additionally, the role of firm size as a determinant of heterogeneous sensitivities helps rationalize the income effect identified in our reduced-form regression. We find that regions with higher levels of economic development exhibit a greater dispersion of firm sizes, which leads to greater differences in the adaptability to shocks among firms. This, in turn, results in a higher dispersion of persistent sensitivity across firms, and thus, an increased susceptibility to misallocation due to temperature shocks at the aggregate level.

Next, we estimate and evaluate the quantitative implications of the level and forecast error effects using model-implied regressions. We empirically test the level effect by estimating how temperature levels non-linearly affect TFP volatility and MRPK dispersion across firms at the region-sector level. Our findings confirm the model's predictions that temperature extremes increase damage volatility: TFP volatility exhibits a U-shaped relationship with temperature. We identify an optimal temperature of around 13°C, at which point TFP volatility reaches the lowest level, thereby imposing the least burden on allocative efficiency and aggregate TFP through the level effect of misallocation. We also provide direct evidence of the forecast error effect using forecast data from the monthly long-range temperature forecasts released by ECMWF (Copernicus Climate Change Service and Climate Data Store 2018). By aggregating these monthly long-run temperature forecast errors at the region-year level, the model-induced regression shows that conditional on the realized temperature, a 1°C error in temperature forecast for all months would lead to at least a 1.6 log point increase in MRPK dispersion. Such an increase in capital misallocation is equivalent to an approximate 0.58% annual aggregate TFP loss when compared to the perfect information counterfactual. Our findings suggest that temperature forecast errors are costly: unexpected temperature shocks lead to dispersion in investment mistakes among firms due to their varying sensitivity to heat. Therefore, in our context, the aggregate importance of temperature forecasts is highlighted through a new channel: accurate forecasting increases the allocative efficiency of capital.

Using the model parameters identified in the model-induced regression, we quantitatively examine the contributions of the level and forecast error effects of temperature to misallocation in our sample period. We find that, on average, the level effect of temperature accounts for 8.4 log points of MRPK dispersion, equivalent to a TFP loss of 3%. However, the forecast error effect contributes approximately 0.023 log points to MRPK dispersion, implying a TFP loss of 0.81%. The magnitude of the level effect exceeds that of the forecast error effect by more than three times. Broadly consistent with our reduced-form projections, these estimates suggest that the level effect of global warming might play a more significant role through the misallocation channel, as rising temperatures are likely to lead to increased damage volatility in firms' productivity and make efficient investment more difficult.

Lastly, we discuss how our findings shed new light on the design and effects of climate mitigation and adaptation policies. Specifically, we discuss three types of policies that could potentially reduce the cost of climate-induced misallocation. First, we consider the mitigation policy that reduces the end-of-century temperature rise from 4°C to 2°C. Our results project an avoidable TFP loss of 22% globally under RCP 2.6 compared to RCP 7.0. Compared to the benefits of avoided misallocation losses, the estimated cost of optimal mitigation policy from DICE-2016R is very moderate and largely outweighed by the benefits by 2100. Second, we evaluate the potential of mid-range weather forecast accuracy improvement as an adaptation policy. We predict future regional weather forecast accuracy by extrapolating from past technological progress and assuming that poorer regions will gradually invest more in climate information services as they become richer. The predicted forecast accuracy implies an average reduction of 0.7 in annual mean squared forecast errors by the end of the century, which could result in an aggregate TFP gain of 0.41% due to increased investment efficiency (i.e., a reduction in return dispersion). Therefore, our results suggest that continuously improving mid-range weather forecast accuracy is an essential and potentially cost-effective adaptation policy. Finally, from a micro perspective, our results broadly suggest that any policies that reduce the "climate inequality" of impact sensitivity among firms could reduce the misallocation loss from extreme climate events. Policies should be targeted to identify and subsidize firms that are productive but lack the resources to defend against heat. Our results also highlight that there need not be an equity-efficiency trade-off in the context of heterogeneous firms. If more firms become more "equal" in their sensitivity to temperature, the aggregate economy will also feature higher allocative efficiency.

We conclude that capital misallocation is a quantitatively important channel for how climate change affects the aggregate economy. Climate-induced misallocation stems from substantial cross-sectional firm-level heterogeneity in temperature sensitivity. The estimated loss due to misallocation across firms is considerable, indicating that the average effect of firm-level productivity loss alone is insufficient to capture the aggregate cost of climate change in the economy. Our results suggest that climate policies that solely target the average effect, while overlooking firm heterogeneity, may have limited efficacy.

Contributions to the Literature. This paper relates to a large literature on measuring the economic damages from temperature shocks and climate change. One canonical approach is to directly estimate the effect of temperature shocks on aggregate region-sector, country, or global level outcomes (See Dell, Jones, and Olken 2012; Burke, Hsiang, and Miguel 2015; Lemoine 2018; Carleton et al. 2022; Nath, Ramey, and Klenow 2023; Bilal and Känzig 2024, among many others). Another strand of work estimates the *average* firm- or worker-level productivity damages from climate change and explores the underlying micro-level mechanisms (Somanathan et al. 2021; Acharya, Bhardwaj, and Tomunen 2023; Ponticelli, Xu, and Zeume 2023). Most studies interpret their findings as physical productivity losses resulting from climate shocks. This paper contributes to this literature by taking a conceptually different approach: we focus on how climate change could drive down aggregate productivity by causing the *across-firm* misallocation of capital. We show that a sizable portion of aggregate climate impact is *allocative* rather than purely *physical*. Our approach estimates a large causal effect of the misallocation channel from climate shocks and projects a substantial TFP loss across all future climate change scenarios. Quantitatively, we uncover novel heterogeneity of the climate-induced misallocation losses across regions with different levels of development and climates.

Second, on the macroeconomic modeling of climate change, the existing studies have incorporated climate change into workhorse macro and trade models of efficient economies (Nath 2023; Cruz and Rossi-Hansberg 2023; Bakkensen and Barrage 2021; Casey, Fried, and Gibson 2022; Rudik et al. 2021). Naturally, these models remain silent on the causes and effects of how climate change would drive distortions and misallocation of productive factors in the economy. This paper provides a static general equilibrium framework to measure the costs of the temperature-induced misallocation channel using an easy-to-implement sufficient statistics approach. We also build a firm dynamics model to better understand the endogenous mechanisms behind climate-induced misallocation, which stem from *firm-level heterogeneity*, a previously overlooked but quantitatively significant dimension in the climate-macro literature. Very few studies have explored the allocative effect of climate change. Perhaps the closest to our paper is the contemporaneous work by Caggese et al. (2023). They project how the future geographical distribution of temperature shocks in Italy might lead to differential factor productivity of firms across micro-regions under future global warming, and thus allocative efficiency losses could be predicted. By contrast, our paper provides a direct causal estimate of climate on within-region *marginal product dispersion* across firms using historical regional climate variations and firm-level data in 32 countries globally. It is a direct measure of misallocation (as in (Hsieh and Klenow 2009) and (Sraer and Thesmar 2023)) and captures *all channels* of climate-induced misallocation, not just those stemming from the geographical distribution of temperature.

Third, our research contributes to the burgeoning literature on the impacts and economic value of weather forecasts. Recent work evaluates the market internalization of weather forecasts (Schlenker and Taylor 2021), agents updating beliefs in responses to forecasts (Shrader 2023; Kala 2017), and the economics values of reducing mortality with more accurate forecasts (Shrader, Bakkensen, and Lemoine 2023). We show evidence of how inaccuracies in forecasts result in more frequent investment mistakes in the cross-section of firms and thus reduce aggregate productivity. Our research supports micro-level findings at the macro level and emphasizes the vital role of accurate weather forecasting in reducing economic disruptions and boosting productivity.

Finally, we contribute to the literature on misallocation. Since the seminal contributions by Restuccia and Rogerson (2008) and Hsieh and Klenow (2009), a large body of work has been studying the aggregate (e.g. Gopinath et al. 2017, David and Zeke 2021) and firm-level (e.g. Asker, Collard-Wexler, and Loecker 2014, David and Venkateswaran 2019, Baqaee and Farhi 2019) drivers of misallocation. Our paper adds to this literature by demonstrating that environmental factors, such as temperature variations and climate change, are also sources of misallocation and might become increasingly important in the future as global warming worsens. Additionally, our paper connects to a small but growing body of literature that studies the causal identification of the drivers of misallocation using (quasi-)natural experiments (Sraer and Thesmar 2023, Bau and Matray 2023, among others). These studies employ exogenous shocks to explore the causes and consequences of misallocation. We expand on this literature by using exogenous temperature variations to examine the impacts of climate change as a driver of misallocation.

The structure of the paper is organized as follows. In Section 2, we develop our climate growth accounting framework. Our data sources and methodology for constructing variables are detailed in Section 3. Section 4 presents our empirical identification strategy and reduced-form results. Section 5 presents the firm dynamics model to explain the underlying mechanisms. Evidence at the firm level, which tests the proposed channels, is provided in Section 6. Section 7 offers evidence at the aggregate level. We discuss implications on mitigation and adaptation policies in Section 8. And we conclude with Section 9.

2 A Framework for Climate TFP Accounting

In this section, we develop a framework for TFP accounting in the presence of climate conditions to illustrate the effect of climate-induced misallocation on aggregate productivity. The economic structure follows the seminal work by Hsieh and Klenow (2009), a closed economy model featuring heterogeneous firms that face various input and output distortions. Additionally, we allow firm-specific productivities, demand shifters, and distortions to respond endogenously to climate conditions in a flexible manner. We show how climate conditions might affect aggregate productivity through two distinct channels in a distorted economy: micro-level productivity (technology) and the dispersion in distortions (misallocation). We also derive measurable sufficient statistics for the misallocation channel that will guide our empirical strategy in Section 4. Our framework will focus on the measurement of the misallocation channel in a general set-up, without taking a stand on the specific mechanisms. We will study and quantify the potential mechanisms in Section 5, 6, and 7.

2.1 Model Preliminaries

Consider an economy comprised of R regions indexed by r, and S sectors indexed by s. We use $n = (r, s)$ to denote a region-sector pair and there are $N = R \cdot S$ region-sector pairs. We focus on the aggregation of firm-level economic activities within a region-sector pair. We allow all fundamentals of firm i in market $n = (r, s)$ to be arbitrary functions of a general array of (current and past) regional climate conditions, $\tilde{\mathbf{T}}_{rt}$, the aggregate state of the economy, $\tilde{\mathbf{X}}_{nt}$, and the idiosyncratic state of firm i, $\tilde{\mathbf{Z}}_{nit}$.

For concreteness, one can think of current climate conditions, $\mathbf{T}_{rt}$, as realizations of daily temperature, precipitation, and other types of extreme weather events. $\mathbf{X}_{nt}$ and $\mathbf{Z}_{nit}$ can be interpreted as other aggregate and firm-specific productivity or demand shocks that are unrelated to temperature. We use the tilde notation, $(\tilde{\mathbf{T}}_{rt}, \tilde{\mathbf{X}}_{nt}, \tilde{\mathbf{Z}}_{nit})$, to denote the history of realizations up to date t.

2.2 Aggregation Model with Micro Effects of Climate Conditions

We now describe the aggregation model and how we incorporate the micro effects of climate conditions into the model.

Industry Production. Industry output Y_{nt} for region-sector n is given by a constant elasticity of substitution (CES) production function of differentiated products of measure J_n[1]:

$$Y_{nt} = \left(\int_0^{J_n} B_{nit}^{\frac{1}{\sigma_n}} Y_{nit}^{\frac{\sigma_n - 1}{\sigma_n}} \, di \right)^{\frac{\sigma_n}{\sigma_n - 1}}, \tag{1}$$

where B_{nit} is a good-specific preference shifter, Y_{nit} denotes the output of firm i and $\sigma_n > 1$ is the elasticity of substitution between products within region-sector n. Profit maximization of industrial output producers leads to the inverse demand function for the output of each firm, Y_{nit}:

$$Y_{nit} = B_{nit} Y_{nt} \left[\frac{P_{nit}}{P_{nt}} \right]^{-\sigma_n}, \tag{2}$$

where $P_{nt} = \left(\int_0^{J_n} B_{nit} P_{nit}^{1-\sigma_n} di \right)^{\frac{1}{1-\sigma_n}}$ is the price index of the region-sector. The demand shifter $B_{nit} := B_{ni}(\tilde{\mathbf{T}}_{rt}, \tilde{\mathbf{X}}_{nt}, \tilde{\mathbf{Z}}_{nit})$ is a firm-specific function of climate and economic conditions to capture the possibility that some goods and services might be less preferable in hotter climates,

1. In theory, we could allow J_n to be time-varying as well to account for the effect of potential entry-exit. However, accurately measuring these dynamics within a granular region-sector pair is challenging given the data limitations. Therefore, the model does not address this aspect.

even in the same region and sector. [2]

Firm-level Production. Each product is produced by a unique firm. The production function for each firm is given by a Cobb-Douglas function of capital and labor:

$$Y_{nit} = A_{nit} K_{nit}^{\alpha_{Kn}} L_{nit}^{\alpha_{Ln}}, \tag{3}$$

where A_{nit} is physical productivity,[3] K_{nit} is capital stock and L_{nit} is labor input employed by firm i. The production function exhibits constant returns to scale, with $\alpha_{Kn} + \alpha_{Ln} = 1$. The physical productivity of firm i is modeled as a firm-specific function, $A_{nit} := A_{ni}(\tilde{\mathbf{T}}_{rt}, \tilde{\mathbf{X}}_{nt}, \tilde{\mathbf{Z}}_{nit})$, to capture the different sensitivity to heat (or cold) among different types of firms within and across various region-sectors. The heterogeneity of productivity damage across firms has been well documented in the literature, and can be potentially attributed to the distinct nature of production processes across firms and varying levels of adaptability to climate conditions.[4] Such heterogeneity is present even within the same region-sector. For example, in agriculture, rainfed farms often suffer more than irrigated farms when facing heat (Piao et al. 2010). In manufacturing, the productivity of a firm with AC installation is less susceptible to heat shocks than those without ACs (Somanathan et al. 2021).

Distortions. Each firm faces a variety of distortions, represented as an output wedge on revenue τ^Y and a set of wedges on all inputs τ^F. Subject to the inverse demand and wedges, each firm i engages in monopolistic competition and optimally chooses its quantity of inputs and price to maximize profits:

$$\max_{P_{nit}, K_{nit}, L_{nit}} \left(1 - \tau_{nit}^Y\right) P_{nit} \underbrace{A_{nit} K_{nit}^{\alpha_{Kn}} L_{nit}^{\alpha_{Ln}}}_{Y_{nit}} - \left(1 + \tau_{nit}^K\right) R_{nt} K_{nit} - \left(1 + \tau_{nit}^L\right) W_{nt} L_{nit} \tag{4}$$

$$\text{subject to} : Y_{nit} = B_{nit} Y_{nt} \left[\frac{P_{nit}}{P_{nt}}\right]^{-\sigma_n}, \tag{5}$$

where R_{nt} is the user cost of capital, W_{nt} denotes the wage and P_{nt}^M denotes the price for the intermediate input bundles. τ_{nit}^Y is the firm-specific wedge that distorts output, and τ_{nit}^F denotes the input-specific wedge on factor $F \in \{K, L\}$. For example, τ_{nit}^K denotes capital distortion that raises the marginal cost of capital relative to the market rental rate R_{nt}. We assume all firms take these wedges as exogenous for now and turn to model the endogenous nature of these frictions and their relationship with climate change in Section 5.

These wedges are reduced-form representations of all the frictions in the economy that

2. This is more evident in service industries where climate variations directly affect consumer behavior more saliently. For instance, Zivin and Neidell (2014) found that Americans are more likely to shift to indoor recreational activities from outdoor ones (such as recreational fishing (Dundas and Haefen 2020)) when exposed to heat shocks.

3. It is a measure of quantity-based total factor productivity (TFPQ), reflecting the overall efficiency with which the firm uses its inputs to produce units of physical output (Bils, Klenow, and Ruane 2021).TFPQ cannot be directly measured in the absence of price or quantity data, barring any additional structural assumptions. In a Cobb-Douglas production function, the notion of physical productivity (TFPQ) nests the effect of factor-specific productivity.

4. For the cross-country heterogeneity in productivity damage due to adaptation, see Nath (2023).

prevent the optimal allocation of inputs in our static ex-post accounting exercise,[5] including climate-related frictions. Thus, similar to demand shifters and productivity, we assume them to be firm-specific functions of climate as well as the states of the region-sector and the firm itself.

Specifically, the output wedge $\tau^Y_{nit} := \tau^Y_{ni}(\tilde{\mathbf{T}}_{rt}, \tilde{\mathbf{X}}_{nt}, \tilde{\mathbf{Z}}_{nit})$ captures the distortions (or exogenous markups) the firm faces on prices or quantities relative to the Dixit-Stigliz benchmark.[6] These distortions can arise from policy interventions or market imperfections. For example, some firms might have relatively higher markups as temperature shocks increase the local industry concentration Ponticelli, Xu, and Zeume (2023), which is not captured by the Dixit-Stigliz markup. Similarly, input wedges denoted as $\tau^F_{nit} = \tau^F_{ni}(\tilde{\mathbf{T}}_{rt}, \tilde{\mathbf{X}}_{nt}, \tilde{\mathbf{Z}}_{nit})$, disincentivize firms from using input $F \in \{K, L\}$ as if they were effectively paying a higher factor price.[7] Any channels through which climate conditions prevent the optimal allocation of inputs would be captured by the function τ^F_{ni}, such as weather-induced capital depreciation (Hsiang and Jina 2015; Bilal and Rossi-Hansberg 2023). Importantly, in the context of dynamic input choices such as capital, the wedge function $\tau^K_{ni}(\tilde{\mathbf{T}}_{rt}, \cdot)$ would capture the different degrees of investment mistakes induced by unexpected temperature shocks (e.g. when a heat-averse firm invested too much capital before a heat shock hits).

Factor Supply. The total productive factors in the region-sector n follows that $K_{nt} = \sum_{i=1}^{J_n} K_{nit}$, $L_{nt} = \sum_{i=1}^{J_n} L_{nit}$. The total factor supply is treated as exogenously given every period.[8]

Equilibrium. The equilibrium allocations in a region-sector depend on the set of fundamentals $(B_{nit}, A_{nit}, \tau^Y_{nit}, \tau^F_{nit})$, $\forall i$ and $\forall F \in \{K, L\}$. Given preference shifter B_{nit}, physical productivity A_{nit}, output distortions $\tau^Y_{nit} < 1$, factor distortions $\tau^F_{nit} > -1$ for all firms i, and total factor supply of K_{nt} and L_{nt}, a general equilibrium consisting of goods prices P_{nit}, factor prices, and equilibrium factor allocation F_{nit} is defined where all markets clear. We call the equilibrium defined by $(B_{nit}, A_{nit}, \tau^Y_{nit}, \tau^F_{nit})$ the *distorted equilibrium* and the equilibrium defined by $(B_{nit}, A_{nit}, 0, 0)$ the *efficient equilibrium*[9] to denote the first best outcome in this economy without distortions.

Distortions and Misallocation. We now examine how climate-related input frictions could shape the differences in marginal products in the cross-section of firms. For any input $F \in \{K, L\}$, the firm's optimality condition with respect to F_{it} will yield that the marginal revenue product of factor F (MRPF) equals to the factor price P^F_{nt} times the weather-affected wedges

5. "Ex-post" is in a sense that we use the set of wedges to rationalize the firm's behavior in the static accounting framework after the input and production has taken place.

6. τ^Y_{nit} also represent price distortions that reflect potential heterogeneity in revenue taxes, markups, or prices across firms not captured by the constant Dixit-Stiglitz markup.

7. For a firm to be (boundedly) productive, it is necessary that all prices are positive, which requires $1 - \tau^Y_{nit} > 0$ and $1 + \tau^F_{nit} > 0$.

8. We could also model the total factor supply to be region-sector specific functions of the form: $L_{nt} := L_n(\tilde{\mathbf{T}}_{rt}, \cdot), K_{nt} := K_n(\tilde{\mathbf{T}}_{rt}, \cdot)$, but this plays little role in our analysis.

9. In the accounting framework, efficiency is defined in a static and unconstrained sense (similar to Carrillo et al. 2023).

$\frac{1+\tau^F_{ni}(\tilde{\mathbf{T}}_{rt},\cdot)}{1-\tau^Y_{ni}(\tilde{\mathbf{T}}_{rt},\cdot)}$:

$$MRPF_{nit} = \alpha_{F_n}\frac{\sigma_n - 1}{\sigma_n}\frac{P_{nit}Y_{nit}}{F_{nit}} = \frac{1+\tau^F_{ni}(\tilde{\mathbf{T}}_{rt},\cdot)}{1-\tau^Y_{ni}(\tilde{\mathbf{T}}_{rt},\cdot)}P^F_{nt}. \tag{6}$$

Equation 6 states that any shift in climate conditions would affect the input (and output) wedges and thus MRPF. Moreover, any heterogeneity in the way wedges respond to temperature would result in unequal marginal revenue return to factors among firms in the cross-section. Such dispersion of marginal revenue return to factors is often referred to as "misallocation", indicating there are potential gains from reallocating the factor from firms with a low marginal product to the ones with a high marginal product. We can explicitly link these distortions to equilibrium (mis-)allocation of factors as follows.

Proposition 1 ***Equilibrium (Mis)Allocation.*** *The distorted equilibrium allocation of capital, labor, and material inputs must satisfy that for any factor $F \in \{K, L\}$,*

$$\begin{aligned}\log(\frac{F_{nit}}{F^*_{nit}}) =& -\log(1+\tau^F_{nit}(\tilde{\boldsymbol{T}}_{rt},\cdot))\\ &+\sigma_n\log(1-\tau^Y_{nit}(\tilde{\boldsymbol{T}}_{rt},\cdot)) - (\sigma_n - 1)\sum_{F'=\{K,L\}}\alpha_{F'_n}\log(1+\tau^{F'}_{ni}(\tilde{\boldsymbol{T}}_{rt},\cdot))\\ &+\log(C_{Fnt}(\tilde{\boldsymbol{T}}_{rt},\cdot)),\end{aligned} \tag{7}$$

where C_{Fnt} is a region-sector-year specific constant and F^*_{nit} is the efficient equilibrium allocation of factors that are entirely determined by preference shifter and physical productivity within the region-sector:

$$F^*_{nit} = \frac{B_{ni}(\tilde{\boldsymbol{T}}_{rt},\cdot)A_{ni}(\tilde{\boldsymbol{T}}_{rt},\cdot)^{\sigma_n-1}}{\int_0^{J_n} B_{nj}(\tilde{\boldsymbol{T}}_{rt},\cdot)A_{nj}(\tilde{\boldsymbol{T}}_{rt},\cdot)^{\sigma_n-1}dj}F_{nt} \tag{8}$$

Proof. See Appendix A.2. ■

The relative gap $\log(F_{nit}) - \log(F^*_{nit})$ decreases with factor-specific wedges $\log(1+\tau^F_{ni}(\tilde{\mathbf{T}}_{rt},\cdot))$ due to increased effective cost of the factor. The second line of 7 captures how other wedges affect the input usage F_{nit} in the distorted equilibrium by reducing the size of the firm. A firm with a higher output wedge and overall lower input wedges has greater price incentives and faces lower unit costs in production. Thus, more input F_{nit} will be used in production. The aggregate constant $C_{Fnt}(\tilde{\mathbf{T}}_{rt},\cdot)$ captures how distorted factor F is in the aggregate economy. Holding the firm-level distortion τ^F_{ni} constant, if the aggregate distortion is larger, then firm i would hire more of factor F since it is less distorted compared to the aggregate.

Equation 8 reveals that in an efficient economy free of distortions, climate only affects preferences and physical productivity, leading to a resource allocation favoring firms whose products are preferred by customers and those with higher physical productivity. On the other hand, in a distorted equilibrium with temperature-sensitive wedges, less factors are allocated to firms with higher input distortions (i.e. higher factor prices), even if they are more productive. This results in a state of misallocation of F_{nit} compared to its efficient counterpart, F^*_{nit}.

In the context of temperature effects, if firm A's capital wedge increases with the current temperature (a variable in $\tilde{\mathbf{T}}_{rt}$), while firm B's decreases, a temperature shock would raise the effective price of capital for firm A. As a result, firm A would allocate less capital than is efficient for its production compared to firm B, thereby creating a misallocation of resources. We will remain agnostic on the endogenous mechanism for now and leave the detailed discussion and identification of mechanisms driving these climate-induced distortions in Section 5, 6, and 7.

A Remark on Climate Conditions and Firm-level Fundamentals. Recall that we have assumed that all firm-level fundamentals $\{B_{nit}, A_{nit}, \tau^Y_{nit}, \tau^F_{nit}\}$ to be firm-specific and smooth functions based on the realized histories of three key factors, including climate conditions ($\tilde{\mathbf{T}}_{rt}$), aggregate economic conditions ($\tilde{\mathbf{X}}_{nt}$), and firm-level states ($\tilde{\mathbf{Z}}_{nit}$):

$$A_{nit} = A_{ni}(\tilde{\mathbf{T}}_{rt}, \tilde{\mathbf{X}}_{nt}, \tilde{\mathbf{Z}}_{nit}), \quad B_{nit} = B_{ni}(\tilde{\mathbf{T}}_{rt}, \tilde{\mathbf{X}}_{nt}, \tilde{\mathbf{Z}}_{nit}),$$

$$\tau^Y_{nit} = \tau^Y_{ni}(\tilde{\mathbf{T}}_{rt}, \tilde{\mathbf{X}}_{nt}, \tilde{\mathbf{Z}}_{nit}), \quad \tau^F_{nit} = \tau^F_{ni}(\tilde{\mathbf{T}}_{rt}, \tilde{\mathbf{X}}_{nt}, \tilde{\mathbf{Z}}_{nit}), \quad \forall F \in \{K, L\}.$$

Allowing these relationships to be firm-specific is essential as it implies that the same regional climate conditions $\tilde{\mathbf{T}}_{rt}$ could have heterogeneous effect on physical productivity A_{nit}, demand B_{nit}, and input distortions τ^Y_{nit} and τ^F_{nit}, across different firms. This heterogeneous impact leaves room for differential response of marginal products to climate variations, which will be the key mechanisms to be inspected in this paper.

2.3 Aggregation, TFP Decomposition and Misallocation

We proceed to perform aggregation in this accounting framework. We adopt a widely-used assumption in the misallocation literature (see Hsieh and Klenow (2009) and Sraer and Thesmar (2023)) that productivity and all associated wedges follow a joint log-normal distribution across firms in any region-sector-year pair, which holds very well in the data. More formally, we assume that for any given set of arguments $\left(\tilde{\mathbf{T}}_{rt}, \tilde{\mathbf{X}}_{nt}, \left\{\tilde{\mathbf{Z}}_{nit}\right\}_i\right)$, the joint distribution of the realized values of the sets of functions, $\mathbf{S}_{nit} = (B_{nit}, A_{nit}, 1+\tau^Y_{nit}, 1+\tau^K_{nit}, 1+\tau^L_{nit})$, can be characterized as follows:

$$\log(\mathbf{S}_{nit}(\tilde{\mathbf{T}}_{rt}, \tilde{\mathbf{X}}_{nt}, \tilde{\mathbf{Z}}_{nit})) \sim \mathcal{N}\left(\mu^{(\mathbf{n})}_{\mathbf{s}}(\tilde{\mathbf{T}}_{\mathbf{rt}}, \tilde{\mathbf{X}}_{\mathbf{nt}}), \mathbf{\Sigma}^{(\mathbf{n})}_{\mathbf{ss}}(\tilde{\mathbf{T}}_{\mathbf{rt}}, \tilde{\mathbf{X}}_{\mathbf{nt}})\right). \tag{9}$$

Here, $\boldsymbol{\mu}^{(n)}_s$ represents the mean vector of firm-level fundamentals, while $\Sigma^{(n)}_{ss}$ is the covariance matrix of these fundamentals across firms. Each element of these are smooth functions of their respective arguments.[10] For tractability, we adopt the aggregation notation of Krusell and Smith (1998) that the distribution of firm-level fundamentals $\tilde{\mathbf{Z}}_{nit}$ (over i) can be summarized by a finite set of moments and stacked into the aggregate states of the economy $\tilde{\mathbf{X}}_{nt}$. The log-normality assumption allows us to transparently show how micro-level wedges are translated into losses in aggregate productivity:

Proposition 2 ***Aggregation and TFP Decomposition.*** *Under the log-normality assumption, each*

10. This smoothness follows the principle that population moments are smooth functions of the variables $\mathbf{S}_{nit}$.

region-sector n admits an aggregate production function of the form

$$Y_{nt} = TFP_{nt} K_{nt}^{\alpha_{Kn}} L_{nt}^{\alpha_{Ln}}, \tag{10}$$

where the region-sectoral aggregate Total Factor Productivity $TFP_{nt} := TFP_n\left(\tilde{\mathbf{T}}_{rt}, \tilde{\mathbf{X}}_{nt}\right)$ can be decomposed as follows:

$$\begin{aligned}
\log TFP_n(\tilde{\mathbf{T}}_{rt}, \cdot) = & \underbrace{\frac{1}{\sigma_n - 1} \log \left[J_n \mathbb{E}_i \left[B_{ni}(\tilde{\mathbf{T}}_{rt}, \cdot) \left(A_{ni}(\tilde{\mathbf{T}}_{rt}, \cdot) \right)^{\sigma_n - 1} \right] \right]}_{\textit{Technology}(\log TFP_n^E)} - \underbrace{\frac{\sigma_n}{2} \operatorname{var}_{\log\left(1-\tau_{ni}^Y\right)}(\tilde{\mathbf{T}}_{rt}, \cdot)}_{\textit{Output Wedge Dispersion}} \\
& \underbrace{- \sum_{F \in \{K,L\}} \frac{\alpha_{Fn} + \alpha_{Fn}^2(\sigma_n - 1)}{2} \operatorname{var}_{\log\left(1+\tau_{ni}^F\right)}(\tilde{\mathbf{T}}_{rt}, \cdot)}_{\textit{Factor Wedge Dispersion}} \\
& \underbrace{+ \sigma_n \sum_{F \in \{K,L\}} \alpha_{Fn} \operatorname{cov}_{\log\left(1-\tau_{ni}^Y\right), \log\left(1+\tau_{ni}^F\right)} \left(\tilde{\mathbf{T}}_{rt}, \cdot \right)}_{\textit{Output-Factor Mixed Distortion}} \\
& \underbrace{- (\sigma_n - 1) \alpha_{Kn} \alpha_{Ln} \operatorname{cov}_{\log\left(1+\tau_{ni}^K\right), \log\left(1+\tau_{ni}^L\right)} \left(\tilde{\mathbf{T}}_{rt}, \cdot \right)}_{\textit{Factor Mixed Distortion}}.
\end{aligned} \tag{11}$$

Proof. See Appendix A.3. ■

All the variance and covariance terms are elements in the variance matrix $\Sigma_{ss}^{(n)}(\tilde{\mathbf{T}}_{rt}, \tilde{\mathbf{X}}_{nt})$ in Equation 9. Each of them is a region-sector-specific function of weather conditions and other economic fundamentals. They describe how these conditions would alter the distribution of wedges over the cross-section of firms.

The efficient TFP level is given by $\log \text{TFP}_n^E = \frac{1}{\sigma_n - 1} \log \left[J_n \mathbb{E}_i \left[B_{ni}(\tilde{\mathbf{T}}_{rt}, \cdot) \left(A_{ni}(\tilde{\mathbf{T}}_{rt}, \cdot) \right)^{\sigma_n - 1} \right] \right]$ in the absence of distortions, which is determined by the variety, preference shifter and love-for-variety-adjusted physical productivity of the firm. This represents the production possibility frontier of the economy. We call this **technology** in the spirit of Basu and Fernald (2002) and Baqaee and Farhi (2019). The rest of the terms represent the costs of distortions in the economy, referred to as **misallocation loss**. Dispersion in output wedges $\operatorname{var}_{\log\left(1-\tau_{ni}^Y\right)}$ and factor input wedges $\operatorname{var}_{\log\left(1+\tau_{ni}^F\right)}$ will both lead to dispersion in the marginal revenue product of factors, creating more misallocation of factors and lowering sectoral TFP.

The impact of factor wedge dispersion on TFP is determined by two key parameters: σ_n and α_{F_n}. A greater σ_n implies higher product substitutability and, consequently, larger gains from reallocation. α_{F_n} indicates the factor's importance in production. For a factor F, a higher α_{F_n} renders the dispersion of factor wedges more costly. Furthermore, the interactions of wedges also impact productivity. All else being equal, greater productivity losses occur when firms with lower markups are also likely to endure higher input distortions ($\operatorname{cov}_{\log\left(1-\tau_{ni}^Y\right), \log\left(1+\tau_{ni}^F\right)} < 0$). Similarly, misallocation costs tend to be higher in cases where firms experiencing capital distortions are also more likely to face higher labor distortions ($\operatorname{cov}_{\log\left(1+\tau_{ni}^F\right), \log\left(1+\tau_{ni}^{F'}\right)} > 0$). These interactions are often referred to as "mixed" distortions.

2.4 Decomposing the Impact of Climate Change on TFP

Our decomposition framework shows that aggregate TFP depends on moments concerning technology and misallocation, which are endogenous to climate conditions. Since we have assumed that all moments are smooth functions of climate conditions $\tilde{\boldsymbol{T}}_{rt}$, we can decompose the first-order impact of climate change on TFP via a set of causal elasticities for each relevant moment. We formalize this in a case when only capital wedges are present.

Benchmark case: only capital wedges are present. An economy with only capital wedges is also considered in Asker, Collard-Wexler, and Loecker (2014), David and Venkateswaran (2019), and Sraer and Thesmar (2023), and with a view that capital is more of a dynamic input than labor or material. The dispersion of capital distortions is also measured to be larger than that of labor (Gorodnichenko et al. 2018) as they cannot be adjusted easily in the short run. Therefore, how capital misallocation is affected by climate conditions will be the main focus of empirical analysis throughout the paper.

When the capital wedge is the only source of distortions in the economy within region-sector n, the MRPK of each firm i satisfies that:

$$\text{MRPK}_{nit} = \alpha_{Kn} \frac{\sigma_n - 1}{\sigma_n} \frac{P_{it} Y_{it}}{K_{it}} \propto (1 + \tau^K_{nit}) R_{nt}.$$

The dispersion of capital is therefore given by the variance of log(MRPK) across firms

$$\text{var}(\log(1 + \tau_{nit})) = \text{var}(mrpk_{nit}) = \text{var}\left(\log\left(\frac{P_{it} Y_{it}}{K_{it}}\right)\right), \tag{12}$$

where we define $mrpk = \log(\text{MRPK})$. Equation 12 shows that the cross-sectional variance of (log) capital distortions across firms is identical to the dispersion of (log) MRPK, which can be computed via the variance of log sales over capital stock given the Cobb-Douglas technologies. Now, the effect of climate conditions on aggregate TFP can be written as:

$$\begin{aligned} \frac{\partial \log TFP_n(\tilde{\mathbf{T}}_{rt}, \cdot)}{\partial \tilde{\mathbf{T}}_{rt}} &= \frac{\partial \text{Technology}_{nt}}{\partial \tilde{\mathbf{T}}_{rt}} - \frac{\partial \text{ Misallocation Loss}_{nt}}{\partial \tilde{\mathbf{T}}_{rt}} \\ &= \frac{1}{\sigma_n - 1} \frac{\partial \log \mathbb{E}_i \left[B_{ni}(\tilde{\mathbf{T}}_{rt}, \cdot) \left(A_{ni}(\tilde{\mathbf{T}}_{rt}, \cdot) \right)^{\sigma_n - 1} \right]}{\partial \tilde{\mathbf{T}}_{rt}} \\ &\quad - \underbrace{\frac{\alpha_{Kn} + \alpha^2_{Kn}(\sigma_n - 1)}{2} \frac{\partial \, \text{var}_{mrpk,n}(\tilde{\mathbf{T}}_{rt}, \cdot)}{\partial \tilde{\mathbf{T}}_{rt}}}_{\text{The Misallocation Channel}}, \end{aligned} \tag{13}$$

such that the (first-order) cost of climate-induced misallocation would be reduced to the estimation of elasticity $\frac{\partial \, \text{var}_{mrpk_n}(\tilde{\mathbf{T}}_{rt}, \cdot)}{\partial \tilde{\mathbf{T}}_{rt}}$, i.e. "the misallocation channel". The decomposition shows that the first-order effect of climate conditions on aggregate TFP can be captured entirely through the effect on technology and the effect on inefficiency losses through capital misallocation. This proposition also provides practical guidance on the reduced-form identification in Section 4.4, which will be dedicated to causally estimate $\frac{\partial \, \text{var}_{mrpk_n}(\tilde{\mathbf{T}}_{rt}, \cdot)}{\partial \tilde{\mathbf{T}}_{rt}}$.

In theory, the derivatives of our structural objects with respect to climate conditions are globally well-defined and could vary with various histories of climate and economic conditions. However, in practice, it is preferable to think of them as ”reduced form,” which means that they can only be well estimated with respect to observed equilibrium allocations and are not necessarily invariant to the evolving climate conditions in the long run. For example, these marginal (first-order) effects could increase with worsening global warming or decrease with gradual adaptation. We will address this explicitly in Section 4.3 to capture the heterogeneous effect related to long-run climate conditions and economic development.

3 Data

3.1 Global Firm-level Microdata

We compile a global sample of firm-level microdata from both developed and developing economies that include 30 European countries, China and India, which covers 38.6% of world GDP. The firm-level panels for the 30 European countries are from Bureau van Dijk's (BvD) Orbis database, and the data for China and India are obtained from government-conducted surveys, China National Bureau of Statistics (NBS), and India ASI. The datasets contain financial accounting information such as revenue, fixed assets, wage bills, and employment. The three datasets have been widely employed in the literature and could be regarded as nationally representative.

Table B.1 provides a comprehensive list of countries, year coverage, and data sources for the three datasets. For all datasets, we harmonize the sectoral classifications of all firms into eight major divisions according to the U.S. Standard Industrial Classification (USSIC) code.[11] Regions are defined to be the NUTS 3 regions in Europe, prefectures in China, and districts in India. The size of these regions is close to the size of a county in the US.

Our key economic variables of interest are the sufficient statistics of firm-level activities that map directly into aggregate TFP at the region-sector-year level, in particular, the variance of marginal revenue product of capital across firms. Thus, for all datasets we use, we restrict ourselves to work with firm-year observations that report data on both revenue and capital stock. We measure revenue $P_{it}Y_{it}$ with the reported operating revenue in both Orbis and China NBS data, and the reported total sales in India ASI. We use the book value of gross fixed assets as a measure of firm-level capital stock K_{it}.[12] For each country, we trim the observations of extreme values of MRPK and TFPR at 0.1%.

For all reduced-form analysis using region-sector-year level sufficient statistics, we restrict our sample to the region-sector-year pairs with more than 30 firm-year observations of revenue and capital stock data, to minimize the noises in the variance measures and preserve log-normality in the data. To make sure variations in these sufficient statistics are not due to changes in data collection patterns and measurement errors, we also drop the observa-

11. The industries included are agriculture, mining, construction, manufacturing, transportation & utilities, wholesale trade, retail trade, finance, insurance, and real estate(FIRE) and Services. We choose the SIC classification mainly due to its availability in the Orbis Data.

12. Only exception is India ASI, which reports the book value of net fixed assets in a much more consistent manner while the gross values are reported with a major amount of missing values.

tions after which there are sudden jumps in the number of firms and aggregate sales in the region-sector. The final region-sector sample is an unbalanced sample consisting 124,567 of region-sector-year observations, covering 76,826,956 firm-year observations. For the firm-level analysis in Section 6, we include all firm-year observations in the raw data after trimming the 0.1% extreme values of all firm-level dependent variables and covariates. Below, we provide a brief overview of each of the datasets.

BvD Orbis. The firm-level data for the 30 European countries are drawn from Orbis, a database maintained by Bureau van Dijk (BvD). Orbis originates from administrative records collected at the firm level, primarily by each country's local Chambers of Commerce. A significant advantage of focusing on European countries with Orbis is that company reporting is regulatory, even for small private firms. It covers firms from all sectors and approximately 99 percent of the companies included are private entities.

To organize and clean the Orbis dataset, we follow the approach in Kalemli- Özcan et al. (2024), Gopinath et al. (2017), and Nath (2023). A notable departure from the papers cited earlier lies in our method for expanding MRPK's coverage. We include firms that have complete data on revenue and capital (fixed assets) while allowing for variability in the extent of coverage for other variables such as material costs, wage bills, and employee numbers.[13] Each firm in the Orbis data has its associated USSIC sector code, and its various address information can be matched with a NUTS3 region in Europe. Different countries in Orbis have different years of data coverage, detailed in Table B.1. We use the sample period of 1998-2018.

China NBS. The annual firm-level data for China is derived from surveys conducted by the National Bureau of Statistics (NBS) in China. These surveys encompass all industrial firms with annual sales exceeding nominal CNY 5 million (approximately USD 0.61 million) from 1998 to 2007. Such firms are commonly referred to as "above-scale" industrial firms.[14] The NBS data includes sectors such as mining, manufacturing, and utilities, with manufacturing constituting more than 90% of the total observations in the dataset. In processing the NBS data, we follow the methodology outlined in Zhang et al. (2018). Each firm in the dataset is categorized using a four-digit Chinese Industry Classification (CIC) code and is harmonized to the USSIC division level. Each firm's reported location can be mapped into a prefecture-level division. We only use the sample period of 1998-2007 due to inconsistent reporting after 2008 as discussed in Brandt, Van Biesebroeck, and Zhang (2014) and Nath (2023).

India ASI. Our data for India are drawn from India's Annual Survey of Industries (ASI). ASI is a census of large plants employing more than 100 workers and a random sample of about one-fifth of smaller plants that are registered under the Indian Factories Act.[15] The

13. Nath (2023) keeps the firms with complete revenue and labor data, while Gopinath et al. (2017) use a more restrictive sample that only preserves observations having all production-related information in south European countries.

14. Brandt, Van Biesebroeck, and Zhang (2014) shows that when comparing to the 2004 NBS census of industrial firms that covers all industrial plants in China, these above-scale firms in the sample account for over 90.7% of the total output.

15. As noted by Allcott, Collard-Wexler, and O'Connell (2016), large plants in the census scheme are defined as

sampling procedure assures representativeness at the state and industry levels. Almost all plants included in the ASI data are in the manufacturing sector. We match the plants to the Indian districts following the approach of Somanathan et al. (2021). From 2001 to 2014, ASI also collects whether the plant is AC equipped which we will utilize as a proxy variable for a firm's adaptability. We use the sample period of 1998 to 2018.

3.2 Weather and Forecast Data

Climate. For climate data, we use the land component of the European ReAnalysis, known as ERA5-Land (Sabater 2019), produced by the European Centre for Medium-Range Weather Forecasts (ECMWF). ERA5-Land is a reanalysis dataset that combines historical observations with models to create a consistent time series of various climate variables. A main advantage of ERA5-Land is its enhanced temporal and horizontal resolution. It provides hourly data on surface variables at a spatial resolution of 0.1°longitude $\times$ 0.1°latitude (approximately 9 km), covering the entire world. Such high resolution allows for a clearer depiction of the spatial patterns of surface temperature between neighboring locations.

Our analysis uses variables of air temperature at 2 meters above the land surface. We aggregate daily average temperatures[16] up to the annual level. Specifically, in our main specification, we bin daily temperature every 5°C from -5°C to 30°C. Each temperature bin counts the number of days in a year when the daily average temperature falls within specific temperature ranges. This is calculated for every region in each year.

Figure 1a plots the difference of the number of hot days above 25°C in a year between periods of our sample firm coverage, 1999-2008 and 2009-2018, and the baseline periods, from 1951 to 1980. The dark red color represents an increase of more than 13.2 days in a year with temperatures above 25°C. Figure 1b depicts the daily temperature distributions in baseline periods, sample periods, and the projection year of 2100. The global warming trend reveals that the number of days above 25 has increased, and the number of days below 10 has reduced in each country in the past decades. The temperature distribution shifts rightward when we compare across and within countries, as climates grow warmer.

The use of temperature bins in our analysis better conceptualizes climate. Because climate change represents a long-term shift in weather patterns, the year-to-year variation in the whole temperature distribution offers a more accurate depiction of climate change than merely examining year-to-year variations in mean temperature. A key feature of climate change is the increased frequency of extreme heat events (Oudin Åström et al. 2013; Christidis, Mitchell, and Stott 2023), therefore the increase in the number of extreme hot bins, indicative of a rightward shift in the tail of the weather distribution, captures the idea of global warming more accurately.

factories with 100 or more workers in all years except 1997-2003 when it included only factories with 200 or more workers. The sampling scheme for smaller registered plants included one-third of factories until 2004 and one-fifth since then.

16. The daily average temperature is the simple geometric average of the maximum and minimum temperatures. The daily maximum temperature is identified by the highest value among the hourly temperatures, and the daily minimum temperature is the lowest recorded value.

Projection and Forecast. We collect global projection data computed by the sixth phase of the Coupled Model Intercomparison Project (CMIP6).[17] We use the SSP3-4.5 experiment in our main analysis, which is based on the SSP3 scenario that involves high mitigation and adaptation challenges, along with the RCP4.5 pathway with a radiative forcing of 4.5 $\mathrm{W/m^2}$ in the year 2100. The SSP3-4.5 scenario represents the intermediate greenhouse gas emissions level with modest mitigation policy and is described as a more likely path (O'Neill et al. 2016). We use SSP3-4.5 projection in the main analysis and present results from other scenarios in Appendix C.4.

For weather forecast data, we collect the long-range (seasonal) forecast from ECMWF (Copernicus Climate Change Service and Climate Data Store 2018), which provides information about atmospheric and oceanic conditions up to seven months into the future. The forecast data have a spatial resolution of 1°longitude by 1°latitude.[18] We collect forecast daily maximum and minimum 2m temperature from the first day of each month from January to December with forecasts up to 30 days measured in 724 lead-hours.

3.3 Other Data

Regional GDP. We collect regional-level global GDP data from DOSE (Wenz et al. 2023). We then clean and map global GDP data to our firm and weather datasets using spatial coordinates. This involves aligning different geographical units with administrative divisions like NUTS, prefectures, and districts.

Income Projection Projections of national income per capita are collected from the SSP Database, using the OECD EnvGrowth model (Dellink et al. 2017) hosted by the International Institute for Applied Systems Analysis.

4 Estimating the Misallocation Effect of Climate Change

4.1 Identification of the Causal Elasticities on Misallocation

We now estimate the first-order causal elasticities on capital misallocation $\frac{\partial \operatorname{var}_{mrpk_{ni}}(\tilde{\mathbf{T}}_{rt},\cdot)}{\partial \tilde{\mathbf{T}}_{rt}}$. Note that for each region-sector $n = (r, s)$, a Taylor expansion around the observed steady-state $(\overline{\operatorname{var}_{mrpk_{(s,r)i}}}, \overline{\tilde{\mathbf{T}}}_r, \overline{\tilde{\mathbf{X}}_{s,r}})$ can be written as

$$\begin{aligned}\operatorname{var}_{mrpk_{(s,r)i}}(\tilde{\mathbf{T}}_{r,t}, \tilde{\mathbf{X}}_{s,r,t}) &= \overline{\operatorname{var}_{mrpk_{(s,r)i}}} + \boldsymbol{\lambda}^{s,r}_{\sigma^2_{mrpk}} \cdot (\tilde{\mathbf{T}}_{r,t} - \overline{\tilde{\mathbf{T}}_r}) + \boldsymbol{\delta}^{s,r}_{\sigma^2_{mrpk}} \cdot (\tilde{\mathbf{X}}_{s,r,t} - \overline{\tilde{\mathbf{X}}_{s,r}}) + H.O.T. \\ &\approx \boldsymbol{\lambda}^{s,r}_{\sigma^2_{mrpk}} \cdot \tilde{\mathbf{T}}_{r,t} + \boldsymbol{\delta}^{s,r}_{\sigma^2_{mrpk}} \cdot \tilde{\mathbf{X}}_{s,r,t} + \eta_{s,r},\end{aligned} \tag{14}$$

where $\eta_{s,r}$ is a sector-region specific constant. For our benchmark exercise, we first estimate the average causal elasticity $\boldsymbol{\lambda}_{\sigma^2_{mrpk}} = \mathbb{E}[\boldsymbol{\lambda}^{s,r}_{\sigma^2_{mrpk}}]$ across all climates and sectors. We will revisit the nature of heterogeneity across climates and sectors in Section 4.3.

17. We use the GFDL-ESM4 model with a 1-degree nominal horizontal resolution produced by the National Oceanic and Atmospheric Administration, Geophysical Fluid Dynamics Laboratory (NOAA-GFDL).

18. From 1981 to 2016, the forecast values were hindcasts generated with a 25-member ensemble. Starting in 2017,

Figure 1: Climates of our sample regions

(a) Number of Hot Days Deviation Relative to 1951-1980 (b) Average Daily Temperature Distribution

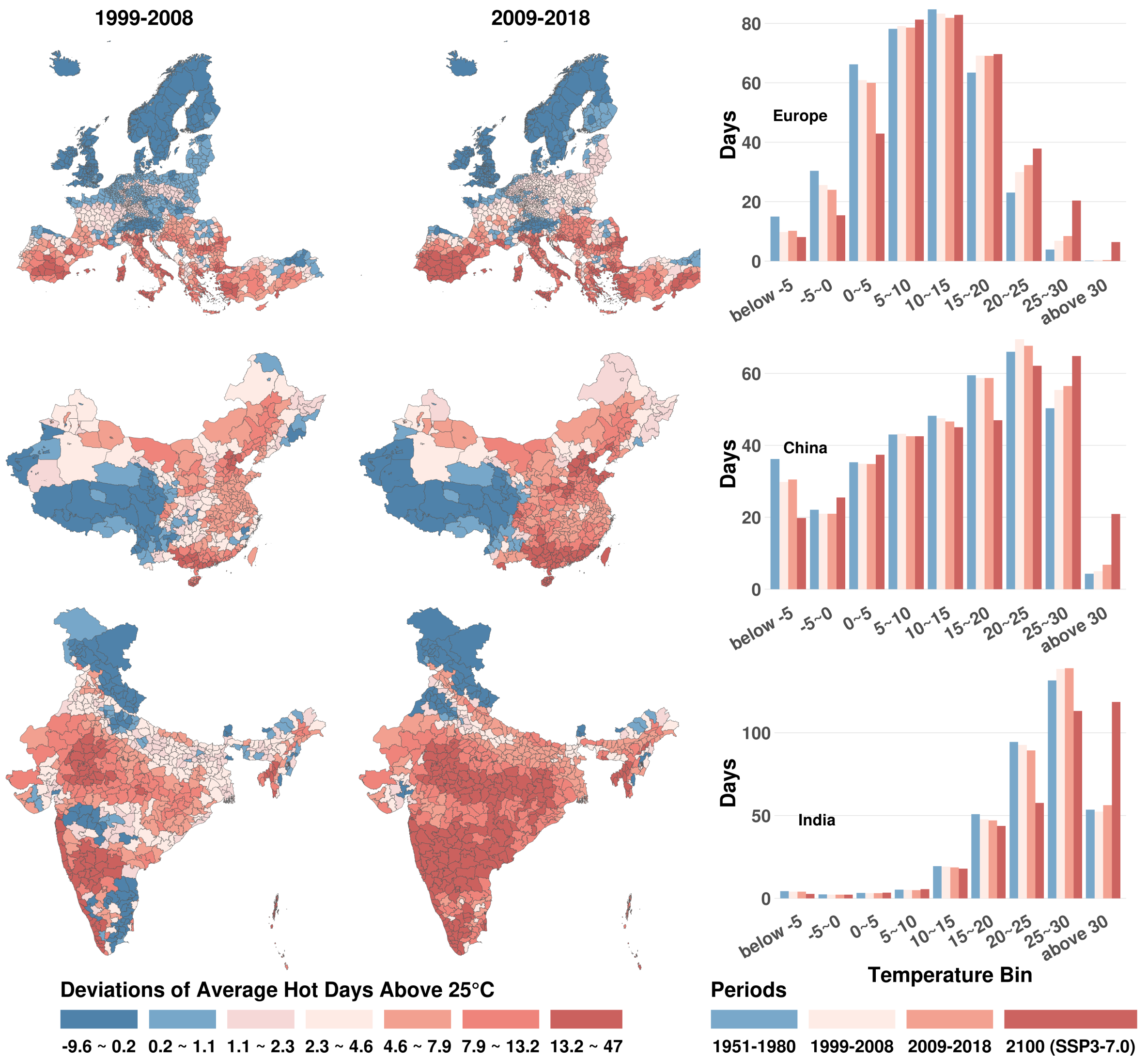

Notes: Figure 1a plots the difference of average number of days above 25°C between sample periods and baseline periods. The baseline period is from 1950 to 1980. The sample periods consist of two parts, 1999 to 2008, and 2009 to 2018. We calculate the 10-year average number of days above 25°C and deduct the 30-year baseline average number of days to obtain the difference. Figure 1b plots the average daily temperature distributions for baseline periods 1950-1980, two sample periods, and the projection year of 2100 under the SSP3-7.0 scenario.

We define current climate conditions, $\mathbf{T}_{r,t}$, in terms of temperature bins, following the approach by Carleton et al. (2022), Deschênes and Greenstone (2011), and Nath (2023). These bins, spanning the vector space $\mathbf{T}_{r,t} = \{\text{Tbin}_{r,t}^{<-5°C}, \text{Tbin}_{r,t}^{-5\sim0°C}, \text{Tbin}_{r,t}^{0\sim5°C}, \text{Tbin}_{r,t}^{5\sim10°C}, \text{Tbin}_{r,t}^{10\sim15°C}, \text{Tbin}_{r,t}^{15\sim20°C}, \text{Tbin}_{r,t}^{20\sim25°C}, \text{Tbin}_{r,t}^{25\sim30°C}, \text{Tbin}_{r,t}^{>30°C}\}$, capture the number of days within specific temperature ranges for region r in year t. Structured in 5-degree Celsius increments, these bins cover a broad spectrum of temperature variations, including extreme heat and cold. Thus, as noted in Deschênes and Greenstone (2011), using daily temperature data enables us to capture weather's nonlinear effects using linear regression models.

To estimate the causal effect of temperature on MRPK dispersion (i.e., misallocation), we exploit the inter-annual variation in the distribution of daily temperatures through the following panel regression:

$$\text{var}_{mrpk_{(s,r),t}} = \sum_{b \in B/(5\sim10°C)} \lambda^b_{\sigma^2_{mrpk}} \times \text{Tbin}^b_{r,t} + \boldsymbol{\delta}_{\sigma^2_{mrpk}} \mathbf{X}_{s,r,t} + \alpha_{c(r),t} + \eta_{s,r} + \varepsilon_{r,s,t}, \tag{15}$$

where $\eta_{s,r}$ is the region-sector fixed effects, accounting for the unvarying attributes of MRPK dispersion specific to each region-sector pair over time, consistent with the formulation in Equation 14. $\alpha_{c(r),t}$ is the country-by-year fixed effects, capturing the aggregate shocks to the country c that region r resides in. Standard errors are clustered at the region level to account for both serial and spatial correlations between all sectors across all years within each region (NUTS 3 in Europe, province in China, first-level administrative divisions in India).

$\lambda^b_{\sigma^2_{mrpk}}$ are coefficients measuring the causal effect of one additional day in temperature bin b on contemporaneous MRPK dispersion. Each $\text{Tbin}^b_{r,t}$ indicates the number of days whose average temperature falls within a specific range $b \in B$, where B is the set of ranges defined in 5-degree Celsius increments. We use the temperature bin ranging from 0°C to 5°C as the reference category, meaning that the coefficient for this category is normalized to zero.

$\mathbf{X}_{s,r,t}$ is a vector of logged control variables at the region-sector-year level, including the total number of observed firms, average firm-level sales, and average MRPK.[19] The first two control for the observed sample size and region-sector-level business cycle fluctuations, respectively. By controlling for the average (log)MRPK across firms at the region-sector-year level, we aim to demonstrate that the observed dispersion in MRPK is not primarily driven by the mechanisms through which temperature influences the average MRPK.[20]

4.2 Average Effects of Temperature on Capital Misallocation

The baseline estimates and inferred TFP loss are reported in Table 1 columns (1) and (5) and visualized in Figure 2. Figure 2 plots our baseline estimates of the effects of heat exposure on annual MRPK dispersion and the implied TFP loss. Specifically, the values on the left Y-axis

they are forecasts produced monthly with a 51-member ensemble. These ensembles are run on the first day of each month, providing forecasts for up to seven months ahead.

19. We exclude these controls in our preferred specification as they may block a potential pathway for affecting dispersion, although adding these controls have very little effect on our estimates.

20. This control allows us to isolate the specific impact of temperature on MRPK dispersion, independent of its effects on the average level of MRPK. Controlling for average MRPK also reflects the average financial constraints across firms.

represent the regression coefficients, denoted as $\hat{\lambda}^b_{\sigma^2_{mrpk}}$, for each bin b. Each $\hat{\lambda}^b_{\sigma^2_{mrpk}}$ quantifies the estimated impact of an additional day in temperature bin b on MRPK dispersion, compared to a day within the 5°C - 10°C range. To facilitate interpretation, we translate the estimates $\hat{\lambda}^b_{\sigma^2_{mrpk}}$ into the marginal effect on aggregate TFP through the misallocation channel using $-\frac{\alpha_{Kn}+\alpha^2_{Kn}(\sigma_n-1)}{2}\hat{\lambda}^b_{\sigma^2_{mrpk}}$ from Equation 13 under the choice of a well-established conservative choice of $\alpha_{Kn} = 0.35$ and $\sigma_n = 4$ across all n.[21] The right Y-axis corresponds to the values of the implied TFP loss.

Figure 2: Estimated impact of daily temperature shocks on annual MRPK dispersion and implied TFP loss

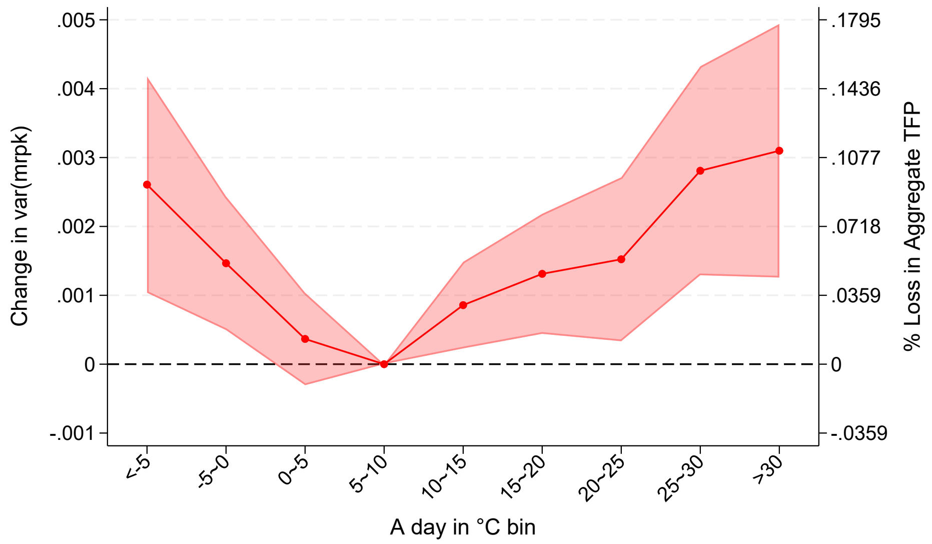

Notes: This figure shows the aggregate impact linking annual MRPK dispersion and TFP loss to average daily temperatures. The formula for computing TFP loss from misallocation is $-\frac{\alpha_{Kn}+\alpha^2_{Kn}(\sigma_n-1)}{2}\hat{\lambda}^b_{\sigma^2_{mrpk}}$. The estimation is normalized by setting the range of 5°C - 10°C as the reference category. Therefore, each $\lambda^b_{\sigma^2_{mrpk}}$ represents the estimated effect of an additional day in temperature bin b on annual MRPK dispersion or TFP loss, relative to a day with temperatures between 5°C - 10°C. The figure also includes the 90% confidence interval for these estimates where standard errors are clustered at the region level.

The estimated coefficients reveal that MRPK dispersion and the inferred TFP loss from temperature-induced misallocation peak at the most extreme temperatures, both coldest and hottest. This observed U-shape pattern between MRPK dispersion and temperature can also be translated into an inverted U-shape pattern between TFP and temperature, which is well known in the climate econometrics literature (Burke, Hsiang, and Miguel 2015; Nath 2023).

For temperatures above 25°C and below -5°C, the effects on MRPK dispersion are both economically and statistically significant at 1% level. Specifically, the point estimates indicate that substituting a day in the 5-10°C range with a day exceeding 30°C results in an increase of 0.31 log points in MRPK dispersion, translating to a decrease of 0.11% in annual aggregate TFP due to capital misallocation. On the cold end, we find that an additional day colder than -5°C in a year leads to an approximate 0.26 log points increase in annual MRPK dispersion and

21. For the elasticity of substitution, we choose $\sigma_n = 4$ as in Bils, Klenow, and Ruane (2021). For capital share, we pick a common value of $\alpha_{Kn} = 0.35$.

0.09% loss in annual TFP.

Robustness. Table 1 columns (2)-(4) present results with different specifications of fixed effects, inclusions of control variables, and weighting method. We introduce country-sector-year fixed effects instead of country-year fixed effects in column (2), absorbing all unobserved country and year-specific, region-invariant factors affecting MRPK dispersion in each sector. Column (3) adds control variables, including total number of observed firms, average firm-level sales, and average level of MRPK across firms in a region-sector-year, all in logarithmic form. Column (4) reports the results of the weighted OLS using the 1995 region-sector value-added as the regression weight. The objective is to assess whether assigning greater influence to region-sector observations with a larger size would affect our analysis. Our results, in particular the "U-shaped" pattern, remain robust under various specifications.

4.3 Heterogeneous Effect by Climate and Development

Our benchmark specification in Equation 15 captures the average effect of temperature on capital misallocation $\mathbb{E}[\boldsymbol{\lambda}^{s,r}_{\sigma^2_{mrpk}}]$. We now try to estimate the heterogeneous impact of temperature shocks across regions with different long-run climate and development levels.

It is not immediately clear if a hot day would consistently cause more or less misallocation in regions that are already warm or economically thriving. The ambiguity arises from two potentially counteracting factors. For simplicity, consider a case where the mass of firms can be divided into two groups: heat-loving and heat-averse. On the one hand, heat-averse firms in warmer climates might already adapt to high temperatures and thus experience less damage. However, it's also possible that in warmer regions, heat-averse businesses might still face greater damages with any additional heat shocks due to their limited adaptability (e.g., Moscona and Sastry 2023) and the damage convexity due to cumulative exposure of heat, as found by the observed non-linear effects in Burke, Hsiang, and Miguel (2015). Similarly, in regions with higher income levels, while firms may possess greater resources for adaptation to heat shocks, these economies often have highly specialized productions and exhibit larger dispersion in firm sizes (e.g., Chen (2022) and Poschke (2018)), which leads to more heterogeneous responses to climate conditions, as later shown in Section 6 that differences in firm sizes contributes to the MRPK divergence when facing heat shocks.

Therefore, to more precisely account for the heterogeneous impact stemming from different long-run climate and development levels across regions, we follow the approach of Carleton et al. (2022) and Nath (2023) by interacting a time-invariant measure of climate (i.e., long-run average temperature) and GDP per capita with each temperature bin. This approach allows us to capture how climate and income jointly influence the effects of temperature variations on capital misallocation. The modified regression model is formulated as follows:

$$\begin{aligned}\sigma^2_{mrpk_{s,r,t}} &= \sum_{b\in B_{/(5\sim 10^\circ C)}} \lambda^b \times \text{Tbin}^b_{r,t} + \sum_{b\in B_{/(5\sim 10^\circ C)}} \lambda^b_{\overline{T}} \times \text{Tbin}^b_{r,t} \times \overline{T}_r \\ &+ \sum_{b\in B_{/(5\sim 10^\circ C)}} \lambda^b_{\text{GDP}_{\text{pc}}} \times \text{Tbin}^b_{r,t} \times \ln \overline{\text{GDP}_{\text{pc}}}_r + \boldsymbol{\delta}\tilde{\mathbf{X}}_{s,r,t} + \alpha_{c,t} + \eta_{s,r} + \varepsilon_{s,r,t},\end{aligned} \tag{16}$$

Table 1: Effects of daily mean temperature bins on MRPK dispersion and TFP loss

	(1) σ^2_{mrpk}	(2) σ^2_{mrpk}	(3) σ^2_{mrpk}	(4) σ^2_{mrpk}	(5) Implied TFP Loss
< -5°C	0.0026***	0.0025***	0.0028***	0.0012	0.0935***
	(0.0010)	(0.0009)	(0.0009)	(0.0023)	(0.0342)
$-5 \sim 0$°C	0.0015**	0.0013**	0.0016***	0.0006	0.0526**
	(0.0006)	(0.0006)	(0.0006)	(0.0013)	(0.0212)
$0 \sim 5$°C	0.0004	0.0002	0.0005	-0.0019**	0.0131
	(0.0004)	(0.0004)	(0.0004)	(0.0009)	(0.0146)
$10 \sim 15$°C	0.0009**	0.0008**	0.0008**	0.0036***	0.0308**
	(0.0004)	(0.0004)	(0.0004)	(0.0010)	(0.0137)
$15 \sim 20$°C	0.0013**	0.0012**	0.0014***	0.0045***	0.0471**
	(0.0005)	(0.0005)	(0.0005)	(0.0013)	(0.0190)
$20 \sim 25$°C	0.0015**	0.0015**	0.0015**	0.0080***	0.0546**
	(0.0007)	(0.0007)	(0.0007)	(0.0020)	(0.0259)
$25 \sim 30$°C	0.0028***	0.0027***	0.0027***	0.0095***	0.1008***
	(0.0009)	(0.0009)	(0.0009)	(0.0021)	(0.0331)
> 30°C	0.0031***	0.0030***	0.0030***	0.0090***	0.1112***
	(0.0011)	(0.0011)	(0.0011)	(0.0021)	(0.0401)
Controls	No	No	Yes	No	No
Region-Sector FE	Yes	Yes	Yes	Yes	Yes
Country-Year FE	Yes	No	Yes	Yes	Yes
Country-Sector-Year FE	No	Yes	No	No	No
1995 VA Weighted	No	No	No	Yes	No
Observations	124,065	123,518	124,065	123,847	124,065
R^2	0.876	0.903	0.878	0.897	0.876

Notes: Standard errors in parentheses. We cluster standard errors at the regional level (NUTS3 level for European countries, prefecture level for China, and district level for India). Dependent variables in columns (1) to (4) represent the variance of log MRPK. Results from estimating Equation 15 are displayed in columns (1) to (4), with controls in column (3) and weighted OLS regression in column (4). Column (5) is the implied TFP loss calculated using the formula, $-\frac{\alpha_{Kn}+\alpha_{Kn}^2(\sigma_n-1)}{2}\hat{\lambda}^b_{\sigma^2_{mrpk}}$, and the regression estimates. Countries included are China, India, and 30 European countries.

* $p < 0.10$, ** $p < 0.05$, *** $p < 0.01$

where $\overline{T}_r$ represents the long-run annual average temperature for region r and $\ln \overline{\text{GDP}_{\text{pc}_r}}$ is the log of long-run average GDP per capita in region r.[22] Both long-run temperature and GDP per capita are computed as sample averages from 1997-2018. The coefficients λ_T^b and $\lambda_{\text{GDP}_{\text{pc}}}^b$ quantify how the impact of daily temperature shocks on MRPK dispersion varies across regions with different income levels and climates.[23]

Figure 3 presents the results from estimating Equation 16. We predict the impact of temperature shocks on MRPK dispersion and its equivalent TFP loss across three levels of income and long-run climate. The left Y-axis indicates the projected effects of temperature shocks on MRPK dispersion, while the right Y-axis shows the implied TFP loss suggested by the estimates.

Figure 3: MRPK Dispersion and TFP Loss Across Climates and Income

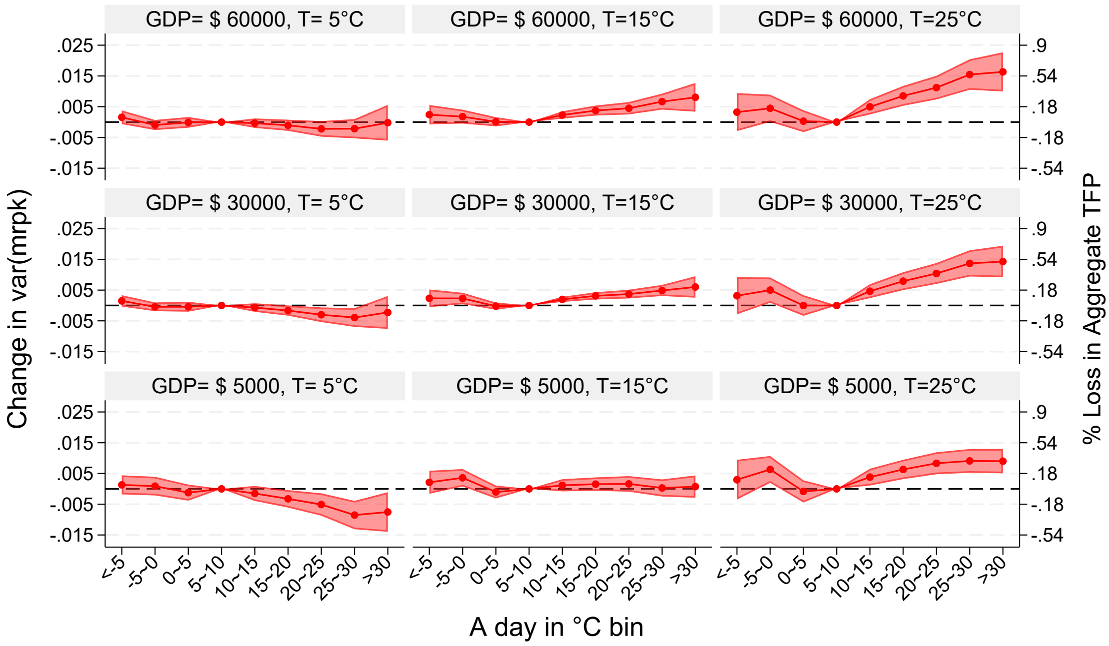

Notes: The graphs plot the predicted effect of exposure to daily mean temperature bins on MRPK dispersion and TFP loss at varying levels of income and climates. These predicted effects are derived from the interacted panel regression specified in Equation 16. The graphs include 90% confidence intervals, and standard errors are clustered at the regional level. The left y-axis indicates changes in MRPK dispersion, and the right y-axis shows the calculated TFP loss. The reference temperature is at 5∼10°C.

Level Effect: Hotter regions suffer more from the misallocation channel. Figure 3 shows that an extremely hot day (above 30°C) would result in greater MRPK dispersion in regions with a hotter average level of temperature. In regions of comparable wealth, the adverse effects of extreme heat on misallocation intensify as the regional climate becomes warmer, as observed when moving from the left column to the right for each income level. For regions

22. The sub-national level (PPP-adjusted) GDP per capita data is from DOSE. It is important to use sub-national level data as countries like India and China admit large income heterogeneity across the districts or prefectures. The GDP per capita data is in 2017 International Dollars.

23. Interacting temperature bins with the region's long-term average temperature allows us to analyze how an additional hot day has differential effects across areas with varying baseline climates. Similarly, by interacting temperature bins with a country's annual per capita income, we evaluate how the same heat shock impacts developed and developing economies differently.

with a high average temperature of 25°C, experiencing an additional day over 30°C leads to a notable TFP loss (ranging from 0.3% to 0.58%) due to misallocation, regardless of income levels. In contrast, in colder climates (e.g., where $\overline{T}_r \approx 5$°C), heat shocks appear to have negligible or even reducing effects on MRPK dispersion, thereby decreasing TFP loss. Interestingly, even a cold shock, such as an additional day below 0°C, tends to increase misallocation more significantly in hotter regions than colder ones. In general, compared to the reference level, the effect of a cold shock (<0°C) is always economically less significant than a heat shock (>30°C), with the notable exception being hot and low-income regions like India (GDP=$5000, $\overline{T} = 25$°C).

The quantitative implications can be best understood by comparing two regions with the same income level but different climates. For example, Arizona (US) and Norway have similar average per capita income across the sample period, around $60000, while their annual average temperature largely differs: 14.84°C in Arizona but only 1.97°C in Norway. Extrapolating using our estimates, an additional day with a temperature above 30°C compared to a 5-10°C day in Norway will lead to a 0.29 log points decrease in MRPK dispersion, which translates to a 0.1% increase in TFP, whereas in Arizona, the same heat shock leads to 0.8 log points increase in MRPK dispersion and a 0.3% decrease in TFP. In Section 5, we will explore how the divergent results across climates in our reduced-form regressions can be explained by regions' deviations from the optimal "'bliss-point' temperature for production, estimated to be around 13°C.

Income Effect: Richer economies suffer more from the misallocation Channel. A second key finding is that wealthier economies are more adversely affected by the misallocation channel due to extreme heat; we call this the *Income Effect*. This can be better understood by comparing countries across different income levels within similar climates. As presented in Figure 3, in each column with fixed long-run temperature, moving from the bottom (low income) to the top (high income) would increase the misallocation effect of the same heat shocks and make the response function more and more U-shaped. As a more concrete example, France and Turkey have similar average temperatures of around 10.5°C, while the income per capita of France ($45922) is over 1.5 times higher than that of Turkey ($28150). Our estimates suggest that the effect of an additional hot day >30°C would lead to a 0.08% TFP loss for Turkey and a 0.14% TFP loss for France. To explain the income effect, in Section 6, we will show that firm size dispersion increases with the region's economic development, resulting in greater MRPK divergence in response to the same heat shocks.

To sum up, the heterogeneous effect shows that the nature of the misallocation channel of climate change might be significantly different from other channels, such as labor productivity (Nath 2023) and mortality risk (Carleton et al. 2022). Previous empirical analysis showed that richer economies and hotter regions suffer much less from heat shocks regarding labor productivity and mortality, suggesting that some effects of climate change are somewhat adaptable.[24] However, the cost of climate shocks through the misallocation channel reveals an opposite pat-

24. For example, the estimates in Nath (2023) show that as a region becomes consistently hotter, workers are more adapted to the hotter climate and would not find a heat shock damaging to its productivity. Secondly, as an economy grows richer, workers suffer less from the temperature extremes. Both channels suggest that the cost of climate change might be lower in developed economies.

tern[25] by incurring a larger loss in hotter and richer countries, suggesting that market-based adaptation might have limited effect. Interestingly, the *average effect* of temperature on MRPK also exhibits similar heterogeneity. Estimates can be found in Figure C.1. As an economy develops to be more sophisticated in its techniques of production among firms (along with rising incomes), it might become more vulnerable in the sense that achieving efficient resource allocations becomes more challenging.

4.4 End-of-the-century Projection of the Misallocation Channel

In this subsection, we utilize the empirical estimates from Section 4.3 to project the effect of climate-induced misallocation on aggregate TFP loss by the end of the 21st century (2081-2100) for 4,881 regions in 172 countries around the world.[26]

Such projections require detailed region-level daily temperature projections, average levels of temperature, and GDP per capita at the end of the century. We use near-surface air temperature projection in RCP4.5 from the sixth phase of the Coupled Model Intercomparison Project (CMIP6) (Copernicus Climate Change Service 2021). The RCP 4.5 scenario features modest mitigation efforts. To project the daily temperature distribution, we calculate the average number of days in each temperature bin as defined in Section 4.1 and the average temperature from 2081-2100. We use the 20-year average for all variables to avoid inaccurate representations due to year-to-year fluctuations in climate model predictions. We follow Carleton et al. (2022) and use projections of national income per capita derived from the SSP3 scenarios, using the OECD EnvGrowth model (Dellink et al. 2017) projections. For an average region in the sample, the annual mean temperature is projected to increase by about 1.78°C by the end of the century (from 2081 to 2100), compared to a baseline period from 2000 to 2014, and the average GDP per capita is projected to increase by about $20748 (in 2017 International Dollar) compared to 2019. A detailed illustration of the current and projected evolution of income and average temperature can be found in Figure C.2.

Our goal is to compute the following: compared to baseline climate conditions, how much more will global warming contribute to aggregate TFP loss through misallocation by the end of the 21st century (EOC)? To make transparent the forces at play here, we decompose the total

25. In Section 6, we identify some potential mechanisms that could help explain why hotter and richer regions suffer more from heat shocks. Specifically, we find that a positive temperature shock in hotter regions would increase TFP volatility, making firms more prone to input mistakes, while a hot temperature shock in cold regions might enjoy a slight decrease in TFP volatility. Moreover, a firm's adaptability to heat and cold shocks depends heavily on size. On the firm level, we show that smaller firms' MRPK is more sensitive to extreme temperatures than larger firms. Across region-sector pairs, we find that economies with larger size dispersion suffer more misallocation, which is consistent with the firm-level evidence. We find those region-sectors with large size dispersion are also those with higher incomes (i.e., more developed), consistent with Poschke (2018).

26. Regions in our 32-country sample is defined as in Section 3, while the regions in all other countries are defined as GADM1-level region from the GADM dataset.

effect of climate-induced misallocation into three components:

$$\underbrace{\Delta^{\text{Loss}} \ln \text{TFP}_r}_{\text{Total Effect}_r} = \frac{\alpha_{Kn} + \alpha_{Kn}^2(\sigma_n - 1)}{2} \Bigg[\underbrace{\sum_b \left(\lambda^b + \lambda^b_{\text{GDP}_{pc}} \ln \text{GDP}_{pc,r,\text{base}} + \lambda^b_{\bar{T}} \bar{T}_{r,\text{base}} \right) \times \Delta \text{Tbin}_r^b}_{\text{Shock Effect}_r}$$
$$+ \underbrace{\sum_b \lambda_{b,\bar{T}} \text{Tbin}^b_{r,\text{EOC}} \times \Delta T_r}_{\text{Level Effect}_r}$$
$$+ \underbrace{\sum_b \lambda^b_{\text{GDP}_{pc}} \text{Tbin}^b_{r,\text{EOC}} \times \Delta \ln \text{GDP}_{pc,r}}_{\text{Income Effect}_r} \Bigg], \tag{17}$$

where we use Δ to denote the change in a variable between its end-of-century (EOC) value and its baseline value. The *shock effect* refers to the change in TFP losses due to shifts in daily temperature distributions ΔTbin_r^b, conditional on the baseline income computed in 2019 and baseline long-run temperature from 2000 to 2014; the *level effect* refers to the change in TFP losses due to the change in long-run temperature ΔT_r; and the *income effect* reflects the cost of the region's increasing misallocation due to the shift in economic development, measured by the change in (log) GDP per capita, $\Delta \ln \text{GDP}_{pc,r}$. To make the quantitative results more interpretable, we aggregate all measures of regional TFP loss to the country level by performing a weighted sum using the projected regional GDP share in each country under SSP3.[27]

Figure 4 plots each country's projected TFP loss from the capital misallocation channel in percentage terms. While the overwhelming majority of countries will experience a significant TFP loss, the projected TFP losses exhibit large heterogeneity across countries. The country-level TFP loss projections from other emission scenarios are presented in Figure C.4 and C.5.

In countries most severely affected, such as Tanzania, Malaysia, Honduras, and India, TFP losses are as high as above 40% compared to today. India, for instance, with a current average temperature of 23.29°C and an income per capita of $6608.62, the number of days above 30°C is projected to rise from 76.24 to 99.78 by the end of the century together with a large rise in average temperature to 25.00°C and income to $14615.39. Together, these forces result in a TFP loss of about 48.38%. These projections stem from the results that for countries like India that are already warm (tropical/subtropical) but relatively under-developed, the effect of extreme heat becomes more severe as they get hotter and more developed, as implied by the third column in Figure 3, showing the country moving from the bottom cell to the top right.

Less affected countries, such as the United States, Argentina, and Spain, will see a TFP loss between 20% and 30%. For example, in the United States, the projected change in the TFP losses due to global warming is about 20.99% at the end of the century. On average, in the US, income per capita is expected to rise from $62478.25 to $95800.89, while the annual temperature is expected to rise from 10.07°C to 12.45°C with the number of days above 30°C being projected to increase from 3.97 to 8.94. Countries with more mild damage, like France, the United Kingdom, Russia, and Canada, will see TFP losses below 15%. For example, in the

27. We use the grid-level projected SSP3 GDP are from Wang and Sun (2022) to obtain the projected GDP share.

United Kingdom, the national average temperature is predicted to rise from 9.15°C to 10.16°C, the number of days above 25°C is expected to increase from 0.03 to 0.37 days, and income per capita is projected to rise from \$47362.27 to \$85615.36. Together, the TFP losses in the UK are projected to be 7.25% due to misallocation. For developed countries in temperate and maritime climates, climate change might shift up the average temperature, but the extreme heat exposure is still quite limited. Therefore, while large in terms of absolute value, the increase in climate-induced misallocation is still more moderate compared to tropical countries.

Figure 4: End-of-century Projected TFP Loss Due to the Misallocation Channel

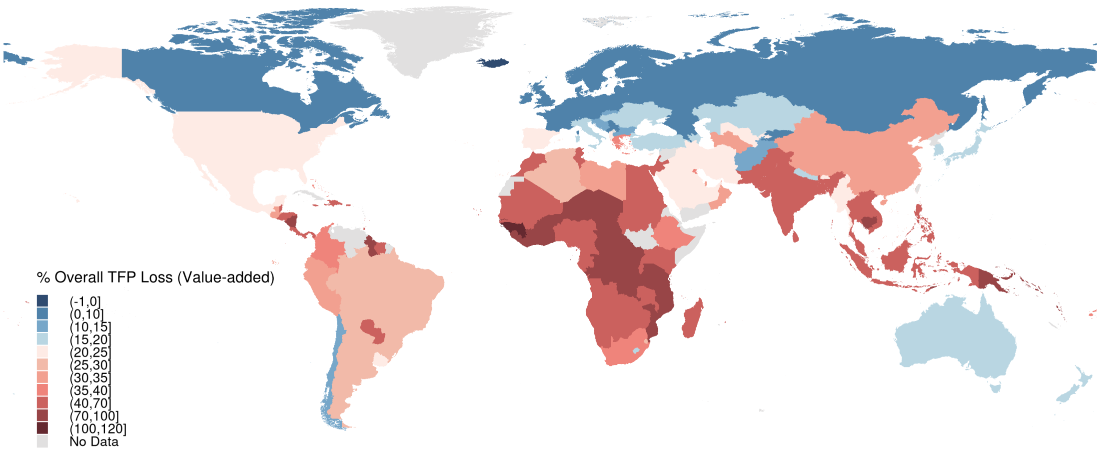

Notes: Figure shows the projected TFP losses from capital misallocation under SSP3-4.5 scenarios. The estimation follows Equation 17 where we estimate the total effect in MRPK dispersion and compute the equivalent value of TFP losses.

Figure 5: Projected Global TFP Loss and Its Decomposition: 2030-2100

(a) Total TFP Loss from the Misallocation Channel

(b) TFP Loss Decomposition

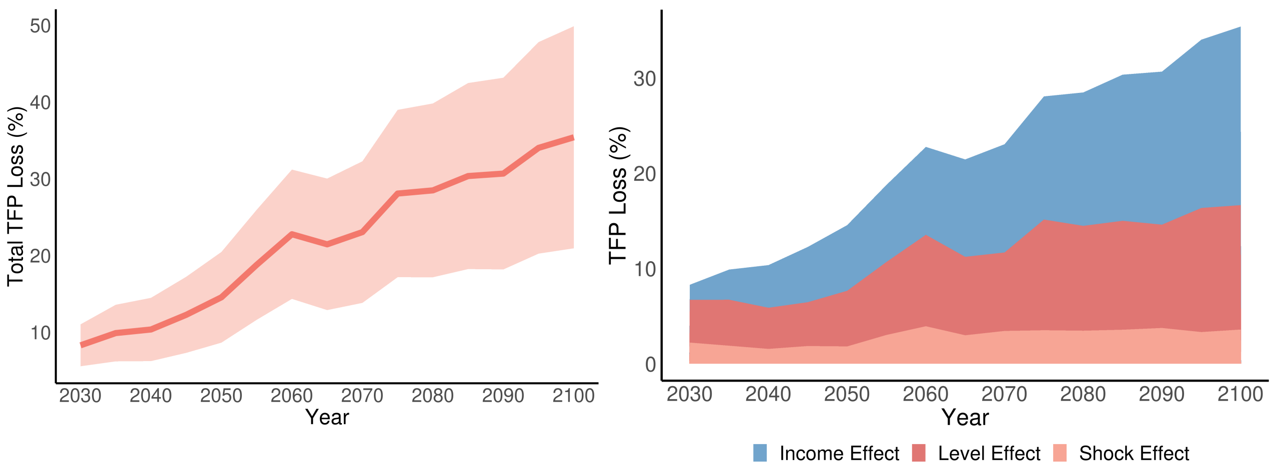

Notes: Figure 5a plots the total TFP loss across years. The dark red line plots the estimates and the shaded area is 90% confidence intervals from the parameter uncertainty. Figure 5b plots the three effects contributing to total TFP loss. All computations are under the SSP3-4.5 scenario and the percentage loss is compared to the baseline level.

Finally, using each country's projected GDP share,[28] we compute the global average TFP loss due to climate-induced misallocation can be computed as:

$$\underbrace{\Delta^{\text{Loss}} \ln \text{TFP}}_{\text{Total Effect}=35.40\%} = \underbrace{\text{Shock Effect}}_{3.60\%} + \underbrace{\text{Level Effect}}_{13.06\%} + \underbrace{\text{Income Effect}}_{18.74\%},$$

where we project that relative to today, the global cost of climate-induced misallocation to be 35.4% of aggregate TFP (GDP), with the shock effect from daily temperature distribution contributing to 3.60%, income effect contributing to 18.74% and the level effect of average temperature increase takes 13.06%. We present the evolution of TFP losses from the misallocation channel in Figure 5a, along with the 90% confidence interval that account for parameter uncertainty. This graph shows a projected increase in TFP losses from 8.30% in 2030 to 35.40% by 2100. Additionally, Figure 5b breaks down the projected TFP losses into three components over time and indicates that the income effect and the level effect are the primary drivers of the increasing TFP losses from the misallocation channel over the years.

The size of these estimates is large and is comparable to the overall projected impact by Burke, Hsiang, and Miguel (2015) and more recently by Bilal and Känzig (2024). Much of the projected total effect comes from the sharp rise in the semi-elasticities of daily temperature shocks due to the projected rise in temperature and income. These, of course, are subject to a range of caveats, including out-of-sample extrapolation, as the income and temperature levels by the end of the century are unprecedentedly high compared to the records in the past. However, even if we only account for the projected daily temperature variations and keep the first-order semi-elasticities of temperature shocks constant as the ones estimated today, we still project a global aggregate TFP loss of 3.60% coming from the misallocation channel, which should serve as a lower bound for our estimate.[29] Country-level misallocation loss projections under other climate change scenarios are provided in .

5 A Firm Dynamics Model of Temperature Shocks and MRPK Dispersion

In the previous section, we empirically demonstrated how temperature shocks lead to increased misallocation, particularly in countries with hotter long-run climates and more developed economies. We now explore why both temperature shocks and their levels can generate dispersion in capital returns within a standard dynamic investment model. Given the time-to-build nature of capital inputs, a natural explanation is that temperature influences the dispersion of expectation errors in capital returns across firms. We present two mechanisms in the model: (i) firms do not have perfect foresight of the future temperature and are heterogeneous in temperature sensitivity, and (ii) firms do not have perfect foresight of their sensitivity to temperature so that temperature extremes could lead to unexpected extreme losses in the

28. The TFP losses from this weighting scheme would exactly correspond to a model-implied aggregate TFP loss where the total global output is defined as a Cobb-Douglas aggregator of country-level value-added output and can be viewed as a first-order approximation for the TFP loss under any other constant returns to scale aggregator for global output.

29. A detailed breakdown of each effect on the country level is presented in Figure C.3.

firm level. These two mechanisms imply that misallocation depends on both the "level" and the "shock" of temperature. We will generate regression equations with model interpretations to test them empirically in Section 6 and Section 7.

5.1 Setup

Similar to the accounting framework in Section 2, our model describes the action of firms and the aggregate economy within a region-sector $n = (r, s)$. We suppress the region-sector label to avoid notation burdens. Our model follows a partial equilibrium set-up similar to that of David and Zeke (2021).

Production and Demand. We begin by describing the production side of the economy. Each firm i produces a differentiated product of quantity Y_{it} with Cobb-Douglas technology:

$$Y_{it} = \tilde{A}_{it} K_{it}^{\tilde{\alpha}_K} N_{it}^{\tilde{\alpha}_N}, \quad \tilde{\alpha}_K + \tilde{\alpha}_N = 1, \tag{18}$$

where $\tilde{A}_{it}$ is the physical productivity, K_{it} is the capital input (which is dynamic) and N_{it} represents labor. The firm's product faces a constant elasticity downward-sloping demand curve with demand shifter B_{it}:

$$Y_{it} = B_{it} P_{it}^{-\sigma}.$$

Combing production and demand functions, we obtain the equilibrium revenue function of the form:

$$P_{it} Y_{it} = \hat{A}_{it} K_{it}^{\alpha_K} N_{it}^{\alpha_N} \tag{19}$$

where $\alpha_F = (1 - \frac{1}{\sigma})\tilde{\alpha}_F, \forall F \in \{K, N\}$ and $\hat{A}_{it} = B_{it}^{\frac{1}{\sigma}} \left(\tilde{A}_{it}\right)^{(1-\frac{1}{\sigma})}$ is the revenue-based productivity (TFPR). We will be referring to this simply as productivity.

Productivity and Heterogeneity in Temperature Sensitivity. We now introduce how firms' productivity is heterogeneously impacted by temperature. For parsimony, we allow the annual temperature to be a sufficient statistic for climate conditions in the structural model (as in Dell, Jones, and Olken (2012) and Cruz and Rossi-Hansberg (2023)). We assume that firms' (log) productivity, $\hat{a}_{it} \equiv \ln(\hat{A}_{it})$, is determined by:

$$\hat{a}_{it} = \hat{\beta}_{it}(T_t - T^*) + \hat{z}_{it}, \tag{20}$$

where T_t is the realized temperature at year t, and T^* is the optimal temperature for firms' production. We assume that each firm i's (log) productivity changes linearly with temperature's deviation from optimum, $T_t - T^*$, subject to the sensitivity $\hat{\beta}_{it}$.[30] $\hat{z}_{it}$ denotes the firm-specific idiosyncratic productivity, which captures all the variations apart from the effect of temperature.

We allow a firm i's temperature sensitivity $\hat{\beta}_{it}$, to be firm-specific and time-varying. There

30. The heterogeneity of $\hat{\beta}_{it}$ reflects the composite effect of how both physical productivity and demand shifter are impacted by temperature across firms.

are two sources of heterogeneity in a firm's sensitivity to temperature:

$$\hat{\beta}_{it} = \underbrace{\hat{\beta}_i}_{\substack{\text{Persistent}\\ \text{sensitivity}}} + \underbrace{\hat{\xi}_{it}}_{\substack{\text{Idiosyncratic}\\ \text{sensitivity}}} + \mathcal{O}_t$$

(1) The persistent sensitivity to temperature, $\hat{\beta}_i$, is assumed to be observable and known to firms (e.g., a ski resort's $\hat{\beta}_i$ might be negative, and the owner knows about it). We assume that $\hat{\beta}_i$ is distributed as $\hat{\beta}_i \sim \mathcal{N}\left(\overline{\hat{\beta}}, \sigma^2_{\hat{\beta}}\right)$ across firms, where $\sigma^2_{\hat{\beta}}$ measures the dispersion of persistent sensitivity within a region-sector. A higher $\sigma^2_{\hat{\beta}}$ implies a more dispersion sensitivity across firms.

(2) The idiosyncratic sensitivity, $\hat{\xi}_{it}$, is i.i.d. across firm and time and cannot be predicted. It follows a normal distribution, $\hat{\xi}_{it} \sim \mathcal{N}\left(0, \sigma^2_{\hat{\xi}}\right)$, where $\sigma^2_{\hat{\xi}}$ measures the damage uncertainty within a region-sector. The impact of idiosyncratic sensitivity on TFP scales with $T_t - T^*$ to capture the increased damage uncertainty associated with extreme temperature (e.g. plant-level fire hazards are more likely to happen during heat waves).

$\mathcal{O}_t$ denotes the adjustment to offset the Jensen's inequality terms when aggregating across firms such that the aggregate productivity is log-linear in temperature in the absence of marginal product dispersion. Since $\mathcal{O}_t$ is common across all firms, it plays no role in our analysis of misallocation across firms.

Jointly, we model $\hat{\beta}_{it}$ to capture the idea that a firm would react to (realized and expected) temperature conditions according to their known knowledge of the firm's characteristics. However, with the presence of dynamic inputs that take time to build, firms could not act optimally as there is always some unknown damage sensitivity to temperature every period.

Law of Motion for Productivity and Temperature. We assume (agents perceive that) temperature and (log) idiosyncratic productivity $\hat{z}_{it} = \log \hat{Z}_{it}$[31] follow an AR($p$) process, with persistence ρ_T and ρ_z, respectively:

$$\begin{aligned}(T_{t+1} - \bar{T}) &= \sum_{h=1}^{p} \rho_{T,h}(T_{t+1-h} - \bar{T}) + \eta^T_{t+1},\\ \hat{z}_{it+1} &= \rho_z \hat{z}_{it} + \hat{\varepsilon}_{it+1},\end{aligned} \tag{21}$$

where we assume that temperature oscillates around a local average $\bar{T}$. $\eta^T_{t+1} \sim \mathcal{N}\left(0, \sigma^2_\eta\right)$ is the temperature shock. The idiosyncratic productivity shocks $\hat{\varepsilon}_{it+1} \sim \mathcal{N}\left(0, \sigma^2_{\hat{\varepsilon}}\right)$ are independent across firms and time.

At the firm level, uncertainty arises from three sources: 1) idiosyncratic damage sensitivity $\hat{\xi}_{it}$, normally distributed with variance $\sigma^2_{\hat{\xi}}$; 2) aggregate temperature uncertainty with variance σ^2_η; and 3) idiosyncratic uncertainty, with variance $\sigma^2_{\hat{\varepsilon}}$. We assume firms have full information regarding all realized shocks and hold rational expectations regarding the future states of the economy. We refer to the cross-sectional variance of unexpected firm-level TFP shocks as *TFP Volatility*, following Asker, Collard-Wexler, and Loecker (2014).[32]TFP volatility in the model

31. We use lower case to denote variables in logs, except for temperature T_t.
32. This can also be viewed as a theoretical counterpart to the cross-sectional measures of uncertainty as in Bloom

depends endogenously on temperature levels T_t and the temperature shocks η_t^T:

Lemma 1 *TFP Volatility,* $\mathrm{Var}(\hat{a}_{it} - \mathbb{E}_{t-1}[\hat{a}_{it}])$*, and can be written as:*

$$\mathrm{Var}(\hat{a}_{it} - \mathbb{E}_{t-1}[\hat{a}_{it}]) = (T_t - T^*)^2 \sigma_{\hat{\xi}}^2 + \hat{\eta}_t^{T2} \sigma_{\hat{\beta}}^2 + \sigma_{\hat{\varepsilon}}^2. \tag{22}$$

TFP Volatility reaches its minimum when the temperature reaches its optimum $T_t = T^*$*, and when there is no unexpected change in temperature,* $\eta_t^T = 0$.

This lemma illustrates that TFP volatility is dependent on the regional climate. Suppose a region is too hot or cold compared to T^*. In that case, firm-level productivity is too volatile due to the damage uncertainty $\sigma_{\hat{\xi}}^2$. We will test this empirically in Section 7.1.

Temperature and wages. Firms hire a composite of flexible inputs, “labor”, on a period-by-period basis at a competitive wage, W_t. For simplicity in modeling the temperature-related supply- and demand-side frictions in the labor market (e.g., temperature-related disutility of work or temperature-induced loss of labor productivity), we assume the equilibrium wage is given by:

$$W_t = \overline{W} \exp\left(\chi (T_t - T^*)\right),$$

where the wage is a function of temperature (deviation from T^*) with constant elasticity χ, indicating the sensitivity of which wages respond to temperature.[33].

Flexible Input Choice and Profits. Optimal choice of flexible inputs is made after capital inputs are allocated and all shocks are realized. The static input choice solves

$$\max_{N_{it}} \exp\left(\hat{\beta}_{it}\left(T_t - T^*\right)\right) \hat{Z}_{it} K_{it}^{\alpha_K} N_{it}^{\alpha_N} - W_t N_{it},$$

and results in the operating profits Π_{it}, calculated as revenue minus labor costs, expressed as

$$\Pi_{it} = G A_{it} K_{it}^{\alpha} := G \exp\left(\beta_{it}(T_t - T^*) + z_{it}\right) K_{it}^{\alpha}, \tag{23}$$

where $G := \overline{W}^{-\frac{\alpha_N}{1-\alpha_N}} \alpha_N^{\frac{\alpha_N}{1-\alpha_N}} (1-\alpha_N)$, $z_{it} = \frac{1}{1-\alpha_N} \hat{z}_{it}$, and $\alpha = \frac{\alpha_K}{1-\alpha_N}$. We define capital profitability as $A_{it} := \exp\left(\beta_{it}(T_t - T^*) + z_{it}\right)$, where $\beta_{it} = \frac{\hat{\beta}_{it} - \chi \alpha_N}{1-\alpha_N}$ is the sensitivity of capital profitability to temperature, transformed from the firm's productivity's temperature sensitivity, $\hat{\beta}_{it}$, and the wage's temperature sensitivity, χ. α is the curvature of the profit function.

Dynamic Capital Investment. Capital is a dynamic input that takes time to build. It needs to be invested one period ahead before all shocks (including temperature) are realized. Naturally,

(2009).

33. This assumption is commonly used in business cycle analysis. See Blanchard and Galí (2010), Alves et al. (2020), and Flynn and Sastry (2023).

the investment problem of a firm i can be formulated into the Bellman equation of the form:

$$V\left(T_t, Z_{it}, K_{it}\right) = \max_{K_{it+1}} \quad G\exp\left(\beta_{it}(T_t - T^*) + z_{it}\right) K_{it}^{\alpha} - K_{it+1} + (1-\delta)K_{it} + \frac{1}{1+r}\mathbb{E}_t\left[V\left(T_{t+1}, Z_{it+1}, K_{it+1}\right)\right],$$

where $\frac{1}{1+r}$ is the discount factor. Firms are risk-neutral and face no adjustment costs in the model.[34]. The optimal investment K_{it+1} solves the Euler equation:

$$1 = \underbrace{\frac{1}{1+r}}_{\text{Discount Factor}} \left(\underbrace{\alpha G K_{it+1}^{\alpha-1}\mathbb{E}_t\left[\exp\left(z_{it+1} + \beta_{it+1}(T_{t+1} - T^*)\right)\right]}_{\text{Expected Value of Marginal Profits of Capital}} + \underbrace{(1-\delta)}_{\substack{\text{Value of} \\ \text{Undepreciated Capital}}} \right). \tag{24}$$

Equation 24 shows that capital investment is increasing in the forecast of capital profitability, which in turn depends on the expectation of profitability-based idiosyncratic productivity z_{it+1} and temperature sensitivity β_{it+1}, as well as temperature T_{t+1}.

Solving the Euler Equation yields the firm's optimal investment policy as a function of expectations in logs (while suppressing some higher-order "risk-adjusted" terms):

$$\begin{aligned} k_{it+1} \approx & \frac{1}{1-\alpha}\mathbb{E}_t[a_{it+1}] + k_0 \\ = & \frac{1}{1-\alpha}\left(\frac{1}{1-\alpha_N}\mathbb{E}_t[\hat{a}_{it+1}] - \frac{\alpha_N}{1-\alpha_N}\mathbb{E}_t[w_{t+1} - \overline{w}]\right) + k_0 \\ = & \frac{1}{1-\alpha}\left(\frac{1}{1-\alpha_N}\left(\mathbb{E}_t[\hat{z}_{it+1}] + \mathbb{E}_t[\hat{\beta}_{it+1}(T_{t+1} - T^*)]\right) - \frac{\alpha_N \chi}{1-\alpha_N}\mathbb{E}_t[T_{t+1} - T^*]\right) + k_0, \end{aligned} \tag{25}$$

where $k_0 = \frac{1}{1-\alpha}\left(\log\left[\frac{\alpha G}{r+\delta}\right]\right)$ and lowercase denotes logs. The derivations illustrate the following logic: investment is proportional to the expected profitability of capital, which is increasing in expected (revenue) productivity and decreasing in expected wages. These are, in turn, dependent on the firm's expectation of future temperature sensitivity and future temperature.

The size of persistent temperature sensitivity $\hat{\beta}_i$ will determine how a firm's investment decision responds to expected temperature. Firm i's investment, relative to the average firm in the economy at date t, would be:

$$k_{it+1} - \overline{k_{it+1}} = \frac{1}{1-\alpha}\left(\mathbb{E}_t[\hat{z}_{it+1}] + \frac{(\hat{\beta}_i - \overline{\hat{\beta}_i})}{1-\alpha_N}\mathbb{E}_t[(T_{t+1} - T^*)]\right). \tag{26}$$

Specifically, for a *heat-averse firm* with $\hat{\beta}_i < \overline{\hat{\beta}_i}$ (say, a ski resort), a higher temperature forecast

34. Our benchmark model abstracts from the presence of adjustment costs in capital investment. If we introduce an adjustment cost of the form $-\frac{\kappa}{2}(\frac{I_{it}}{K_{it}} - \delta)^2$ at the time of investment, then the MRPK dispersion in the economy would take the form:

$$\sigma^2_{mrpk,(r,s),t} = \left(\frac{1}{1-\alpha_N}\right)^2 \left[(T_{r,t} - T^*)^2\sigma^2_{\xi,(r,s)} + {\eta^T_{r,t}}^2\sigma^2_{\beta,(r,s)} + \sigma^2_{\varepsilon,(r,s)}\right] + (\alpha-1)^2\phi_A^2\sigma^2_{k,t-1} + \text{Adj. Cost Channel}_{(r,s),t},$$

for some constant ϕ_A. The Adj. Cost Channel$_{(r,s),t}$ captures how adjustment costs interact with past and present

$\mathbb{E}_t[T_{t+1}]$ will lead to a relatively lower level of expected productivity and consequently lower investment compared to an average firm with $\overline{\hat{\beta}_i}$. In contrast, a *heat-loving firm* with $\hat{\beta}_i > \overline{\hat{\beta}_i}$ (say, a water park), would invest more than an average firm due to the relatively positive productivity effect from higher expected heat.

MRPK. Upon the realization of idiosyncratic productivity and temperature conditions, firms' labor choice is made and production takes place. From Equation 23, realized marginal revenue product of capital ($MPRK_{it} \propto \alpha_K \frac{P_{it}Y_{it}}{K_{it}}$)[35] of firm i can be derived as (in logs):

$$mrpk_{it} = a_{it} + (\alpha - 1)k_{it} + \log(\alpha_K \bar{G})^{36} \tag{27}$$

Plugging in the policy function k_{it} as a function of past expectation, we write down find how $mrpk_{it}$ depends on the realization of shocks in the next proposition.

Proposition 3 *A firm with higher unexpected change in productivity exhibit a higher MRPK relative to the average level:*

$$mrpk_{it} - \overline{mrpk_{it}} = \frac{1}{1-\alpha_N}\left\{ \underbrace{(\hat{\beta}_i - \overline{\hat{\beta}_i})\eta_t^T}_{\substack{\text{Unexpected} \\ \text{Temperature Shock} \\ \text{on Productivity}}} + \underbrace{\hat{\xi}_{it}(T_t - T^*)}_{\substack{\text{Unexpected} \\ \text{Damage} \\ \text{Sensitivity}}} + \hat{\varepsilon}_{it} \right\}, \tag{28}$$

where the relative MRPK of heat-averse firms ($\hat{\beta}_i < \overline{\hat{\beta}_i}$) will decrease with a positive temperature shock η_t^T; while the relative MRPK of heat-loving firms ($\hat{\beta}_i > \overline{\hat{\beta}_i}$) will increase with a positive temperature shock.

Proof. See Appendix. ■

First, notice that Equation 28 suggests that $mrpk_{it}$ would be the same across all firms when productivity is perfectly known at the time of investment. Otherwise, the MRPK would increase with forecast error of (revenue) productivity in the cross-section.

This reveals the key mechanism in the model. All firm's MRPK would change with (1) the unexpected temperature shock η_t^T due to their temperature sensitivity $\hat{\beta}_i$ and (2) with the level of temperature $T_t - T^*$ since part of their damage sensitivity $\hat{\xi}_{it}$ was unknown to them at the time of investment. In a region-sector with an unexpected heat shock, $\eta_t^T > 0$, the firms with relatively low MRPKs in the cross-section are those that are (1) heat-averse ($\hat{\beta}_i < \overline{\hat{\beta}_i}$) such that the productivity suffers unexpectedly more than an average firm, (2) unexpectedly damaged with heat sensitivity $\hat{\xi}_{it}(T_t - T^*) < 0$. Judging from the ex-post, these firms invested too much capital due to their erroneous expectation of higher-than-realized productivity, and the capital

climate conditions. It includes terms that are linear in $\eta_{r,t}^T$, as well as the interactions of past temperature conditions with $\eta_{r,t}^T$. The interaction between adjustment costs and climate conditions operates separately from our main mechanisms. It is unlikely to affect the identification of the damage volatility channel and climate volatility channel in the data when additional controls are added.

35. Note that the marginal revenue product of capital and the marginal profitability of capital are the same up to a transformation, which implies that their cross-sectional log dispersion should be the same.

36. $\overline{G} = \overline{W}^{-\frac{\alpha_N}{1-\alpha_N}} \alpha_N^{\frac{\alpha_N}{1-\alpha_N}}$ is the constant associated with the revenue function $P_{it}Y_{it} = \overline{G}A_{it}K_{it}$.

in those firms cannot be used as productively as those firms that are heat-loving ($\hat{\beta}_i > \overline{\hat{\beta}_i}$) or those experiencing unexpectedly less productivity damages ($\hat{\xi}_{it}(T_t - T^*) > 0$).

The large heterogeneity of firm-level sensitivity implies that temperature conditions could change the dispersion in capital return and thus capital misallocation across firms, summarized by the following proposition, where we add back the notation for a region-sector pair $n = (r, s)$:

Proposition 4 *Within a region-sector pair $n = (r,s)$, the $mrpk$ dispersion across firms is increasing in TFP Volatility, $\mathrm{Var}(\hat{a}_{nit} - \mathbb{E}_{t-1}[\hat{a}_{nit}])$, and can be decomposed into:*

$$\begin{aligned} \sigma^2_{mrpk,(r,s),t} &= \left(\frac{1}{1-\alpha_N}\right)^2 \mathrm{Var}(\hat{a}_{nit} - \mathbb{E}_{t-1}[\hat{a}_{nit}]) \\ &= \left(\frac{1}{1-\alpha_N}\right)^2 \Bigg[\underbrace{(T_{r,t} - T^*)^2 \sigma^2_{\hat{\xi},(r,s)}}_{\substack{\textit{Damage Volatility} \\ \textit{(Level Effect)}}} + \underbrace{{\eta^T_{r,t}}^2 \sigma^2_{\hat{\beta},(r,s)}}_{\substack{\textit{Climate Uncertainty} \\ \textit{(forecast error Effect)}}} + \sigma^2_{\hat{\varepsilon},(r,s)}\Bigg] \end{aligned} \tag{29}$$

Within $n = (r,s)$, $mrpk$ dispersion is increasing in:
(1) squared deviation from optimal temperature, $(T_{r,t} - T^*)^2$,
(2) squared (unexpected) temperature shocks ${\eta^T_{r,t}}^2$.

As the cross-sectional MRPK differences depend solely on the unexpected shocks on productivity in the model, it follows naturally that MRPK dispersion scales with the dispersion in the unexpected shocks on productivity among firms. The higher the TFP volatility, the larger the dispersion of the input mistakes that would take place. Using our decomposition of TFP Volatility in Equation 51, we find temperature variations contribute to misallocation through two channels: level effect (due to damage volatility) and forecast error effect (due to climate uncertainty).

(1) Level Effect. The level of temperature affects misallocation through the change in damage volatility. As the temperature deviates more from the "bliss point" T^*, firms who receive extreme realizations of the idiosyncratic damage sensitivity $\hat{\xi}_{it}$ will get larger unexpected damage (e.g., a larger fraction of firms will experience severe factory fire). Therefore, the productivity becomes harder to forecast, and more investment mistakes are made. The economy will thus suffer from more misallocation as $(T_{r,t+1} - T^*)^2$ rises.

(2) Forecast Error Effect. The magnitude of the climate uncertainty channel relies on the size of unexpected temperature shocks. As different firms have heterogeneous sensitivity to these shocks, larger unexpected temperature shocks, say a heat shock, will make the return to investment of heat-averse firms unexpectedly low and the heat-loving firms unexpectedly high. The opposite is true for an unexpected cold shock. Therefore, we will see an increasing level of capital misallocation with a more considerable unexpected temperature shock ${\eta^T_{r,t}}^2$.

These two effects help explain how a region-sector's geographical locations and long-run climate might matter for capital misallocation, as we have identified in Figure 3 in Section 4.

Regions experiencing extreme temperatures - either too hot or too cold - or those subject to uncertain temperature conditions are prone to higher levels of capital misallocation. In Section 7, we will try to gauge the quantitative importance of how the level effect and the forecast error effect contribute to climate-induced capital misallocation through the lens of model-induced regressions.

Equation 29 also has predictions across region-sectors on how the average degree of misallocation in the region-sector depends on the average climate conditions and the distribution of the firm's weather-related characteristics. For example, when given the same climate conditions, a region-sector with higher dispersion in persistent sensitivity $\sigma^2_{\hat{\beta},(s,r)}$ or larger damage uncertainty $\sigma^2_{\hat{\xi},(s,r)}$ will suffer more climate-induced misallocation.

Paired with the model's implication that the average level of temperature sensitivity $\overline{\hat{\beta}}_{(s,r)}$ in a region-sector does not matter for the degree of misallocation, we can try to rationalize why developed countries suffer more from temperature shocks via the misallocation channel. Although developed countries might feature a higher level of "heat preparedness" $\overline{\hat{\beta}}_{(s,r)}$, but might have a larger dispersion $\sigma^2_{\hat{\beta},(s,r)}$ due to the larger scope of specialized production and more extensive variety. More developed countries also have a larger dispersion of firm sizes (Poschke 2018), which would naturally matter for dispersion of temperature sensitivity as larger firms have more resources and working capital to defend against sudden climate shocks. Although we do not model this explicitly in the benchmark model, we will empirically test how firm sizes might proxy for temperature sensitivity in Section 6.

TFP Loss from Misallocation. Finally, we formalize how temperature-induced misallocation affects region-sector aggregate TFP in the model. In the Appendix, we show that under a CES aggregator,[37] the economy admits an aggregate production function of the form:

$$y_{nt} = a_{nt} + \tilde{\alpha}_K k_{nt} + \tilde{\alpha}_N n_{nt},$$

where the cost of misallocation can be expressed as the deviation from the level of TFP, a^*_{nt} when MRPKs are equalized across firms:

$$a_{nt} - a^*_{nt} = -\frac{\tilde{\alpha}_K + \tilde{\alpha}^2_K(\sigma - 1)}{2}\sigma^2_{mrpk,nt} \tag{30}$$

This formula is reminiscent of Equation 9 in the accounting framework and shows that the intuitions behind the cost of misallocation are similar in the firm dynamics model.

6 Firm-level Evidence: Heterogeneous Sensitivity, Temperature Shocks, and MRPK Divergence

We now provide direct evidence from firm-level data on how temperature shocks could lead to heterogeneous responses in the MRPK among firms with differing levels of persistent tem-

37. Following Midrigan and Xu (2014), in a partial equilibrium context, one can define aggregate production and misallocation by considering the problem of a planner with a CES aggregator and faces no restrictions on how to reallocate inputs across firms.

perature sensitivity,[38] $\hat{\beta}_i$. Since directly measuring $\hat{\beta}_i$ for each firm is challenging, we instead explore two possible major factors contributing to this heterogeneity: firm size and adaptability, particularly regarding the installation of air conditioning (AC) facilities. We investigate whether firms of different sizes and levels of adaptability (those equipped with AC versus those without) exhibit distinct responses to identical temperature shocks in their MRPKs.

The choice to use firm size and AC installation as proxies for temperature sensitivity is grounded in the empirical literature. Regarding size, studies have shown that larger firms are less sensitive to temperature shocks and better equipped to cope with extreme heat compared to smaller firms (Ponticelli, Xu, and Zeume 2023), leading to a higher level of $\hat{\beta}_i$ in the model. As for the importance of AC, Somanathan et al. (2021) demonstrates that hot days significantly suppress output for plants without climate control, whereas plants with climate control facilities are unaffected.

We test the key prediction by the model from Equation 28 (reproduced below). In the same region-sector pair, a more heat-averse firm (i.e. lower $\hat{\beta}_i$) would have a lower MRPK from an unexpected positive temperature shock compared to the average. As the temperature shock was not expected at the time of investment decisions, a more heat-averse firm would be seen to have made a bigger "investment mistake" as the return on the capital can be lower.

$$mrpk_{it} - \overline{mrpk_{it}} = \frac{1}{1-\alpha_N}\left\{ \underbrace{(\hat{\beta}_i - \overline{\hat{\beta}_i})\eta_t^T}_{\substack{\text{Unexpected}\\ \text{Temperature Shock}\\ \text{on Productivity}}} + \underbrace{\hat{\xi}_{it}(T_t - T^*)}_{\substack{\text{Unexpected}\\ \text{Damage}\\ \text{Sensitivity}}} + \hat{\varepsilon}_{it} \right\},$$

$\hat{\beta}_i$ and MRPK: Empirical Approach We run the following regression as the empirical counterpart of the Equation 28 to explore whether the two heat-sensitivity proxy variables: firm sizes and AC installation, lead to different responses of MRPK to temperature shocks:

$$\begin{aligned} \log(MRPK_{r,s,i,t}) = & \sum_{b \in B/\{5-10°C\}} \lambda_b \times \text{Tbin}_{r,t}^b \\ & + \sum_{b \in B/\{5-10°C\}} \lambda_{b,\hat{\beta}\text{-proxy}} \times \text{Tbin}_{r,t} \times \hat{\beta}\text{-proxy}_{it}^{r,s} + \boldsymbol{\delta}\mathbf{X}_{i,t} \\ & + \delta_i + \alpha_{s,c(r),t} + \varepsilon_{s,c(r),i,t}, \qquad \hat{\beta}\text{-proxy} \in \{\text{Relative Size, AC}\}. \end{aligned} \tag{31}$$

r represents the region, s the sector, i the firm, and t the year. $\hat{\beta}\text{-proxy}_{it}^{s,r}$ is a firm-level proxy for $\hat{\beta}_i$, defined either as Relative Size_{it}^{sr} or AC_{it}^{sr} in our two settings. η_i indicates firm fixed effects, which remove time-invariant, unobserved firm-level heterogeneity that could otherwise bias the estimates. $\alpha_{s,c(r),t}$ are country-sector-year fixed effects that control for unobserved characteristics specific to each region-sector pair annually, such as country-sector level business cycle fluctuations. Standard errors are clustered at the region level to address serial and spatial correlation within all firm-year observations in a region. The coefficients of interest, $\lambda_{b,\hat{\beta}\text{-proxy}}$, are identified by comparing firms within the same country-sector exposed to identical temperature shocks but show differential response in (log) MRPK. A $\lambda_{b,\hat{\beta}\text{-proxy}} > 0$ indicates a higher

38. This also serves to identify climate-induced misallocation directly using firm-level microdata without the log-normality assumption.

MRPK for heat-tolerant firms compared to heat-averse ones under similar temperature shocks.

Heterogeneous Effect of Temperature Shocks from Firm Size. Following the approach of Bau and Matray (2023), we characterize a firm's size based on the value of its capital stock, as larger firms are typically more financially flexible in adjusting to unexpected heat shocks. For the analysis of firm size, $\hat{\beta}$-proxy$_{it}^{s,r}$ is defined as a continuous variable equal to Relative Size$_{it}^{s,r}$. We measure a firm's relative size using Relative Size$_{it}^{r,s} := \log K_{it}^{s,r} - \overline{\log K_{it}}^{s,r}$, which compares a firm's (log) capital stock, $\log K_{it}^{s,r}$, to the cross-sectional average of firms within the same region-sector-year, $\overline{\log K_{it}}^{s,r}$. We also standardize Relative Size$_{it}^{r,s}$ over the entire sample in the regression. This approach allows us to exploit variations across firms within each region-sector-year, aligning with the level of variations used in our reduced-form analysis, where $\text{var}(mrpk)$ is calculated.

Figure 6a illustrates the effect of temperature shocks on MRPK across firms of varying sizes, $\lambda_{b,\text{Relative Size}}$, for each temperature bin b. The analysis reveals that firms of different sizes respond differently to identical weather shocks. Specifically, larger firms tend to experience a relatively higher MRPK in response to temperature extremes compared to smaller firms. For instance, an additional day with temperatures above 30°C or below -5°C, compared to a day with temperatures ranging from 10-15°C, increases the MRPK difference by around 0.1% between two firms whose sizes differ by one standard deviation. Detailed results of the estimation are presented in Table D.2. The results here validate our hypothesis that the difference in firm sizes is a source of $\hat{\beta}_i$ heterogeneity, and larger firms are more heat-tolerant.

Figure 6: Effects of daily temperature shocks on log MRPK for firms of different sizes and adaptability

(a) Heterogeneous Effect from Firm Size (b) Heterogeneous Effect from Firm Adaptability (AC)

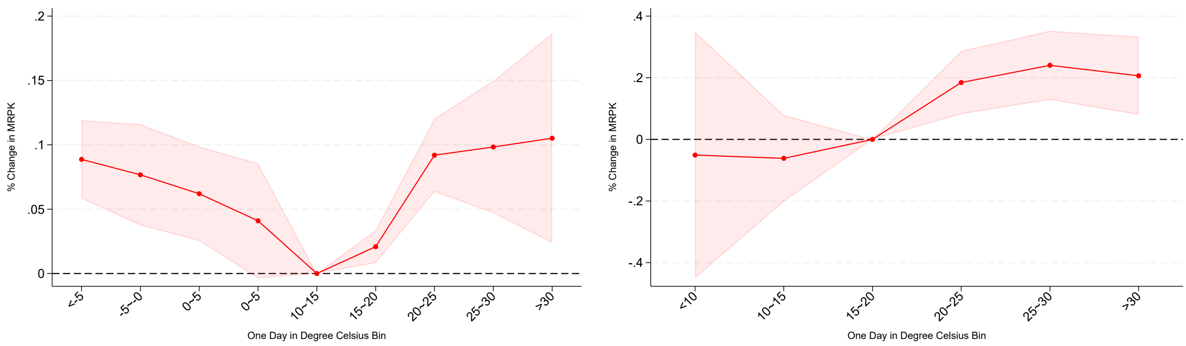

Notes: Graph plots the effects of daily mean temperature bins on firm-level log MRPK. Figure 6a plots the interaction terms of relative firm size and temperature bins. Each point measures the estimated effect on a large firm relative to a firm that is 1 SD smaller. We include firm and country-sector-year fixed effects. Figure 6b plots the estimated effect on firms with and without AC separately. We include firm and sector-year fixed effects (since AC data only covers the India ASI sample). Standard errors are clustered at the regional level. Shaded areas indicate a 90% confidence interval.

More interestingly, drawing back to our empirical findings on the heterogeneous impacts of extreme heat across different income levels, we find that wealthier economies suffer more from capital misallocation under extreme heat. This could be driven by the higher dispersion in firm sizes in more developed economies, as documented by Poschke (2018) and observed in our data in Figure 7.

Figure 7: Firm Size Dispersion and GDP per capita

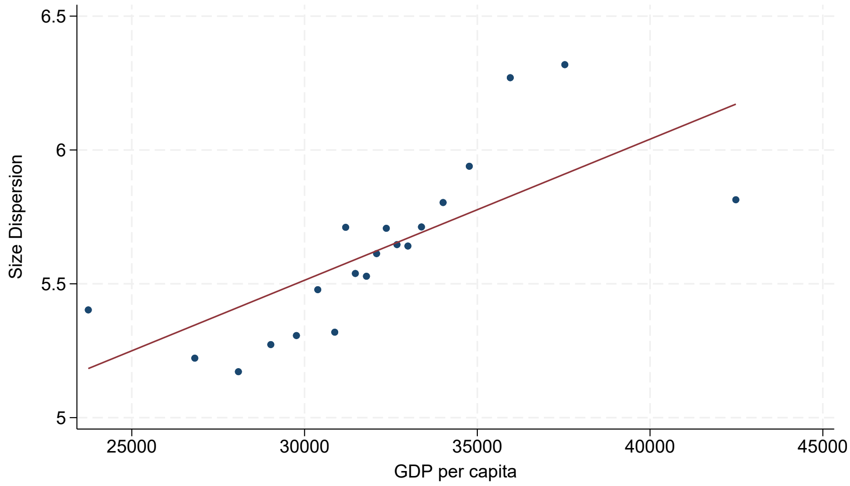

Notes: The graph presents the bin-scatter plots illustrating the relationship between firm size dispersion (measured as the variance of log fixed assets across firms) and annual GDP per capita at the region-sector-year level.

Heterogeneous Effect of Temperature Shocks from Adaptability. Another source of heterogeneity in $\hat{\beta}_i$ could be the varying adaptability to temperature extremes among firms. We expect that firms with greater adaptation measures will be more resilient to heat shocks and thus have a higher $\hat{\beta}_i$. We measure adaptability by the installation of computerized air conditioning (AC) systems, a variable collected annually in the Indian Annual Survey of Industries (ASI) since 2001. Therefore, our analysis for this part focuses on the sample from the Indian ASI.

We implement Equation 31 where $\hat{\beta}$-proxy$_{it}^{s,r}$:= AC$_{it}^{s,r}$ is defined as a dummy variable – it equals 1 for firms equipped with AC and 0 for those without.[39] Figure 6b shows the estimated effects on MRPK for AC-equipped firms compared to those without AC. The impact of temperature shocks on MRPK for AC-equipped firms relative to non-AC firms, $\lambda_{b,\text{AC-equipped}}$, is depicted by the red line for each temperature bin b. Our findings reveal that cold temperature shocks have a negligible difference in MRPK between AC-equipped and non-AC firms. However, heat shocks significantly increase the MRPK difference for AC-equipped firms compared to non-AC firms. For example, an additional day with temperatures above 30°C, compared to a day in the 15-20°C range, leads to a relative increase of about 0.2% in MRPK between AC-equipped and non-AC firms, after controlling for firm capital stock. Detailed results are presented in Table D.3.[40]

39. A firm is defined as AC-equipped if it has reported the installation of AC at least once during the sample period.

40. Our baseline specification in Column 3 analyzes the within-firm variation on the effect of AC installation by including firm fixed effects δ_i and sector-year fixed effects $\theta_{s,t}$, and we include the AC indicator variable AC$_{it}^{s,r}$ and capital stock $\ln K_{it}$ as controls. However, installing air conditioning is a common adaptation strategy for firms to cope with extreme heat, but it also makes them subject to costs of adaptive investment (e.g. Somanathan et al. 2021), which means the investment of AC itself could change the firm's MRPK as well. Following the approach of Asker, Collard-Wexler, and Loecker (2014), we address this in our alternative specification in Column (3) by conditioning on current capital stock to make sure that we are comparing two firms making the same capital decision, but one firm has AC while the other does not. We include sector-year fixed effects in all specifications, such that λ_b and $\lambda_{b,\text{AC}}$ are identified based on the comparison of across-firm differences caused by AC installation within each sector-year.

7 Estimating the Mechanisms of Climate-Induced Misallocation

In this section, we empirically estimate the two effects driving climate-driven misallocation: (1) the level effect due to damage volatility, and (2) the forecast error effect stemming from climate uncertainty, as suggested by the model in Equation 29, which is reproduced below:

$$\sigma^2_{mrpk,(r,s),t} = \left(\frac{1}{1-\alpha_N}\right)^2 \mathrm{Var}(\hat{a}_{nit} - \mathbb{E}_{t-1}[\hat{a}_{nit}])$$
$$= \left(\frac{1}{1-\alpha_N}\right)^2 \Bigg[\underbrace{(T_{r,t} - T^*)^2 \sigma^2_{\xi,(r,s)}}_{\substack{\text{Damage Volatility} \\ \text{(Level Effect)}}} + \underbrace{\eta^{T\;2}_{r,t}\,\sigma^2_{\beta,(r,s)}}_{\substack{\text{Climate Uncertainty} \\ \text{(Forecast Error Effect)}}} + \sigma^2_{\varepsilon,(r,s)} \Bigg]$$

We first test the level effect by empirically estimating how the level of temperature non-linearly shifts the TFP volatility and MRPK dispersion in the cross-section of firms. From this exercise, we can also identify an optimal temperature of around 13°C, which is consistent with Burke, Hsiang, and Miguel (2015). Next, we provide direct evidence of the forecast error effect by showing climate uncertainty, measured by the mean squared forecast errors of monthly temperature, contributes to MRPK dispersion. Based on these estimates, we then quantify the relative contributions of level effect and forecast error effect to climate-induced misallocation.

7.1 Level Effect: Temperature and TFP Damage Volatility

Our theory suggests that MRPK dispersion is proportional to TFP volatility, which in turn is non-linearly dependent on the level of temperature $T_{r,t}$. As the temperature deviates from the optimal level T^*, becoming either too hot or too cold, the likelihood of extreme firm-level events increases. Therefore, temperature's deviation from T^* leads to greater volatility in TFP across different firms. We now test this relationship directly in the data and try to estimate the optimal temperature T^*.

As it is hard to directly measure unexpected TFP shocks ($\hat{a}_{nit} - \mathbb{E}_{t-1}[\hat{a}_{nit}]$) due to possible mis-specifications of the law of motion and agents' information set, we adopt the approach of Asker, Collard-Wexler, and Loecker (2014), and use the variance of 'first-differenced' TFP shocks[41], $\mathrm{Var}_{(r,s)t}(\hat{a}_{it} - \hat{a}_{it-1})$to approximate[42] the TFP volatility[43] in region-sector (r, s). Inspired by Equation 51, we identify the nonlinear impact of temperature on TFP volatility from the following reduced-form specification:

$$\mathrm{Var}_{(r,s),t}(\hat{a}_{it} - \hat{a}_{it-1}) = \alpha + \boldsymbol{\beta f}(T_{r,t}) + \eta_{s,r} + \delta_{c(r),t} + \varepsilon_{s,r,t}, \tag{32}$$

41. Measuring firm-specific productivity shocks is challenging and sensitive to mis-specifications for the TFPR process. This is particularly true in our model, where firm-level productivity responds heterogeneously to temperature shocks. To address this, we adopt the approach of Asker, Collard-Wexler, and Loecker (2014), calculating a proxy of TFP shocks as the difference in firm-level TFP over time, represented as $\hat{a}_{it} - \hat{a}_{it-1}$. In line with the methodology of David and Venkateswaran (2019), we use the model-implied TFP in our specification: $\hat{a}_{it} = \log(P_{it}Y_{it}) - \alpha \log K_{it}$.

42. This approximation would be exact if (all components of) productivity were to follow a random walk pattern.

43. TFP can alternatively be derived as the conventional Solow residuals including labor. However, as noted in David and Venkateswaran (2019), footnote 22, TFP calculated from the Solow residual approach can no longer be directly tied to capital profitability in the presence of labor distortions, while the model-based measure of TFP remains a valid proxy for capital profitability.

where $\boldsymbol{f}(T_{r,t})$ is a polynomial of annual average temperature. $\eta_{s,r}$ and $\delta_{c(r),t}$ denote region-sector and country-year fixed effects, respectively. We include region-sector-year observations with at least 15 recurrent firms in the estimation.[44] The estimation results are reported in Table 2, columns (1)-(3).

Table 2: TFP Volatility and Temperature Levels

	(1) 1st Order	(2) 2nd Order	(3) 3rd Order	(4) Model-Induced
$T_{r,t}$	-0.005319	-0.023121***	-0.012380	
	(0.004573)	(0.007536)	(0.008537)	
$T^2_{r,t}$		0.000841***	-0.000447	
		(0.000303)	(0.000679)	
$T^3_{r,t}$			0.000040**	
			(0.000018)	
$(T^2_{r,t} + T^2_{r,t-1})$				-0.021556***
				(0.005682)
$(T_{r,t} + T_{r,t-1})$				0.000882***
				(0.000216)
$(\Delta T_{r,t})^2$				-0.003604
				(0.002233)
Estimated T^*		13.75 °C	14.64°C	12.22°C
		(3.067678)	(2.173182)	(2.216646)
Region-Sector FE	Yes	Yes	Yes	Yes
Country-Year FE	Yes	Yes	Yes	Yes
Observations	113,765	113,765	113,765	113,765
R^2	0.754	0.754	0.754	0.754

Notes: Standard errors in parentheses. We cluster standard errors at the regional level (NUTS3 level for European countries, prefecture-level for China, and district-level administrative divisions for India).
* $p < 0.10$, ** $p < 0.05$, *** $p < 0.01$

Column (1) reports the estimate of the linear effects of temperature, which is negative but not statistically significant. However, including second- and third-order terms reveals a remarkable nonlinear U-shaped pattern, aligning with our theoretical model. Column (2) shows that the quadratic temperature term is statistically significant and economically meaningful: a 1 °C increase in the annual average temperature in a location with an average of 5°C will lead to a decrease of 2.9 log points in TFP volatility; however, the same 1 °C increase in a place with an average temperature of 20°C will increase the TFP volatility by 2.5 log points. These effects are quantitatively large, especially in the context of global warming projections.[45] The cubic specification in column (3) indicates some asymmetry of the effect around the critical point T^*. Loosely speaking, the same 1°C increase brings more damage in hotter climates than benefits

44. This is to reduce measurement errors from the observations that aggregate statistics with only a few numbers of firms. The measured TFP volatility is winsorized at the top 1 percent level to avoid outliers.

45. To illustrate, let us consider a simple back-of-the-envelope calculation using parameters from our model. Take, for example, a permanent increase from 16 °C to 20 °C, which aligns with an RCP 8.5 climate scenario projected for Southern Spain (*World Bank Climate Change Knowledge Portal* 2023). According to our model's damage uncertainty mechanism, this 4 °C increase would increase TFP Volatility by 4.24 log points. This increment translates into a 12.31 log points increase in MRPK dispersion using Equation 29. Subsequently, under standard elasticity assumptions, this dispersion translates into a 7.6% loss in TFP.

in cooler climates. The U-shaped temperature-volatility relationships from both specifications are plotted in Figure 8.

Figure 8: TFP Volatility and Annual Average Temperature

(a) Second Order Estimation (b) Third Order Estimation

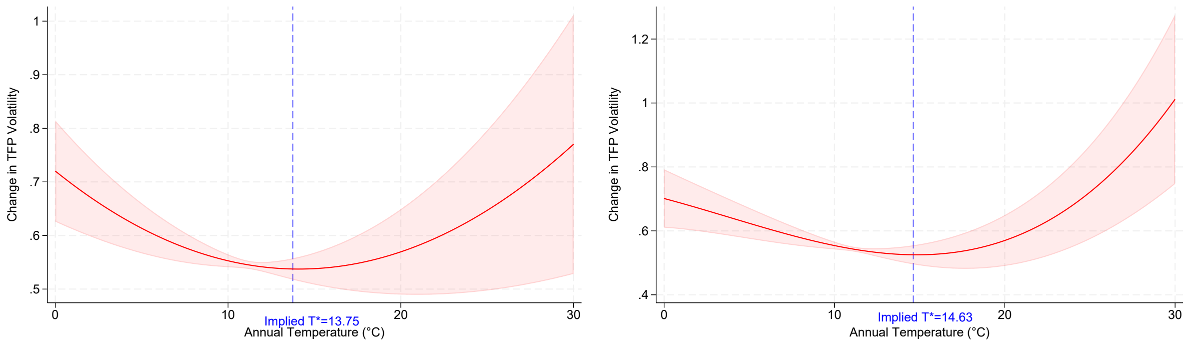

Notes: Graph plots the effects of temperature shocks on TFP volatility, based on a 3-rd order polynomial estimation derived from Equation 32.

Interpreting these estimates through our model, a positive temperature shock in a colder environment will move the economy closer to the optimal temperature T^*, reducing the harmful dispersion of extreme events caused by idiosyncratic temperature sensitivity $\hat{\xi}_{it}$. In contrast, the same positive shock in a hotter climate drives the economy further away from T^*, increasing the damage volatility. This temperature-volatility relationship, as depicted in our reduced-form estimate in Figure 8, also clarifies why the same hot temperature shock in cooler climates leads to a decrease in MRPK dispersion while producing an opposite effect in hotter climates as estimated in Equation 16 and depicted in Figure 3. Next, we will identify T^*.

Identifying the Optimal Temperature T^*. Although easily interpretable, the reduced-form model does not account for how the lagged temperatures might affect the lagged TFP $\hat{a}_{it-1}$. To address this issue, we derive the exact expression for the "first-differenced" volatility:

$$\mathrm{Var}_t(\hat{a}_{it} - \hat{a}_{it-1}) = \sigma^2_{\hat{\xi}}(T_t^2 + T_{t-1}^2) - 2\sigma^2_{\hat{\xi}}T^*(T_t + T_{t-1}) + 2\sigma^2_{\hat{\xi}}T^{*2} + \sigma^2_{\hat{\beta}}(\Delta T_t)^2 + \sigma^2_{\Delta z},$$

and estimate the model-induced specification:

$$\mathrm{Var}_{(s,r),t}(\hat{a}_{it} - \hat{a}_{it-1}) = \alpha + \beta_1(T^2_{r,t} + T^2_{r,t-1}) + \beta_2(T_{r,t} + T_{r,t-1}) + \gamma(\Delta T_{r,t})^2 + \eta_{s,r} + \delta_{c(r),t} + \varepsilon_{s,r,t}, \quad (33)$$

where $\Delta T_{r,t}$ is the first-differenced temperature. The estimates from the model-induced regression are reported in Table 2 column 4 are very close to those obtained from the quadratic specification in column 2. By applying the Delta Method to the estimated coefficients, we can back out the estimate for the optimal temperature $\hat{T}^* = -\frac{\hat{\beta}_2}{2\hat{\beta}_1} = 12.22$°C (SE: 2.21°C). The reduced-form specifications yield $\hat{T}^* = 13.75$°C and $\hat{T}^* = 14.64$°C for the quadratic and cubic specifications, respectively. These estimates align closely with those found by Burke, Hsiang, and Miguel (2015) (and recently Nath, Ramey, and Klenow (2023)), who also estimated that country-level productivity or GDP peaks at the "bliss point" 13°C. Our findings corroborate these findings by suggesting an additional mechanism: the level of temperature contributes to aggregate MRPK dispersion and TFP (output) loss as a volatility shock.

7.2 Forecast Error Effect: Temperature Forecast Errors and Misallocation

The forecast error effect ties misallocation with forecast errors of temperature and climate uncertainty. In our model, even when all the firms face the same temperature forecast as common information, firms' knowledge of their firm-specific sensitivity $\hat{\beta}_i$ would lead them to make differential investment decisions. Thus, any unexpected temperature shock, either cold or hot, would lead to dispersion in capital return. This is summarized as the climate uncertainty channel in Equation 29 as MRPK dispersion increases in the squared forecast error of temperature.

We opt to utilize data directly from the long-range temperature forecasts from ECMWF (Copernicus Climate Change Service and Climate Data Store 2018), instead of relying on proxies or basic statistical models to estimate forecast errors for the company's weather predictions. Extensive research has demonstrated that accurate daily and seasonal temperature and weather forecasts can significantly impact adaptation behaviors (Shrader 2023) and mortality (Shrader, Bakkensen, and Lemoine 2023), as economic agents base their decisions on these signals. Therefore, we also assume that firms actively incorporate month-ahead weather forecasts into their learning processes and adjust investments accordingly.

As data on firm-level MRPK is reported on a yearly frequency while the long-range temperature forecast for a 30-day-ahead period is released every month, we need to create a yearly aggregate measure of squared forecast errors. Let us denote the realized average temperature in the region r at month m and year t as $T_{m,r,t}$ and the month-ahead ECMWF temperature forecast as $\mathbb{E}_{m-1}T_{m,r,t}$. We construct a measure of mean squared forecast errors, $\text{MSFE}_{q,r,t}$, for each time frame q in year t, where we let $q \in \{\text{summer}, \text{winter}, \text{annual}\}$:

$$\begin{aligned}
\text{MSFE}_{\text{summer},r,t} &= \frac{1}{6}\sum_{m=4}^{9}(T_{\text{m},r,t} - \mathbb{E}_{m-1}T_{m,r,t} - \widehat{\text{Bias}}_{m,r})^2, \\
\text{MSFE}_{\text{winter},r,t} &= \frac{1}{6}\sum_{m=\{1,2,3,10,11,12\}}(T_{\text{m},r,t} - \mathbb{E}_{m-1}T_{m,r,t} - \widehat{\text{Bias}}_{m,r})^2, \\
\text{MSFE}_{\text{annual},r,t} &= \frac{1}{12}\sum_{m=1}^{12}(T_{\text{m},r,t} - \mathbb{E}_{m-1}T_{m,r,t} - \widehat{\text{Bias}}_{m,r})^2.
\end{aligned}$$

The reason behind the seasonal aggregation is that the same temperature forecast errors in warm and cold seasons might affect firms' MRPK differently. As all the firms in the sample reside in the Northern Hemisphere, we group all months between April to September as a broadly defined "summer" and the other six months as "winter". We take out the estimated forecast bias, $\widehat{\text{Bias}}_{m,r}$ from forecast error to reduce mechanical differences in temperature measurements due to the positioning of the weather stations and forecasting methods. $\widehat{\text{Bias}}_{m,r}$ is measured as the region-month fixed effect of the monthly forecast error in the past 40 years.

Equation 29 suggests that a larger squared forecast error in a region-sector would lead to more capital misallocation. We directly estimate the empirical version of Equation 29 with the following regression:

$$\sigma^2_{mrpk,(s,r),t} = \boldsymbol{\theta}_q \cdot \text{MSFE}_{q,r,t} + \gamma_1 T_{rt} + \gamma_2 T^2_{rt} + \eta_{s,r} + \delta_{c(r),t} + \varepsilon_{s,r,t}, \tag{34}$$

where $\boldsymbol{\theta}_q$ measures the impact of a one-unit increase in MSFE in the time frame q on annual capital misallocation. We control for the level effect in Equation 29 by adding the linear and quadratic terms of realized annual temperature.

The estimation results are presented in Table 3. Columns (1) and (2) show that the annual MSFE (all-month average) has a positive and statistically significant effect on MRPK dispersion, even after controlling for the level effect of realized temperatures. Columns (2) and (3) display the estimates using "seasonal" MSFEs from both summer and winter. We find that an increase in the MSFE in summer is at least twice as costly as the same increase in winter, suggesting unexpected temperature shocks are more damaging in the warmer season. However, the effect of winter forecast error becomes statistically insignificant when we control for the level of realized temperature.

Table 3: Temperature Forecast Errors and MRPK Dispersion

	(1)	(2)	(3)	(4)
$\text{MSFE}_{\text{annual},r,t}$	0.019114***	0.016249**		
	(0.006675)	(0.006561)		
$\text{MSFE}_{\text{summer},r,t}$			0.014908**	0.016592**
			(0.007115)	(0.007084)
$\text{MSFE}_{\text{winter},r,t}$			0.008536**	0.006096
			(0.004017)	(0.003882)
Quadratic Temperature Control	No	Yes	No	Yes
Region-Sector FE	Yes	Yes	Yes	Yes
Country-Year FE	Yes	Yes	Yes	Yes
Observations	124,065	124,065	124,065	124,065
R^2	0.876	0.876	0.876	0.876

Notes: Standard errors in parentheses. We cluster standard errors at the regional level (NUTS3 level for European countries, prefecture-level for China, and district-levels for India).
$^{*}\ p < 0.10$, $^{**}\ p < 0.05$, $^{***}\ p < 0.01$

The estimates in column (2) can be interpreted in the following way: a 1°C increase in the temperature forecast errors in all months would lead to a 1.6 log point increase in MRPK dispersion, compared to a perfect information counterfactual, equivalent to an approximate 0.58%[46] of annual aggregate TFP loss. Obtained from a small deviation from a perfect information state, this number should be interpreted as a lower bound of the aggregate cost of temperature forecast errors. Moreover, the sample average of $\text{MSFE}_{\text{annual},r,t}$ is 1.39 in our regression, implying the average cost of temperature forecast errors is 0.81% of annual aggregate TFP across India, China, and Europe.

Our findings suggest that temperature forecast errors are costly: unexpected temperature shocks lead to dispersion in investment mistakes among firms due to their varying sensitivity

46. This is obtained by using the calibrated structural parameter, $-\frac{\tilde{\alpha}_K + \tilde{\alpha}_K^2(\sigma-1)}{2} = 0.359$.

to heat. In sum, the value of temperature forecasts is highlighted through a new channel in our context: accurate forecast increases the allocative efficiency of capital.

7.3 Channel Decomposition: Which Effect Has Been More Important in the Past?

After establishing the empirical relevance of the level effect and the forecast error effect in the data, a natural question arises: which channel has contributed more to climate-induced misallocation? To decompose the contribution of the two effects, we run the following model-induced regression directly following Equation 29:

$$\sigma^2_{mrpk,(s,r),t} = \kappa_1 (T_{r,t} - \hat{T}^*)^2 + \kappa_2 \hat{\eta}^{T\,2}_{r,t} + \iota_{s,r} + \iota_{c(r),t} + \varepsilon_{s,r,t}, \tag{35}$$

where $(T_{r,t} - \hat{T}^*)^2$ is computed as the squared deviation of annual temperature from the estimated optimal temperature from Equation 32 ($\hat{T}^* = 12.22°\text{C}$). $\hat{\eta}^{T\,2}_{r,t}$, representing the squared unexpected temperature shocks in the model, is proxied by the annual mean squared forecast error, $\text{MSFE}_{\text{annual},r,t}$ in the data, or by the estimated shock from a climate-specific AR(10) process following the approach in Nath, Ramey, and Klenow (2023). We include region-sector fixed effect, $\iota_{s,r}$, and country-year fixed effect, $\iota_{c(r),s}$ in the regression. The coefficients κ_1 and κ_2 are closely connected to objects in the model. Through the lens of Equation 29, we see that the coefficient $\kappa_1 \approx \mathbb{E}\left[\left(\frac{1}{1-\alpha_N}\right)^2 \sigma^2_{\hat{\xi},(s,r)}\right]$ governs the strength of level effect and reflects the average uncertainty of damage sensitivity across all region-sector pairs. Similarly, $\kappa_2 \approx \mathbb{E}\left[\left(\frac{1}{1-\alpha_N}\right)^2 \sigma^2_{\hat{\beta},(s,r)}\right]$ governs the forecast error effect and reflects the average degree of dispersion in persistent temperature sensitivity.

The estimated coefficients of Equation 35 are presented in Table 4. Under our standard calibration of parameters,[47] we have $\left(\frac{1}{1-\alpha_N}\right)^2 = 1.95$. For the level effect, we estimate $\hat{\kappa}_1$ to be around 0.046 (see column (1)), indicating an average degree of damage uncertainty of $\mathbb{E}[\sigma^2_{\xi,(s,r)}] \approx 0.0023$. For the forecast error effect, we find $\hat{\kappa}_2$ to be around 0.016 to 0.030 in columns (2) and (3), suggesting an average dispersion of persistent climate sensitivity $\sigma^2_{\hat{\beta}}$ to be around 0.008 and 0.015.

With these estimates, we examine which of the two effects could be more prominent across the observed realizations in an average region sector in China, India, and European countries. We compute the average contribution of the two channels to MRPK dispersion and implied TFP loss using the estimated results of our baseline specification and the unweighted average

47. Recall we use a labor share of $\tilde{\alpha}_N = 0.65$ and $\sigma_n = 4$, both of which are standard values in the literature.

Table 4: Model-induced Regressions: Level Effects and Forecast Error Effects

	(1)	(2)
$(T_{r,t} - \hat{T}^{*})^2$	0.004663***	0.004621***
	(0.000868)	(0.000865)
AR(10) Residuals $(\hat{\eta}^T_{r,t})^2$	0.030096**	
	(0.013394)	
Annual MSFE $(\hat{\eta}^T_{r,t})^2$		0.016204**
		(0.006593)
Region-Sector FE	Yes	Yes
Country-Year FE	Yes	Yes
Observations	124,065	124,065
R^2	0.876	0.876

Notes: Standard errors in parentheses. We cluster standard errors at the region level (NUTS 3 level for European countries, province level for China, and first-level administrative divisions for India). * $p < 0.10$, ** $p < 0.05$, *** $p < 0.01$

of climate variables in our regression sample:

$$\Delta\sigma^2_{mrpk,(s,r),t} = \underbrace{\underbrace{\left(\frac{1}{1-\alpha_N}\right)^2 \hat{\sigma}^2_{\hat{\xi},(s,r)} \overline{(T_{r,t} - T^{*})^2}}_{0.0047\times 17.96}}_{\text{Level Effect}=0.084} + \underbrace{\underbrace{\left(\frac{1}{1-\alpha_N}\right)^2 \hat{\sigma}^2_{\hat{\beta},(s,r)} \overline{\eta^{T\,2}_{r,t}}}_{0.016\times 1.39}}_{\text{Forecast Error Effect}=0.023},$$

$$\begin{aligned}
\Delta \log TFP_{(s,r),t} &= -\underbrace{\frac{\tilde{\alpha}_K + \tilde{\alpha}_K^2(\sigma-1)}{2}}_{0.359} \Delta\sigma^2_{mrpk,(s,r),t} \\
&= -\underbrace{\frac{\tilde{\alpha}_K + \tilde{\alpha}_K^2(\sigma-1)}{2} \frac{\hat{\sigma}^2_{\hat{\xi},(s,r)}}{(1-\alpha_N)^2} \overline{(T_{r,t} - T^{*})^2}}_{\substack{\text{Level Effect} \\ =3.00\%}} \\
&\quad -\underbrace{\frac{\tilde{\alpha}_K + \tilde{\alpha}_K^2(\sigma-1)}{2} \frac{\hat{\sigma}^2_{\hat{\beta},(s,r)}}{(1-\alpha_N)^2} \overline{\eta^{T\,2}_{r,t}}}_{\substack{\text{Forecast Error Effect} \\ =0.81\%}} \\
&= 3.81\%
\end{aligned}$$

Through these back-of-envelope calculations, we find that, on average, the level effect of temperature contributes to 8.4 log points of MRPK dispersion, equivalent to a TFP loss of 3%. On the other hand, the contribution of the forecast error effect (proxied by annual MSFE) to MRPK dispersion is around 0.023 log points, implying a TFP loss of 0.81%. Notice that, in our sample from 1998 to 2018, the contribution of the level effect is almost three times as large as the contribution of the forecast error effect. Looking ahead, these estimates suggest that the level effect of increasing global warming would play a more significant role by creating greater damage volatility in productivity losses from temperature among firms, consistent with our reduced-form projections in Section 4.4.

8 Policies to Manage Climate-Induced Misallocation

Our results shed new light on the design and effect of climate mitigation and adaptation policies. We discuss three types of policies that could potentially reduce the cost of climate-induced misallocation: (1) reducing end-of-century temperature rise from 4°C to 2°C ; (2) improving mid-range weather forecast accuracy; and (3) reducing climate sensitivity heterogeneity across firms.

8.1 Mitigating Global Warming: RCP 7.0 vs. RCP 2.6

The most important policy to mitigate the cost of the misallocation channel is to address climate change itself. To illustrate this, we compare the projected misallocation losses between a stringent policy scenario (RCP 2.6) and a business-as-usual scenario (RCP 7.0). RCP 7.0 represents a baseline outcome with limited additional climate policies in place, resulting in a projected 4°C global warming by 2100. In contrast, the RCP 2.6 pathway aligns with the Paris Agreement goals and aims to limit global warming below 2°C.

Figure 9: Cost and Benefit Comparison

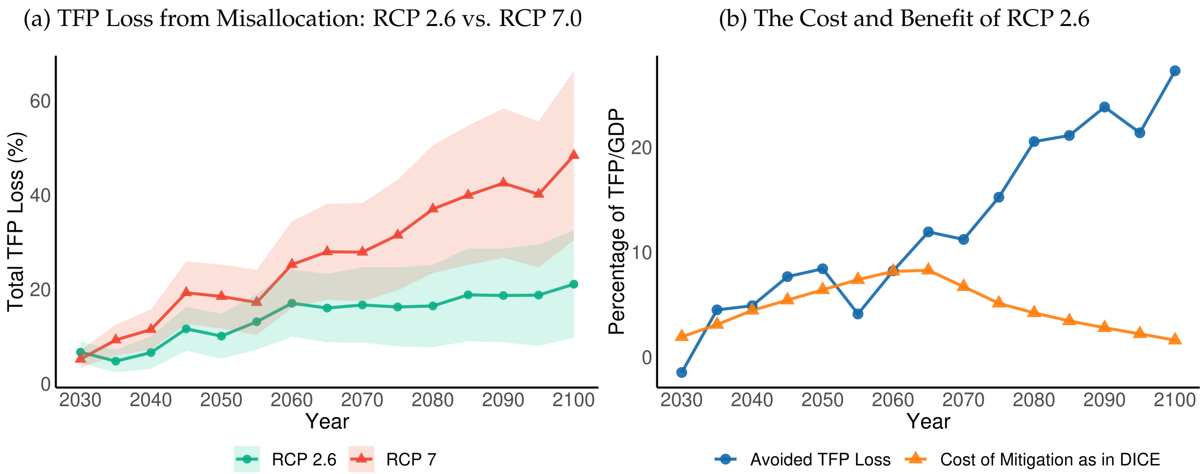

Notes: In Figure 9a, the climate projection data is collected from CMIP6, and the income projection data is from the SSP database. In Figure 9b, the blue line with dot markers represents the difference in TFP losses between the RCP 2.6 and RCP 7.0 scenarios, referred to as the avoided TFP loss or benefit. This is the difference between the two lines in Figure 9a. The orange line with triangle markers shows the estimated cost of mitigation, calculated using the results from DICE-2016R, defined as the percentage difference in post-abatement potential output between the optimal policy scenario to achieve less than 2°C warming (consistent with RCP 2.6) and the baseline scenario with 4°C warming (consistent with RCP 7.0)

Our objective is to compare TFP losses between these two scenarios to assess the effectiveness of mitigation policies in avoiding misallocation losses. Using the approach developed in Section 4.4, we compute the projected TFP losses from the misallocation channel for the two scenarios, as shown in Figure 9a. By the end of the century, TFP losses are projected to be approximately 21% under RCP 2.6, compared to 43% under RCP 7.0. This suggests that a global TFP loss of 22% can be avoided by achieving the Paris Agreement goals.

Using existing estimates from the DICE-2016R model (Nordhaus 2017), we also calculate the potential costs of switching from RCP 7.0 to RCP 2.6 and compare them to our projected benefits. We define the cost of mitigation as the percentage difference in post-abatement potential output between the optimal policy scenario to achieve less than 2°C warming (consistent with RCP 2.6) and the baseline scenario with 4°C warming (consistent with RCP 7.0). Figure 9b shows that the estimated GDP cost of mitigation is moderate; it initially increases over time, peaks at 8% around 2065, and then decreases to less than 2% by 2100. More importantly, while the annual costs closely track the annual benefits from avoided misallocation loss by 2060, the benefits significantly outweigh the policy costs afterward, amounting to a 20% lead by 2100. Therefore, we argue that mitigation policy is extremely beneficial to avoid losses from climate-induced misallocation. Additionally, regardless of the choice of the discount factor, the cost of such a policy is always justified by the large estimated benefits.

8.2 Improving Mid-range Weather Forecast Accuracy

Our model indicates that lowering mid-range weather forecast errors (a reduction in σ_η^2) would reduce capital misallocation. Therefore, we explore how forecast accuracy improvements by the end of the century could serve as an important adaptation channel, and to improve investment efficiency in the aggregate economy and to raise aggregate productivity.

Predicting future forecast accuracy is not an easy task. To make credible inferences, we leverage two key forces identified by Alley, Emanuel, and Zhang (2019) and Linsenmeier and Shrader (2023): the decline in forecasting errors associated with technological progress over time, and the prevalence of this decline in regions with better economic development. We thus estimate the following regression, with the annual MSFE as our measure of weather forecast accuracy:

$$\ln \text{MSFE}_{\text{annual},r,t} = \iota_0 + \iota_1 \ln \text{GDP}_{pc,rt} + \iota_2 t + \iota_3 t^2 + (\iota_4 t + \iota_5 t^2) \times \ln \text{GDP}_{pc,rt} + \gamma_r + \varepsilon_{rt} \quad (36)$$

where γ_r is a region fixed effect. We use the regional per-capita GDP as a proxy for economic development and a quadratic time trend to capture technological progress. We also include interaction terms of the quadratic time trend and $\ln \text{GDP}_{pc,rt}$ to account for the potentially different rates of improvement in regions with varying income levels. Given the non-negativity constraint on MSFE, we estimate Equation 36 using Poisson Pseudo Maximum Likelihood (PPML). Using the estimates, we can predict the end-of-century forecast error, $\widehat{\text{MSFE}_{\text{annual},r,EOC}}$, for each region.[48] Notice that our prediction implicitly assumes that poorer regions will gradually invest more in climate information services as they become richer.

We further leverage the estimated structural elasticity $\hat{\kappa}_2 = 0.016$ in Table 4 to translate the change in forecast accuracy into an aggregate TFP gain in China, India, and Europe. Our

48. Specifically, we predict the end-of-century MSFE as:

$$\begin{aligned}\widehat{\text{MSFE}_{\text{annual},r,EOC}} &= \exp[\Delta \ln(\widehat{\text{MSFE}_{\text{annual},r,EOC}}) + \ln \text{MSFE}_{\text{annual},r,2019}] \\ &= \exp[\hat{\iota}_1 \Delta \ln \text{GDP}_{pc,r} + \hat{\iota}_2 \Delta t + \hat{\iota}_3 \Delta t^2 + \hat{\iota}_4 \Delta(t \times \ln \text{GDP}_{pc,r}) \\ &\quad + \hat{\iota}_5 \Delta(t^2 \times \ln \text{GDP}_{pc,r}) + \ln \text{MSFE}_{\text{annual},r,2019}]\end{aligned}$$

projection implies a sizable average MSFE reduction (weighted by projected GDP share β_r) of 0.7 in the sample, which translates into an aggregate TFP gain of 0.41% according to the formula:

$$
\begin{aligned}
\Delta \log \text{TFP} &= -\sum_r \beta_r \frac{\tilde{\alpha}_K + \tilde{\alpha}_K^2(\sigma-1)}{2} \Delta\sigma^2_{mrpk,r} \\
&= -\underbrace{\frac{\tilde{\alpha}_K + \tilde{\alpha}_K^2(\sigma-1)}{2}}_{0.359} \underbrace{\hat{\kappa}_2}_{0.016} \underbrace{\sum_r \beta_r (\widehat{\text{MSFE}_{\text{annual},r,EOC}} - \text{MSFE}_{\text{annual},r,2019})}_{\substack{\text{Average Forecast Error Reduction} \\ =-0.7}} \\
&= 0.41\%.
\end{aligned}
$$

Our results suggest that continuously improving mid-range weather forecast accuracy is an essential aspect of adaptation. The 0.41% gain in TFP (or GDP) could arguably make forecast-related adaptation investments a cost-effective approach, as these investments are usually well below that scale (currently below 0.15% of GDP). However, our calculations also show that adaptation investment is not a substitute for mitigation policy.

8.3 Reducing "Climate Inequality" Across Firms

The differential response of MRPK to shocks stems from the heterogeneity in temperature sensitivity ($\sigma^2_{\hat{beta}}$ and $\sigma^2_{\hat{\xi}}$) across firms. We also point out that this "climate inequality" among firms could result from various factors, including size-related distortions and adaptability. Therefore, policies should be targeted to identify and subsidize firms that are productive but lack the resources to defend against heat. These policies could include targeted subsidies or credit policies for air conditioning installations and other risk control practices. By harmonizing climate sensitivity among firms, the MRPK dispersion will be less responsive to heat shocks or a warming climate.

Interestingly, our results also highlight that there need not be an equity-efficiency trade-off in the context of heterogeneous firms. If more firms become more "equal" in their sensitivity to temperature, the aggregate efficiency in the economy will also increase. We will leave quantitative explorations of optimal firm-level policies for future research.

9 Conclusion

This paper provides the first causal estimates of the misallocation effect from temperature shocks using firm-level microdata from 32 countries. On average, an additional hot day with $>$ 30°C of temperature increases MRPK dispersion by 0.31 log points and contributes to a 0.11% decline in annual aggregate TFP. Intriguingly, the detrimental impact of extreme heat on capital misallocation is more severe in regions with hotter climates and higher incomes, highlighting a significant market cost of climate change coupled with a limited capacity for adaptation. Using projected temperature and income data, we find that global warming, under the SSP3-4.5 scenario, could lead to an aggregate TFP loss of 35.4%. By writing down a firm dynamics model with heterogeneous temperature sensitivity, climate uncertainty, and damage volatility, we use model-implied regressions to explain the differential effects among regions: regions with higher deviations from the optimal temperature, (around 13°C) and lower temperature forecast accuracy will have larger unexpected volatility in firm-level TFP and investment mistakes. Overall, our results imply that firm-level heterogeneity matters for analyzing the aggregate effect of climate change. This paper suggests an important venue for research in understanding the impact of climate change in a distorted economy.

We conclude with a final suggestion for future research. First, the identified misallocation effect is highly heterogeneous across different geographical locations, implying a different level of TFP losses across regions and sectors globally. This will lead to shifts in comparative advantage and endogenous variations in trade patterns with deteriorating climate conditions caused by global warming. Moreover, as we only focus on the misallocation effect within a region sector as a lower-bound estimate of the climate-induced misallocation, one could also study the misallocation that arises between sectors, regions, and even countries. On the empirical side, it would be important to understand whether demand-side or supply-side factors function as the main drivers of climate-induced misallocation. We leave these questions for future research.

References

Acharya, Viral V, Abhishek Bhardwaj, and Tuomas Tomunen. 2023. *Do Firms Mitigate Climate Impact on Employment? Evidence from US Heat Shocks.* Working Paper, Working Paper Series 31967. National Bureau of Economic Research.

Allcott, Hunt, Allan Collard-Wexler, and Stephen D O'Connell. 2016. "How do electricity shortages affect industry? Evidence from India." *American Economic Review.*

Alley, Richard B, Kerry A Emanuel, and Fuqing Zhang. 2019. "Advances in weather prediction." *Science* 363 (6425): 342–344.

Alves, Felipe, Greg Kaplan, Benjamin Moll, and Giovanni L. Violante. 2020. "A Further Look at the Propagation of Monetary Policy Shocks in HANK." *Journal of Money, Credit and Banking* 52 (S2): 521–559.

Asker, John, Allan Collard-Wexler, and Jan De Loecker. 2014. "Dynamic Inputs and Resource (Mis)Allocation." *Journal of Political Economy* 122 (5): 1013–1063.

Bakkensen, Laura A, and Lint Barrage. 2021. "Going Underwater? Flood Risk Belief Heterogeneity and Coastal Home Price Dynamics." *The Review of Financial Studies* 35 (8): 3666–3709.

Baqaee, David Rezza, and Emmanuel Farhi. 2019. "The Macroeconomic Impact of Microeconomic Shocks: Beyond Hulten's Theorem." *Econometrica* 87 (4): 1155–1203.

Barrage, Lint, and William D Nordhaus. 2023. *Policies, Projections, and the Social Cost of Carbon: Results from the DICE-2023 Model.* Working Paper, Working Paper Series 31112. National Bureau of Economic Research.

Basu, Susanto, and John G. Fernald. 2002. "Aggregate productivity and aggregate technology." *European Economic Review* 46 (6): 963–991.

Bau, Natalie, and Adrien Matray. 2023. "Misallocation and Capital Market Integration: Evidence From India." *Econometrica* 91 (1): 67–106.

Bilal, Adrien, and Diego R Känzig. 2024. *The Macroeconomic Impact of Climate Change: Global vs. Local Temperature.* Technical report. National Bureau of Economic Research.

Bilal, Adrien, and Esteban Rossi-Hansberg. 2023. *Anticipating Climate Change Across the United States.* Technical report. National Bureau of Economic Research.

Bils, Mark, Peter J. Klenow, and Cian Ruane. 2021. "Misallocation or Mismeasurement?" *Journal of Monetary Economics* 124:S39–S56.

Blanchard, Olivier, and Jordi Galí. 2010. "Labor Markets and Monetary Policy: A New Keynesian Model with Unemployment." *American Economic Journal: Macroeconomics* 2, no. 2 (April): 1–30.

Bloom, Nicholas. 2009. "The impact of uncertainty shocks." *econometrica* 77 (3): 623–685.

Brandt, Loren, Johannes Van Biesebroeck, and Yifan Zhang. 2014. "Challenges of working with the Chinese NBS firm-level data." *China Economic Review.*

Burke, Marshall, Solomon M. Hsiang, and Edward Miguel. 2015. "Global non-linear effect of temperature on economic production." *Nature* 527 (7577): 235–239.

Caggese, Andrea, Andrea Chiavari, Sampreet Goraya, and Carolina Villegas-Sanchez. 2023. "Climate Change, Firms, and the Aggregate Productivity." Working Paper.

Carleton, Tamma, Amir Jina, Michael Delgado, Michael Greenstone, Trevor Houser, Solomon Hsiang, Andrew Hultgren, et al. 2022. "Valuing the Global Mortality Consequences of Climate Change Accounting for Adaptation Costs and Benefits." *The Quarterly Journal of Economics* 137 (4): 2037–2105.

Carrillo, Paul, Dave Donaldson, Dina Pomeranz, and Monica Singhal. 2023. *Misallocation in Firm Production: A Nonparametric Analysis Using Procurement Lotteries.* Working Paper, Working Paper Series 31311. National Bureau of Economic Research.

Casey, Gregory, Stephie Fried, and Matthew Gibson. 2022. "Understanding Climate Damages: Consumption versus Investment." Federal Reserve Bank of San Francisco Working Paper 2022-21.

Chen, Zhang. 2022. "Economic Growth and the Rise of Large Firms."

Christidis, Nikolaos, Dann Mitchell, and Peter A. Stott. 2023. "Rapidly increasing likelihood of exceeding 50°C in parts of the Mediterranean and the Middle East due to human influence." *npj Climate and Atmospheric Science* 6, no. 1 (May 26, 2023): 45.

Copernicus Climate Change Service. 2021. *CMIP6 climate projections.* Copernicus Climate Change Service (C3S) Climate Data Store (CDS).

Copernicus Climate Change Service and Climate Data Store. 2018. *Seasonal forecast daily and subdaily data on single levels.*

Cruz, José-Luis, and Esteban Rossi-Hansberg. 2023. *The Economic Geography of Global Warming.*

David, Joel M., and Venky Venkateswaran. 2019. "The Sources of Capital Misallocation." *American Economic Review* 109 (7): 2531–67.

David, Joel M., and David Zeke. 2021. *Risk-Taking, Capital Allocation and Optimal Monetary Policy.* Federal Reserve Bank of Chicago.

Dell, Melissa, Benjamin F Jones, and Benjamin A Olken. 2012. "Temperature Shocks and Economic Growth: Evidence from the Last Half Century." *American Economic Journal: Macroeconomics* 4 (3): 66–95.

Dellink, Rob, Jean Chateau, Elisa Lanzi, and Bertrand Magné. 2017. "Long-term economic growth projections in the Shared Socioeconomic Pathways." *Global Environmental Change.*

Deschênes, Olivier, and Michael Greenstone. 2011. "Climate Change, Mortality, and Adaptation: Evidence from Annual Fluctuations in Weather in the US." *American Economic Journal: Applied Economics* 3 (4): 152–185.

Dundas, Steven J., and Roger H. von Haefen. 2020. "The Effects of Weather on Recreational Fishing Demand and Adaptation: Implications for a Changing Climate." *Journal of the Association of Environmental and Resource Economists* 7 (2): 209–242.

Fan, Jingting. 2024. "Talent, Geography, and Offshore R
amp;D." *The Review of Economic Studies* (April): rdae044. ISSN: 0034-6527.

Flynn, Joel P., and Karthik Sastry. 2023. *Attention Cycles.*

Gopinath, Gita, Sebnem Kalemli-Ozcan, Loukas Karabarbounis, and Carolina Villegas-Sanchez. 2017. "Capital Allocation and Productivity in South Europe." *Quarterly Journal of Economics* 132 (4).

Gorodnichenko, Yuriy, Debora Revoltella, Jan Svejnar, and Christoph T Weiss. 2018. *Resource misallocation in European firms: The role of constraints, firm characteristics and managerial decisions.* Technical report. National Bureau of Economic Research.

Hsiang, Solomon M, and Amir S Jina. 2015. "Geography, depreciation, and growth." *American Economic Review.*

Hsieh, Chang-Tai, and Peter J. Klenow. 2009. "Misallocation and Manufacturing TFP in China and India." *Quarterly Journal of Economics* 124 (4): 1403–1448.

Kala, Namrata. 2017. "Learning, adaptation, and climate uncertainty: Evidence from Indian agriculture." *MIT Center for energy and environmental policy research working paper* 23.

Kalemli- Özcan, Şebnem, Bent E. Sørensen, Carolina Villegas-Sanchez, Vadym Volosovych, and Sevcan Yeşiltaş. 2024. "How to Construct Nationally Representative Firm-Level Data from the Orbis Global Database: New Facts on SMEs and Aggregate Implications for Industry Concentration." *American Economic Journal: Macroeconomics* 16, no. 2 (April): 353–74.

Krusell, Per, and Anthony A. Smith Jr. 1998. "Income and Wealth Heterogeneity in the Macroeconomy." *Journal of Political Economy* 106 (5): 867–896.

Lemoine, Derek. 2018. *Estimating the Consequences of Climate Change from Variation in Weather.* Working Paper, Working Paper Series 25008. National Bureau of Economic Research.

Linsenmeier, Manuel, and Jeffrey Shrader. 2023. "Global inequalities in weather forecasts."

Midrigan, Virgiliu, and Daniel Yi Xu. 2014. "Finance and misallocation: Evidence from plant-level data." *American economic review* 104 (2): 422–458.

Moscona, Jacob, and Karthik A Sastry. 2023. "Does directed innovation mitigate climate damage? evidence from us agriculture." *The Quarterly Journal of Economics* 138 (2): 637–701.

Nath, Ishan. 2023. "Climate Change, The Food Problem, and the Challenge of Adaptation through Sectoral Reallocation."

Nath, Ishan, Valerie Ramey, and Peter Klenow. 2023. "How Much Will Global Warming Cool Global Growth?"

Nordhaus, William D. 2017. "Revisiting the social cost of carbon." *Proceedings of the National Academy of Sciences.*

O'Neill, B. C., C. Tebaldi, D. P. van Vuuren, V. Eyring, P. Friedlingstein, G. Hurtt, R. Knutti, et al. 2016. "The Scenario Model Intercomparison Project (ScenarioMIP) for CMIP6." *Geosci. Model Dev.*

Oudin Åström, Daniel, Bertil Forsberg, Kristie L. Ebi, and Joacim Rocklöv. 2013. "Attributing mortality from extreme temperatures to climate change in Stockholm, Sweden." *Nature Climate Change* 3, no. 12 (December 1, 2013): 1050–1054.

Piao, Shilong, Philippe Ciais, Yao Huang, Zehao Shen, Shushi Peng, Junsheng Li, Liping Zhou, Hongyan Liu, Yuecun Ma, Yihui Ding, et al. 2010. "The impacts of climate change on water resources and agriculture in China." *Nature.*

Ponticelli, Jacopo, Qiping Xu, and Stefan Zeume. 2023. *Temperature and Local Industry Concentration.* Technical report w31533. National Bureau of Economic Research.

Poschke, Markus. 2018. "The Firm Size Distribution across Countries and Skill-Biased Change in Entrepreneurial Technology." *American Economic Journal: Macroeconomics* 10 (3): 1–41.

Restuccia, Diego, and Richard Rogerson. 2008. "Policy distortions and aggregate productivity with heterogeneous establishments." *Review of Economic dynamics* 11 (4): 707–720.

Rudik, I., G. Lyn, W. Tan, and A. Ortiz-Bobea. 2021. *The Economic Effects of Climate Change in Dynamic Spatial Equilibrium.*

Sabater, Joaquin Muñoz. 2019. *ERA5-Land monthly averaged data from 1950 to present.* Copernicus Climate Change Service (C3S) Climate Data Store (CDS).

Schlenker, Wolfram, and Charles A. Taylor. 2021. "Market expectations of a warming climate." *Journal of Financial Economics.*

Shrader, Jeffrey. 2023. "Improving climate damage estimates by accounting for adaptation." *Available at SSRN 3212073.*

Shrader, Jeffrey, Laura Bakkensen, and Derek Lemoine. 2023. "Fatal Errors: The Mortality Value of Accurate Weather Forecasts." National Bureau of Economic Research Working Paper.

Somanathan, E., Rohini Somanathan, Anant Sudarshan, and Meenu Tewari. 2021. "The Impact of Temperature on Productivity and Labor Supply: Evidence from Indian Manufacturing" [in en]. *Journal of Political Economy* 129 (6). Accessed November 27, 2023.

Sraer, David, and David Thesmar. 2023. "How to Use Natural Experiments to Estimate Misallocation." *American Economic Review* 113 (4): 906–38.

Wang, Tingting, and Fubao Sun. 2022. "Global gridded GDP data set consistent with the shared socioeconomic pathways." *Scientific Data.*

Wenz, Leonie, Robert Devon Carr, Noah Kögel, Maximilian Kotz, and Matthias Kalkuhl. 2023. "DOSE – Global data set of reported sub-national economic output." *Scientific Data* 10 (1): 425.

World Bank Climate Change Knowledge Portal. 2023.

Zhang, Peng, Olivier Deschenes, Kyle C Meng, and Junjie Zhang. 2018. "Temperature effects on productivity and factor reallocation: Evidence from a half million Chinese manufacturing plants." *Journal of Environmental Economics and Management* 88:1–17.

Zivin, Joshua Graff, and Matthew Neidell. 2014. "Temperature and the Allocation of Time: Implications for Climate Change." *Journal of Labor Economics* 32 (1): 1–26.

Online Appendix

A Additional Derivations for Section 2

This appendix provides the derivation of the expressions and propositions featured in Section 2.

A.1 Equilibrium Allocations in Distorted Equilibrium

In this appendix, we solve the firm's profit maximization problem in Equation 4 and derive Equation 6.

Subject to the inverse demand and wedges, each firm i in region-sector n engages in monopolistic competition and optimally chooses its quantity of inputs and price to maximize profits

$$\max_{P_{nit},K_{nit},L_{nit}} \left(1-\tau^{Y}_{nit}\right) P_{nit} \underbrace{A_{nit}K_{nit}^{\alpha_{Kn}}L_{nit}^{\alpha_{Ln}}}_{Y_{nit}} - \left(1+\tau^{K}_{nit}\right) R_{nt}K_{nit} - \left(1+\tau^{L}_{nit}\right) W_{nt}L_{nit}$$

$$\text{subject to}: Y_{nit} = B_{nit}Y_{nt}\left[\frac{P_{nit}}{P_{nt}}\right]^{-\sigma_n}.$$

After substituting the demand curve $P_{nit}Y_{nit} = P_{nt}Y_{nt}^{\frac{1}{\sigma_n}} B_{nit}^{\frac{1}{\sigma_n}} Y_{nit}^{\frac{\sigma_n-1}{\sigma_n}}$ into the objective function, we derive the first-order condition with respect to any factor input F_{nit} used (where F_{nit} can be either K_{nit} or L_{nit})

$$MRPF_{nit} = \alpha_{F_n}\frac{\sigma_n-1}{\sigma_n}\frac{P_{nit}Y_{nit}}{F_{nit}} = \frac{1+\tau^{F}_{ni}(\tilde{\mathbf{T}}_{rt},\cdot)}{1-\tau^{Y}_{ni}(\tilde{\mathbf{T}}_{rt},\cdot)}P^{F}_{nt},$$

where P^F_{nt} denotes the factor price, specifically W_{nt} for labor and R_{nt} for capital. $\frac{\sigma_n-1}{\sigma_n}$ is the optimal CES markup. This is Equation 6 in the main text.

Next, we will derive the allocation in the distorted equilibrium. We rewrite the demand curve as

$$P_{nit} = \left(\frac{Y_{nit}}{B_{nit}Y_{nt}}\right)^{-\frac{1}{\sigma_n}} P_{nt} = \left(\frac{\frac{Y_{nit}}{F_{nit}}F_{nit}}{B_{nit}Y_{nt}}\right)^{-\frac{1}{\sigma_n}} P_{nt}. \tag{37}$$

Combining with Equation 6 yields

$$\alpha_{F_n}\frac{\sigma_n-1}{\sigma_n}\left(\frac{\frac{Y_{nit}}{F_{nit}}F_{nit}}{B_{nit}Y_{nt}}\right)^{-\frac{1}{\sigma_n}} P_{nt}\frac{Y_{nit}}{F_{nit}} = \frac{1+\tau^{F}_{ni}(\tilde{\mathbf{T}}_{rt},\cdot)}{1-\tau^{Y}_{ni}(\tilde{\mathbf{T}}_{rt},\cdot)}P^{F}_{nt}.$$

We can rewrite the previous equation as

$$F_{nit} = \alpha_{F_n}^{\sigma_n}\left(\frac{\sigma_n-1}{\sigma_n}\right)^{\sigma_n}\left(\frac{P_{nt}}{P^{F}_{nt}}\right)^{\sigma_n}\frac{(1-\tau^{Y}_{nit})^{\sigma_n}}{(1+\tau^{F}_{nit})^{\sigma_n}}\left(\frac{Y_{nit}}{F_{nit}}\right)^{\sigma_n-1}B_{nit}Y_{nt},$$

and combining with

$$\frac{Y_{nit}}{F_{nit}} = A_{nit}\frac{(1+\tau^F_{nit})}{(1+\tau^K_{nit})^{\alpha_{Kn}}(1+\tau^L_{nit})^{\alpha_{Ln}}}(\frac{\alpha_L}{W_{nt}})^{\alpha_L}(\frac{\alpha_K}{R_{nt}})^{\alpha_K}(\frac{\alpha_F}{P^F_{nt}})^{-1},$$

we can derive an expression for F_{nit} as

$$\begin{aligned} F_{nit} = & \frac{1}{(1+\tau^F_{nit})}\left(\frac{\alpha_{F_n}}{P^F_{nt}}\right)\frac{B_{nit}A_{nit}^{\sigma_n-1}\left(1-\tau^Y_{nit}\right)^{\sigma_n}}{\left(1+\tau^K_{nit}\right)^{\alpha_{Kn}(\sigma_n-1)}\left(1+\tau^L_{nit}\right)^{\alpha_{Ln}(\sigma_n-1)}} \\ & \cdot\left(\frac{\sigma_n-1}{\sigma_n}\right)^{\sigma_n}\left(\frac{\alpha_{Kn}}{R_{nt}}\right)^{\alpha_{Kn}(\sigma_n-1)}\left(\frac{\alpha_{Ln}}{W_{nt}}\right)^{\alpha_{Ln}(\sigma_n-1)}P_{nt}^{\sigma_n}Y_{nt}, \end{aligned} \tag{38}$$

where $F \in \{K, L\}$. Substituting this expression into the production function of firm i for each factor F yields

$$\begin{aligned} Y_{nit} = A_{nit}K_{nit}^{\alpha_{Kn}}L_{nit}^{\alpha_{Ln}} = & \frac{B_{nit}A_{nit}^{\sigma_n}\left(1-\tau^Y_{nit}\right)^{\sigma_n}}{\left(1+\tau^{Kn}_{nit}\right)^{\alpha_{Kn}\sigma_n}\left(1+\tau^{Ln}_{nit}\right)^{\alpha_{Ln}\sigma_n}} \\ & \cdot\left(\frac{\sigma_n-1}{\sigma_n}\right)^{\sigma_n}\left(\frac{\alpha_{Kn}}{R_{nt}}\right)^{\alpha_{Kn}\sigma_n}\left(\frac{\alpha_{Ln}}{W_{nt}}\right)^{\alpha_{Ln}\sigma_n}P_{nt}^{\sigma_n}Y_{nt} \end{aligned} \tag{39}$$

Similarly, we can write the sales of firm i as

$$\begin{aligned} P_{it}Y_{it} &= P_{nt}Y_{nt}^{\frac{1}{\sigma_n}}B_{nit}^{\frac{1}{\sigma_n}}Y_{nit}^{\frac{\sigma_n-1}{\sigma_n}} \\ &= P_{nt}^{\sigma_n}Y_{nt}\frac{B_{nit}A_{nit}^{(\sigma_n-1)}\left(1-\tau^Y_{nit}\right)^{(\sigma_n-1)}}{\left(1+\tau^{Kn}_{nit}\right)^{\alpha_{Kn}(\sigma_n-1)}\left(1+\tau^{Ln}_{nit}\right)^{\alpha_{Ln}(\sigma_n-1)}} \\ &\cdot\left(\frac{\sigma_n-1}{\sigma_n}\right)^{(\sigma_n-1)}\left(\frac{\alpha_{Kn}}{R_{nt}}\right)^{\alpha_{Kn}(\sigma_n-1)}\left(\frac{\alpha_{Ln}}{W_{nt}}\right)^{\alpha_{Ln}(\sigma_n-1)}. \end{aligned} \tag{40}$$

Then the sales share of firm i in region-sector n, θ_{nit}, can be expressed in closed form of the fundamentals as:

$$\theta_{nit} = \frac{P_{nit}Y_{nit}}{\int_0^{J_n}P_{nit}Y_{nit}di} = \frac{\frac{B_{nit}A_{nit}^{(\sigma_n-1)}(1-\tau^Y_{nit})^{(\sigma_n-1)}}{(1+\tau^{Kn}_{nit})^{\alpha_{Kn}(\sigma_n-1)}(1+\tau^{Ln}_{nit})^{\alpha_{Ln}(\sigma_n-1)}}}{\int_0^{J_n}\frac{B_{nit}A_{nit}^{(\sigma_n-1)}(1-\tau^Y_{nit})^{(\sigma_n-1)}}{(1+\tau^{Kn}_{nit})^{\alpha_{Kn}(\sigma_n-1)}(1+\tau^{Ln}_{nit})^{\alpha_{Ln}(\sigma_n-1)}}di} \tag{41}$$

Finally, by combining 38 and 41, we derive the equilibrium allocation of factors in the distorted economy as

$$F_{nit} = \frac{F_{nit}}{F_{nt}}F_{nt} = \frac{\frac{1}{1+\tau^F_{nit}}\theta_{nit}}{\int_0^{J_n}\frac{1}{1+\tau^F_{nit}}\theta_{nit}di}F_{nt} = \frac{1+\tau^F_{nt}}{1+\tau^F_{nit}}\theta_{nit}F_{nt}, \tag{42}$$

where $1+\tau^F_{nt} := \left(\int_0^{J_n}\frac{1}{(1+\tau^F_{nit})}\theta_{nit}di\right)^{-1}$ is a measure of aggregate factor distortion. Mathematically, it is a sales-weighted harmonic mean of all firm-level distortions of input F. Equation 42 states that a firm would use more of input F if it faces smaller distortion than the region-sector aggregate distortion. Moreover, a firm with a larger equilibrium sales share, θ_{it}, is, loosely speaking, more productive and less distorted in production, and will thus use more inputs.

A.2 Proof of Proposition 1

Proposition 1. Equilibrium (Mis)Allocation. The distorted equilibrium allocation of capital, labor, and material inputs must satisfy that for any factor $F \in \{K, L\}$,

$$\begin{aligned}\log(\frac{F_{nit}}{F^*_{nit}}) = &- \log(1+\tau^F_{nit}(\tilde{\mathbf{T}}_{rt},\cdot)) \\ &+ \sigma_n \log(1-\tau^Y_{nit}(\tilde{\mathbf{T}}_{rt},\cdot)) - (\sigma_n - 1)\sum_{F'=\{K,L\}} \alpha_{F'_n} \log(1+\tau^{F'}_{ni}(\tilde{\mathbf{T}}_{rt},\cdot)) \\ &+ \log(C_{Fnt}(\tilde{\mathbf{T}}_{rt},\cdot)),\end{aligned} \tag{43}$$

where C_{Fnt} is a region-sector-year specific constant and F^*_{nit} is the efficient equilibrium allocation of factors that are entirely determined by preference shifter and physical productivity within the region-sector:

$$F^*_{nit} = \frac{B_{ni}(\tilde{\mathbf{T}}_{rt},\cdot)A_{ni}(\tilde{\mathbf{T}}_{rt},\cdot)^{\sigma_n-1}}{\int_0^{J_n} B_{nj}(\tilde{\mathbf{T}}_{rt},\cdot)A_{nj}(\tilde{\mathbf{T}}_{rt},\cdot)^{\sigma_n-1}dj} F_{nt} \tag{44}$$

Proof. Substituting the expression of θ_{it} from 41 into 42 yields an explicit expression of $\frac{F_{nit}}{F_{nt}}$ in terms of micro fundamentals

$$\begin{aligned}\frac{F_{nit}}{F_{nt}} = \frac{\frac{1}{1+\tau^F_{nit}}\theta_{nit}}{\int_0^{J_n}\frac{1}{1+\tau^F_{nit}}\theta_{nit}di} = &\frac{B_{nit}A_{nit}^{\sigma_n-1}\left(1-\tau^Y_{nit}\right)^{\sigma_n}}{\left(1+\tau^F_{nit}\right)\left(1+\tau^K_{nit}\right)^{\alpha_{Kn}(\sigma_n-1)}\left(1+\tau^L_{nit}\right)^{\alpha_{Ln}(\sigma_n-1)}} \\ &\cdot \frac{1}{\int_0^{J_n}\frac{B_{nit}A_{nit}^{\sigma_n-1}\left(1-\tau^Y_{nit}\right)^{\sigma_n}}{\left(1+\tau^F_{nit}\right)\left(1+\tau^K_{nit}\right)^{\alpha_{Kn}(\sigma_n-1)}\left(1+\tau^L_{nit}\right)^{\alpha_{Ln}(\sigma_n-1)}}di}\end{aligned}$$

where it is more transparent that for factor $F \in \{K, L\}$, any increase in input distortion has two effects on the equilibrium allocation: (1) it brings down the sales share of the firm in the economy, limiting the usage of all inputs, and (2) it brings up the cost of the specific factor F.

We can evaluate this expression at the efficient equilibrium (quantities and prices in the efficient allocations are marked with *) where all distortions are eliminated and get

$$\frac{F^*_{nit}}{F_{nt}} = \frac{\theta^*_{nit}}{\int_0^{J_n}\theta^*_{nit}di} = \theta^*_{nit} = \frac{B_{nit}A_{nit}^{\sigma_n-1}}{\int_0^{J_n} B_{nit}A_{nit}^{\sigma_n-1}di}$$

To obtain a more intuitive expression , we use equation 38 to get

$$\frac{F_{nit}}{F^*_{nit}} = \underbrace{\frac{1}{1+\tau^F_{nit}}}_{\substack{\text{own}\\\text{wedge}\\\text{effect}}} \cdot \underbrace{1+\tau^F_{nt}}_{\substack{\text{aggregate}\\\text{wedge}\\\text{effect}}} \cdot \underbrace{\frac{\theta_{nit}}{\theta^*_{nit}}}_{\substack{\text{size}\\\text{effect}}}$$

where we used the fact that $\tau^{F*}_{nit} = 0$ and $\tau^{F*}_{nt} = 0$ in the efficient equilibrium. Writing this out fully in logs yields

$$\log(\frac{F_{nit}}{F^*_{nit}}) = \underbrace{-\log\left(1+\tau^F_{nit}\right)}_{\substack{\text{own}\\ \text{wedge}\\ \text{effect}}} \underbrace{-\log\left(\frac{\int_0^{J_n}\frac{B_{nit}A_{nit}^{(\sigma_n-1)}\left(1-\tau^Y_{nit}\right)^{(\sigma_n-1)}}{\left(1+\tau^F_{nit}\right)\left(1+\tau^K_{nit}\right)^{\alpha_{Kn}(\sigma_n-1)}\left(1+\tau^L_{nit}\right)^{\alpha_{Ln}(\sigma_n-1)}}di}{\int_0^{J_n}\frac{B_{nit}A_{nit}^{(\sigma_n-1)}\left(1-\tau^Y_{nit}\right)^{(\sigma_n-1)}}{\left(1+\tau^K_{nit}\right)^{\alpha_{Kn}(\sigma_n-1)}\left(1+\tau^L_{nit}\right)^{\alpha_{Ln}(\sigma_n-1)}}di}\right)}_{\text{aggregate wedge effect}}$$

$$\underbrace{+\log\left(\frac{\frac{B_{nit}A_{nit}^{(\sigma_n-1)}\left(1-\tau^Y_{nit}\right)^{(\sigma_n-1)}}{\left(1+\tau^{Kn}_{nit}\right)^{\alpha_{Kn}(\sigma_n-1)}\left(1+\tau^{Ln}_{nit}\right)^{\alpha_{Ln}(\sigma_n-1)}}}{\int_0^{J_n}\frac{B_{nit}A_{nit}^{(\sigma_n-1)}\left(1-\tau^Y_{nit}\right)^{(\sigma_n-1)}}{\left(1+\tau^{Kn}_{nit}\right)^{\alpha_{Kn}(\sigma_n-1)}\left(1+\tau^{Ln}_{nit}\right)^{\alpha_{Ln}(\sigma_n-1)}}di}\right) - \log\left(\frac{B_{nit}A_{nit}^{\sigma_n-1}}{\int_0^{J_n}B_{nit}A_{nit}^{\sigma_n-1}di}\right)}_{\text{size effect}}$$

Further simplifying yields

$$\log(\frac{F_{nit}}{F^*_{nit}}) = -\log\left(1+\tau^F_{nit}\right) + \sigma_n\log\left(1-\tau^Y_{nit}\right) - (\sigma_n-1)\sum_{F'\in\{K,L\}}\alpha_{F'n}\left(1+\tau^{F'}_{nit}\right)$$

$$+\log\left(\frac{\int_0^{J_n}B_{nit}A_{nit}^{\sigma_n-1}di}{\int_0^{J_n}\frac{B_{nit}A_{nit}^{(\sigma_n-1)}\left(1-\tau^Y_{nit}\right)^{(\sigma_n-1)}}{\left(1+\tau^F_{nit}\right)\left(1+\tau^K_{nit}\right)^{\alpha_{Kn}(\sigma_n-1)}\left(1+\tau^L_{nit}\right)^{\alpha_{Ln}(\sigma_n-1)}}di}\right),$$

which delivers equation 43 by letting $C_{Fnt} = \frac{\int_0^{J_n}B_{nit}A_{nit}^{\sigma_n-1}di}{\int_0^{J_n}\frac{B_{nit}A_{nit}^{(\sigma_n-1)}\left(1-\tau^Y_{nit}\right)^{(\sigma_n-1)}}{\left(1+\tau^F_{nit}\right)\left(1+\tau^K_{nit}\right)^{\alpha_{Kn}(\sigma_n-1)}\left(1+\tau^L_{nit}\right)^{\alpha_{Ln}(\sigma_n-1)}}di}$.

■

A.3 Proof of Proposition 2

Proposition 2. Aggregation and TFP Decomposition. Under the log-normality assumption, each region-sector n admits an aggregate production function of the form

$$Y_{nt} = \text{TFP}_{nt}K_{nt}^{\alpha_{Kn}}L_{nt}^{\alpha_{Ln}},$$

where the region-sectoral aggregate Total Factor Productivity $\text{TFP}_{nt} := \text{TFP}_n\left(\tilde{\mathbf{T}}_{rt}, \tilde{\mathbf{X}}_{nt}\right)$ can be decomposed as follows:

$$\log \text{TFP}_n(\tilde{\mathbf{T}}_{rt}, \cdot) = \underbrace{\frac{1}{\sigma_n - 1} \log \left[J_n \mathbb{E}_i \left[B_{ni}(\tilde{\mathbf{T}}_{rt}, \cdot) \left(A_{ni}(\tilde{\mathbf{T}}_{rt}, \cdot) \right)^{\sigma_n - 1} \right] \right]}_{\text{Technology}(\log \text{TFP}_n^E)} - \underbrace{\frac{\sigma_n}{2} \text{var}_{\log(1-\tau_{ni}^Y)}(\tilde{\mathbf{T}}_{rt}, \cdot)}_{\text{Output Wedge Dispersion}}$$
$$\underbrace{- \sum_{F \in \{K,L\}} \frac{\alpha_{Fn} + \alpha_{Fn}^2(\sigma_n - 1)}{2} \text{var}_{\log(1+\tau_{ni}^F)}(\tilde{\mathbf{T}}_{rt}, \cdot)}_{\text{Factor Wedge Dispersion}}$$
$$\underbrace{+ \sigma_n \sum_{F \in \{K,L\}} \alpha_{Fn} \text{cov}_{\log(1-\tau_{ni}^Y), \log(1+\tau_{ni}^F)} \left(\tilde{\mathbf{T}}_{rt}, \cdot \right)}_{\text{Output-Factor Mixed Distortion}}$$
$$\underbrace{- (\sigma_n - 1) \alpha_{Kn} \alpha_{Ln} \text{cov}_{\log(1+\tau_{ni}^K), \log(1+\tau_{ni}^L)} \left(\tilde{\mathbf{T}}_{rt}, \cdot \right)}_{\text{Factor Mixed Distortion}} \tag{45}$$

Proof. Using 38, we can derive an expression for the equilibrium aggregate factor demand F_{nt} as

$$F_{nt} = \int_0^{J_n} F_{nit} di = \left(\frac{\sigma_n - 1}{\sigma_n} \right)^{\sigma_n} \left(\frac{P_{nt}^F}{\alpha_{F_n}} \right)^{-1} \left(\frac{R_{nt}}{\alpha_{Kn}} \right)^{\alpha_{Kn}(1-\sigma_n)} \left(\frac{W_{nt}}{\alpha_{Ln}} \right)^{\alpha_{Ln}(1-\sigma_n)} P_{nt}^{\sigma_n} Y_{nt}$$
$$\cdot \int_0^{J_n} \frac{B_{nit} A_{nit}^{\sigma_n - 1} \left(1 - \tau_{nit}^Y\right)^{\sigma_n}}{\left(1 + \tau_{nit}^F\right) \left(1 + \tau_{nit}^K\right)^{\alpha_{Kn}(\sigma_n - 1)} \left(1 + \tau_{nit}^L\right)^{\alpha_{Ln}(\sigma_n - 1)}} di. \tag{46}$$

Substituting the expression of F_{nt} into $\text{TFP}_{nt} := \frac{Y_{nt}}{K_{nt}^{\alpha_{Kn}} L_{nt}^{\alpha_{Ln}}}$ yields

$$\text{TFP}_{nt} = \left\{ \frac{1}{P_{nt}} \frac{\sigma_n}{\sigma_n - 1} \left(\frac{R_{nt}}{\alpha_{Kn}} \right)^{\alpha_{Kn}} \left(\frac{W_{nt}}{\alpha_{Ln}} \right)^{\alpha_{Ln}} \right\}^{\sigma_n}$$
$$\cdot \frac{1}{\left(\int_0^{J_n} \frac{B_{nit} A_{nit}^{\sigma_n - 1} (1 - \tau_{nit}^Y)_n^{\sigma}}{(1 + \tau_{nit}^K)^{\alpha_{Kn}(\sigma_n - 1) + 1} (1 + \tau_{nit}^L)^{\alpha_{Ln}(\sigma_n - 1)}} di \right)^{\alpha_{Kn}}}$$
$$\cdot \frac{1}{\left(\int_0^{J_n} \frac{B_{nit} A_{nit}^{\sigma_n - 1} (1 - \tau_{nit}^Y)_n^{\sigma}}{(1 + \tau_{nit}^K)^{\alpha_{Kn}(\sigma_n - 1)} (1 + \tau_{nit}^L)^{\alpha_{Ln}(\sigma_n - 1) + 1}} di \right)^{\alpha_{Ln}}} \tag{47}$$

Using 40 and the fact that $\int P_{nit} Y_{nit} di = P_{nt} Y_{nt}$, we can derive the aggregate price index as

$$P_{nt} = \left(\frac{\sigma_n}{\sigma_n - 1} \right) \left(\frac{R_{nt}}{\alpha_{Kn}} \right)^{\alpha_{Kn}} \left(\frac{W_{nt}}{\alpha_{Ln}} \right)^{\alpha_{Ln}} \cdot$$
$$\left[\int_0^{J_n} \left(\frac{B_{nit}^{\frac{1}{\sigma_n}} A_{nit} \left(1 - \tau_{nit}^Y\right)}{\left(1 + \tau_{nit}^{Ks}\right)^{\alpha_{Kn}} \left(1 + \tau_{nit}^{Ln}\right)^{\alpha_{Ln}}} \right)^{\sigma_n - 1} di \right]^{\sigma_n - 1} \tag{48}$$

Substituting this back into equation 47 and taking logs to both sides yields

$$\log \mathrm{TFP}_{nt} = \frac{\sigma_n}{\sigma_n - 1} \log \int_0^{J_n} \left(\frac{B_{nit}^{\frac{1}{\sigma_n}} A_{nit} \left(1 - \tau_{nit}^{Y}\right)}{\left(1 + \tau_{nit}^{Ks}\right)^{\alpha_{Kn}} \left(1 + \tau_{nit}^{Ln}\right)^{\alpha_{Ln}}} \right)^{\sigma_n - 1} di$$
$$- \alpha_{Kn} \log \int_0^{J_n} \frac{B_{nit} A_{nit}^{\sigma_n - 1} \left(1 - \tau_{nit}^{Y}\right)_n^{\sigma}}{\left(1 + \tau_{nit}^{K}\right)^{\alpha_{Kn}(\sigma_n - 1)+1} \left(1 + \tau_{nit}^{L}\right)^{\alpha_{Ln}(\sigma_n - 1)}} di \tag{49}$$
$$- \alpha_{Ln} \log \int_0^{J_n} \frac{B_{nit} A_{nit}^{\sigma_n - 1} \left(1 - \tau_{nit}^{Y}\right)_n^{\sigma}}{\left(1 + \tau_{nit}^{K}\right)^{\alpha_{Kn}(\sigma_n - 1)} \left(1 + \tau_{nit}^{L}\right)^{\alpha_{Ln}(\sigma_n - 1)+1}} di$$

Under the assumption that B_{nit}, A_{nit} , $1 + \tau_{nit}^{K}$ and $1 + \tau_{nit}^{L}$ follow a joint log-normal distribution, and all firm-level fundamentals $\{B_{nit}, A_{nit}, \tau_{nit}^{Y}, \tau_{nit}^{F}\}$ to be firm-specific and smooth functions of $(\tilde{\mathbf{T}}_{rt}, \tilde{\mathbf{X}}_{nt}, \tilde{\mathbf{Z}}_{nit})$, expanding all the terms in 49 yields

$$\begin{aligned}
\log \mathrm{TFP}_n(\tilde{\mathbf{T}}_{rt}, \cdot) = & \underbrace{\frac{1}{\sigma_n - 1} \log \mathbb{E}_i \left[B_{ni}(\tilde{\mathbf{T}}_{rt}, \cdot) \left(A_{ni}(\tilde{\mathbf{T}}_{rt}, \cdot) \right)^{\sigma_n - 1} \right]}_{\text{Technology}(\log \mathrm{TFP}_n^E)} - \underbrace{\frac{\sigma_n}{2} \operatorname{var}_{\log\left(1 - \tau_{ni}^{Y}\right)}(\tilde{\mathbf{T}}_{rt}, \cdot)}_{\text{Output Wedge Dispersion}} \\
& - \underbrace{\sum_{F \in \{K, L\}} \frac{\alpha_{Fn} + \alpha_{Fn}^2(\sigma_n - 1)}{2} \operatorname{var}_{\log\left(1 + \tau_{ni}^{F}\right)}(\tilde{\mathbf{T}}_{rt}, \cdot)}_{\text{Factor Wedge Dispersion}} \\
& + \underbrace{\sigma_n \sum_{F \in \{K, L\}} \alpha_{Fn} \operatorname{cov}_{\log\left(1 - \tau_{ni}^{Y}\right), \log\left(1 + \tau_{ni}^{F}\right)} \left(\tilde{\mathbf{T}}_{rt}, \cdot \right)}_{\text{Output-Factor Mixed Distortion}} \\
& - \underbrace{(\sigma_n - 1) \alpha_{Kn} \alpha_{Ln} \operatorname{cov}_{\log\left(1 + \tau_{ni}^{K}\right), \log\left(1 + \tau_{ni}^{L}\right)} \left(\tilde{\mathbf{T}}_{rt}, \cdot \right)}_{\text{Factor Mixed Distortion}}
\end{aligned} \tag{50}$$

which is the Equation 11 in the text.

■

B Data Sources and Variable Construction

This appendix provides details on data sources and variable constructions.

B.1 Orbis Data

Our data of firms from the European countries comes from the Orbis historical Disk Product. We use the sample period 1995-2018 for our analysis. We detail the cleaning process below.

Sample Cleaning. Following the procedure of Kalemli- Özcan et al. (2024), we link multiple vintages of Orbis products over time and link the firm's descriptive information with its financial information via the unique BVD firm identifier (BVDID). We then apply the following standard cleaning procedure:

1. We restrict our analysis to firms that satisfy the following criteria: the country they reside in from their latest address matches with their ISO codes in their BVDID identifier. For

example, if the firm's ISO-2 code in BVDID is FR while its latest address is in Spain, then we exclude this firm from our sample.

2. For some firms that lack address information but have other identifiers such as postcodes, we manually map the postcodes to NUTS3 for each country.

3. We harmonize each firm's fiscal year with the calendar year based on the closing date: if the closing date is on or after July 1st, we use the current year as the calendar year; otherwise, we use the previous year.

4. Firms may report multiple sales figures from different sources (like local registries, annual reports, etc.) for consolidated or unconsolidated accounts. Following Fan (2024), we use the unconsolidated accounts to avoid double-counting that can occur with consolidated accounts.

5. We only keep firms with non-missing and positive sales (`operating_revenue_turnover`) and fixed assets (`fixed_assets`).

6. We calculate firm-level MRPK_{it} for firm i in year t as $\log \text{MRPK}_{it} = \log(\alpha_{Kn} \frac{\sigma_n - 1}{\sigma_n} \frac{P_{it}Y_{it}}{K_{it}})$ where $P_{it}Y_{it}$ is measured with sales and K_{it} is measured with fixed assets.

7. We winsorize the observations of MRPK_{it}, fixed assets, or sales at the top and bottom 0.1% of the distribution in the entire panel for each country. This is to prevent outliers from affecting the variance calculation and estimation.

B.2 China NBS Data

The annual firm-level data for China is derived from surveys conducted by the National Bureau of Statistics (NBS) in China. We only use the sample period of 1998-2007 due to inconsistent reporting after 2008 as discussed in Brandt, Van Biesebroeck, and Zhang (2014) and Nath (2023).

Sample Cleaning. To process the NBS data, we follow the methodology outlined in Zhang et al. (2018). We measure sales using the variable "产品销售收入" (product sales revenue) and capital using the variable "固定资产合计" (total fixed assets). Each firm in the dataset is categorized using a four-digit Chinese Industry Classification (CIC) code and is harmonized to the USSIC division level. Each firm's reported location can be mapped into a prefecture-level division. The rest of the cleaning follows the same procedure as items 5-7 in Appendix B.1.

B.3 India ASI Data

Our data for India are drawn from India's Annual Survey of Industries (ASI). We use the sample period of 1998 to 2018.

Sample Cleaning. We match the plants to the Indian districts following the approach of Somanathan et al. (2021) and harmonize the industries first to the NIC-04 classification, and then to the SIC division level. We measure sales using the gross sale value of all products and capital using an average of the opening and closing gross book value of total capital, as in Bils, Klenow, and Ruane (2021). The rest of the cleaning follows the same procedure as items 5-7 in Appendix B.1.

B.4 Additional Descriptive Statistics

The table below lists out the countries, year coverage, number of regions in each country, and the total number of firm-year pair observations in the final sample we used for the empirical analysis.

Table B.1: Descriptive Table of Dataset by Country

Dataset	Country	Coverage	Number of Regions	Number of Firm-Year Obs
NBS China Industrial	China	1998-2007	325	2069100
India ASI	India	1998-2017	267	473646
	Austria	2004-2018	34	185029
	Belgium	1998-2018	44	781322
	Bulgaria	1998-2018	28	1439871
	Switzerland	2003-2018	3	1701
	Cyprus	2005-2018	1	17356
	Czech Republic	1998-2018	14	1425901
	Germany	1998-2018	346	765981
	Denmark	1999-2018	11	392015
	Estonia	1998-2018	5	791340
	Greece	1998-2018	44	342636
	Spain	1998-2018	52	12210663
	Finland	1998-2018	19	1909080
	France	1998-2018	96	15151185
	Croatia	1998-2018	21	1202515
BvD Orbis	Hungary	2004-2018	20	3095326
	Ireland	2000-2018	8	115344
	Italy	1998-2018	107	12083926
	Lithuania	1998-2018	10	129442
	Luxembourg	1998-2018	1	74287
	Latvia	2010-2018	6	533640
	Malta	2000-2018	1	21249
	Netherlands	1998-2018	36	201182
	Norway	1998-2018	12	2462277
	Poland	1998-2018	73	1207428
	Portugal	1998-2018	24	3882515
	Romania	1998-2018	42	4636047
	Sweden	1998-2018	21	3934403
	Slovenia	1998-2018	12	744495
	Slovakia	1998-2018	8	1008353
	United Kingdom	1998-2018	178	3537701

C Additional Figures for Section 4

This appendix provides additional results and figures to complement the main analysis in Section 4.

C.1 Firm-level MRPK and Temperature

Here we present the *average* effect of temperature on firm-level MRPK across climates and income. We show that heat shocks negatively affect firm-level MRPK across almost all climates and income. As an economy becomes more developed or traditions into a hotter climate, the negative effect of heat shocks on MRPK becomes larger.

Figure C.1: Average Effect of Temperature on firm-level MRPK Across Climates and Income

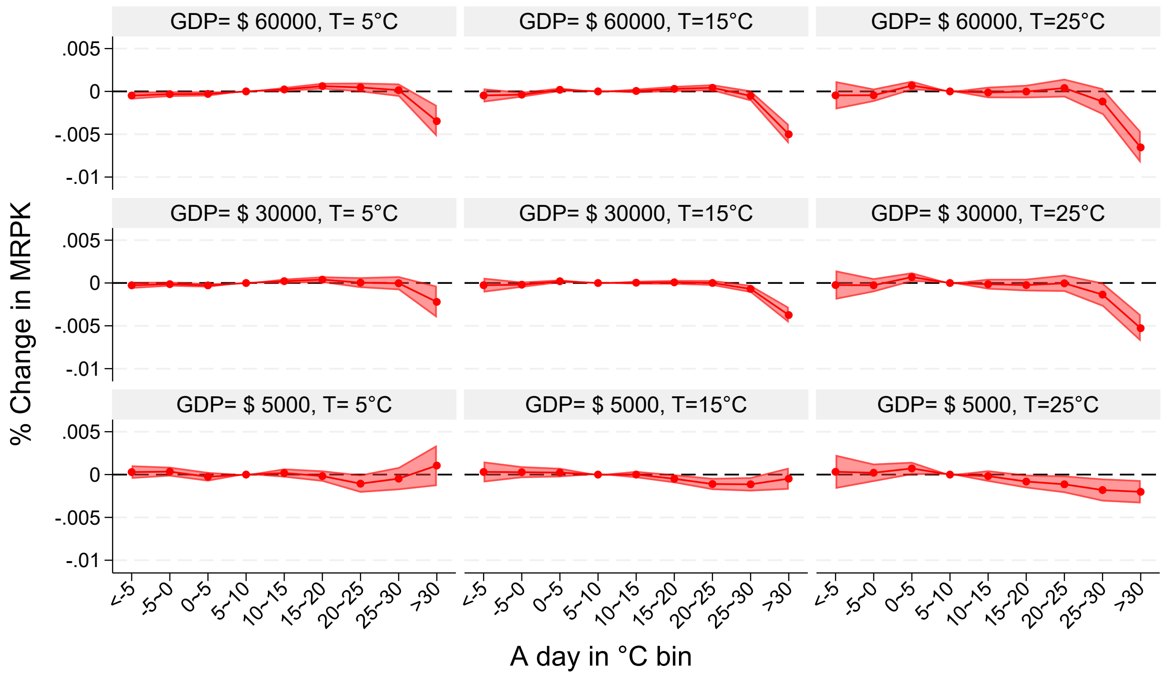

Notes: The graph plots the estimated effect of exposure to daily mean temperature bins on the level of MRPK at varying levels of income and climates. The regression is at the firm-level with firm and country-year fixed effect. The graph includes 90% confidence intervals and standard errors are clustered at the regional level. The reference temperature is at 5-10°C.

C.2 Projected Evolution of Income and Temperature under SSP3-4.5

The figure illustrates the projected evolution of income and average temperature from the 2000-2014 baseline to the end of the century (2081-2100) under the SSP3-4.5 scenarios. Among the 172 countries, All 172 countries show a rightward shift (indicating an increase in temperature), and 96% of them also show an upward shift (indicating an increase in per-capita income). In the baseline period, average temperatures are below 5°C in 11 countries, between 5-15°C in 49 countries, between 15-25°C in 62 countries, and above 25°C in 50 countries. Baseline per capita income is below $5000 in 41 countries, between $5000-$30000 in 83 countries, between

$30000-$60000 in 38 countries and above $60000 in 10 countries. The blue arrow exemplifies the joint evolution of income and temperature.

Figure C.2: Joint Evolution of Income and Average Temperature from Base Period to End of Century (under SSP3-4.5)

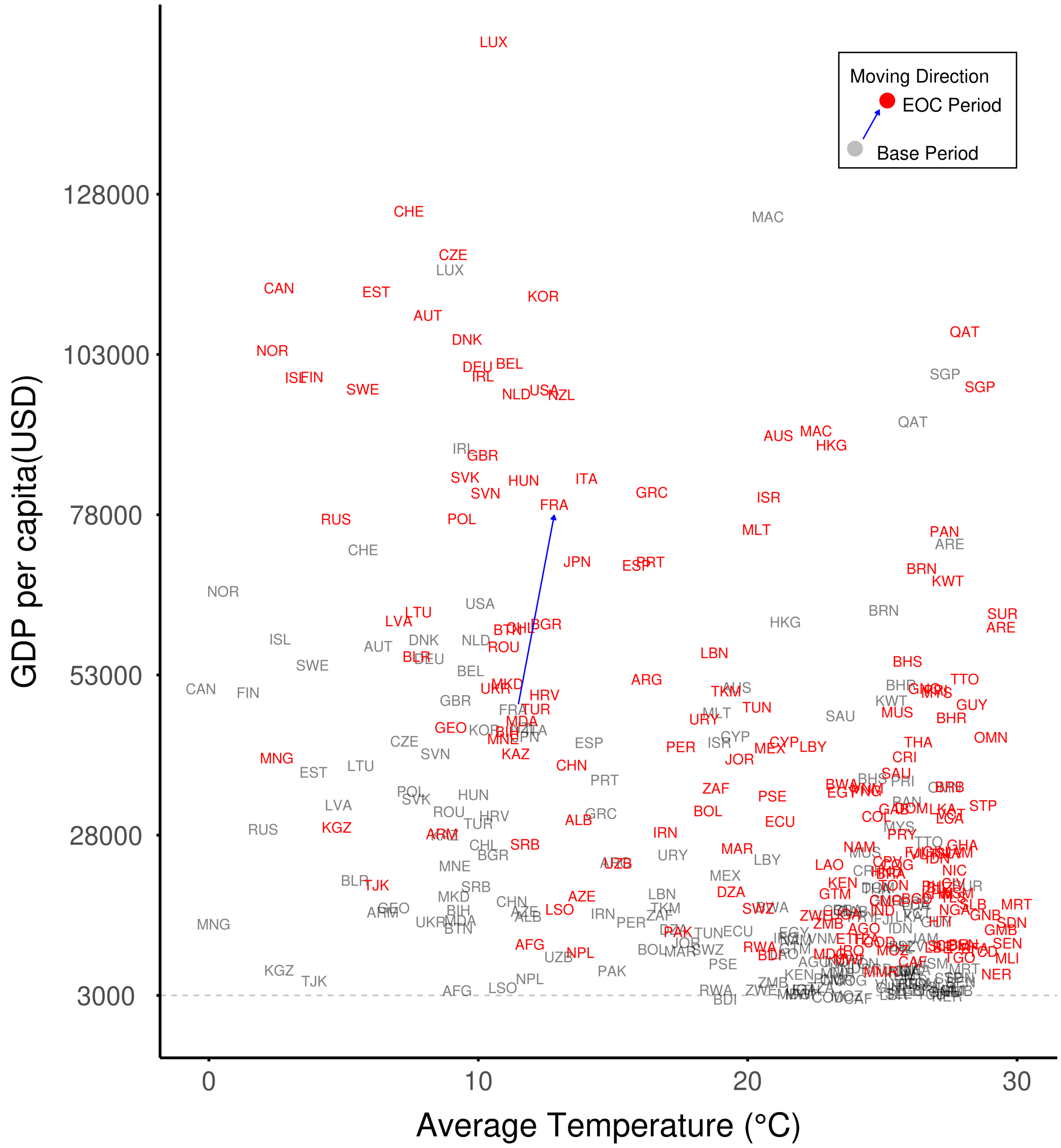

Notes: Grey texts represent the baseline period from 2000 to 2014, and the red texts represent the end of the century (2081 - 2100). End-of-century projection comes from SSP3-4.5 projection. The graph shows the joint evolution of income per capita and average temperature for each country.

C.3 Projection Components

The graph shows a breakdown of the three effects contributing to the total projected TFP loss under SSP3-4.5 scenarios in Section 4.4.

Figure C.3: Three Effects Contribution to Projected TFP Loss (SSP3-4.5)

(a) Shock Effects Projection

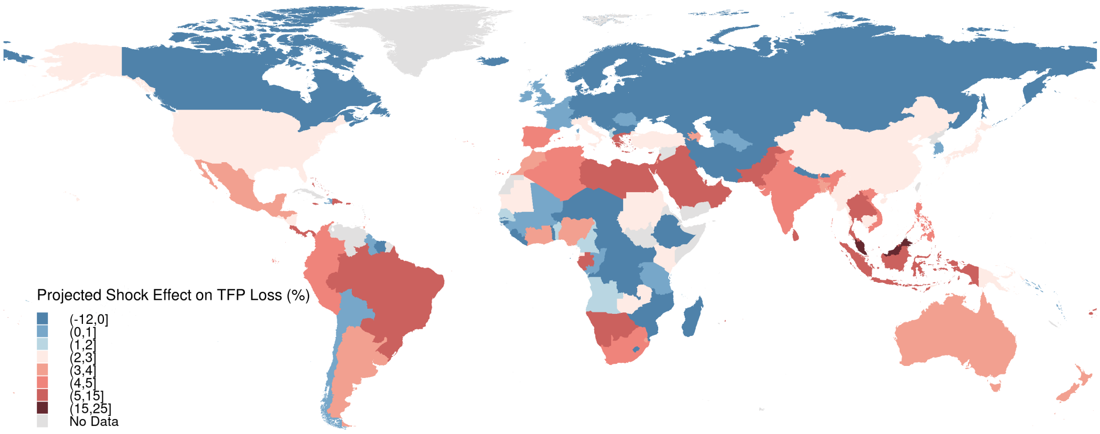

(b) Level Effects Projection

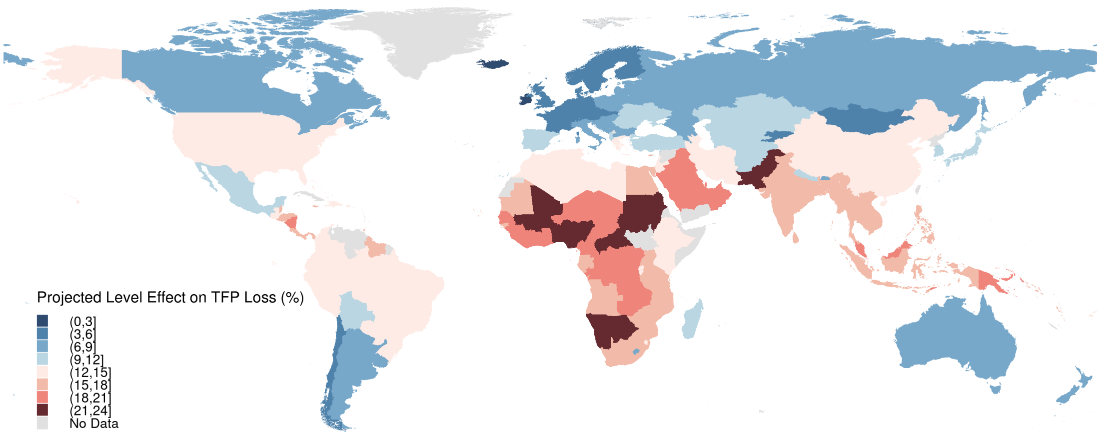

(c) Income Effects Projection

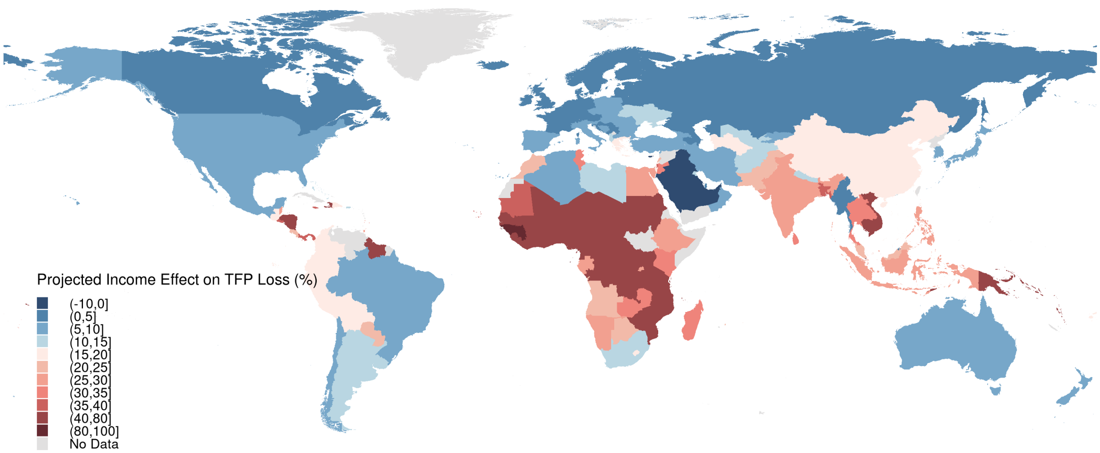

C.4 Projections from Other Scenarios

This appendix presents global TFP loss projections by current income levels under different scenarios. We categorize the countries into four groups based on current GDP per capita quantiles: below the 25th percentile (less than \$5149.8), 25th-50th percentile (\$5149.8-\$13968.3), 50th-75th percentile (\$13968.3-\$32776.8), and above the 75th percentile (greater than \$32776.8). The four scenarios considered are SSP2-4.5, SSP3-7.0, SSP3-4.5, and SSP5-8.5.

Figure C.4: Global TFP Loss Projection By Current Income Levels from Other Scenarios (Part 1)

(a) Income Below 25% Percentile

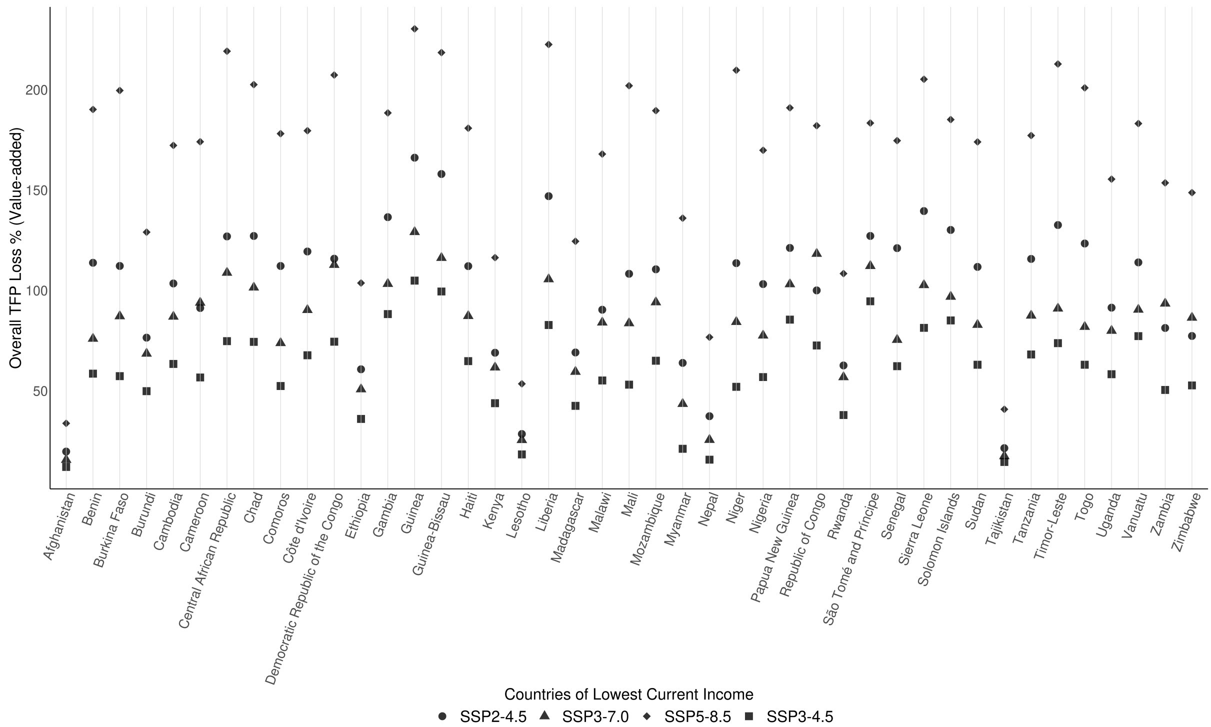

(b) Income at 25% to 50% Percentile

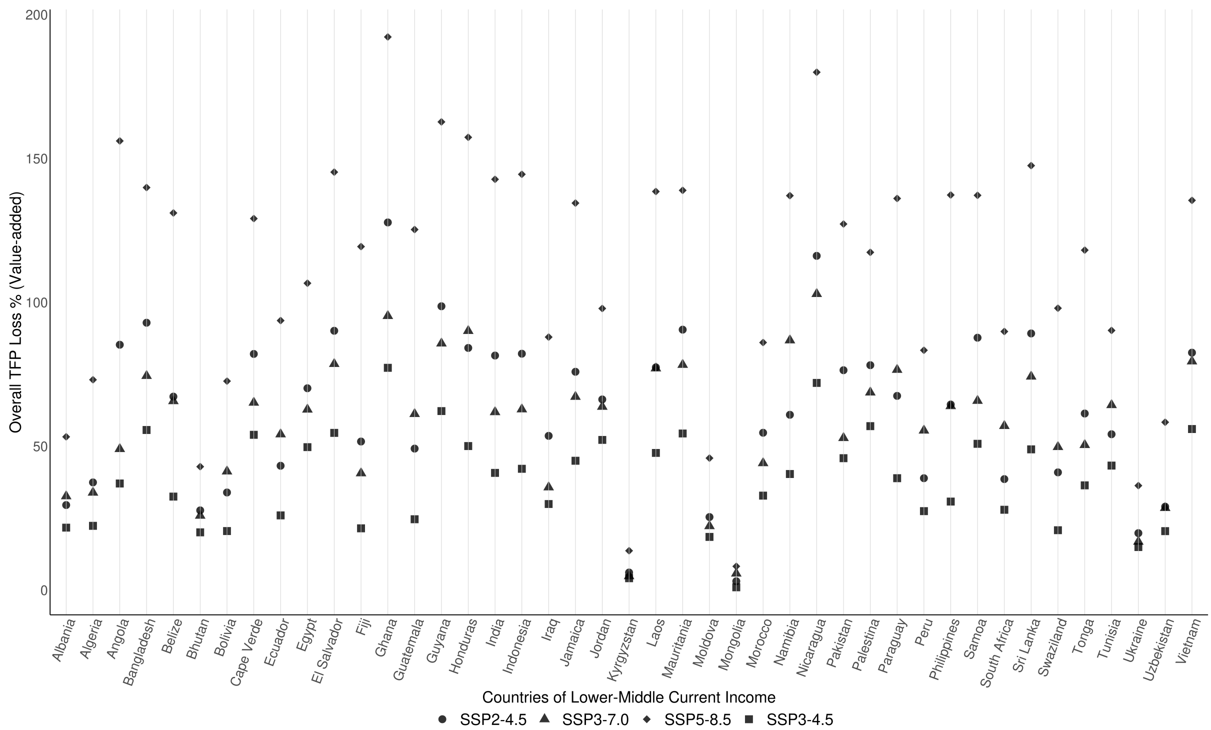

Figure C.5: Global TFP Loss Projection By Current Income Levels from Other Scenarios (Part 2)

(a) Income at 50% to 75% Percentile

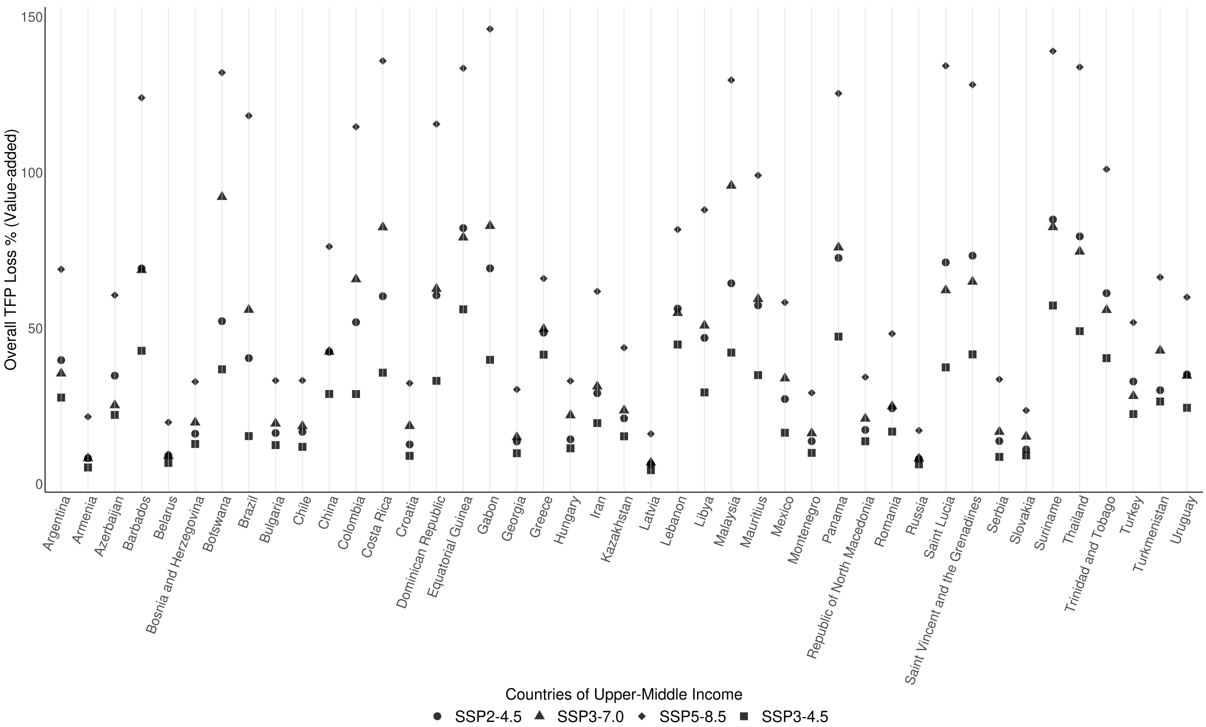

(b) Income above 75% Percentile

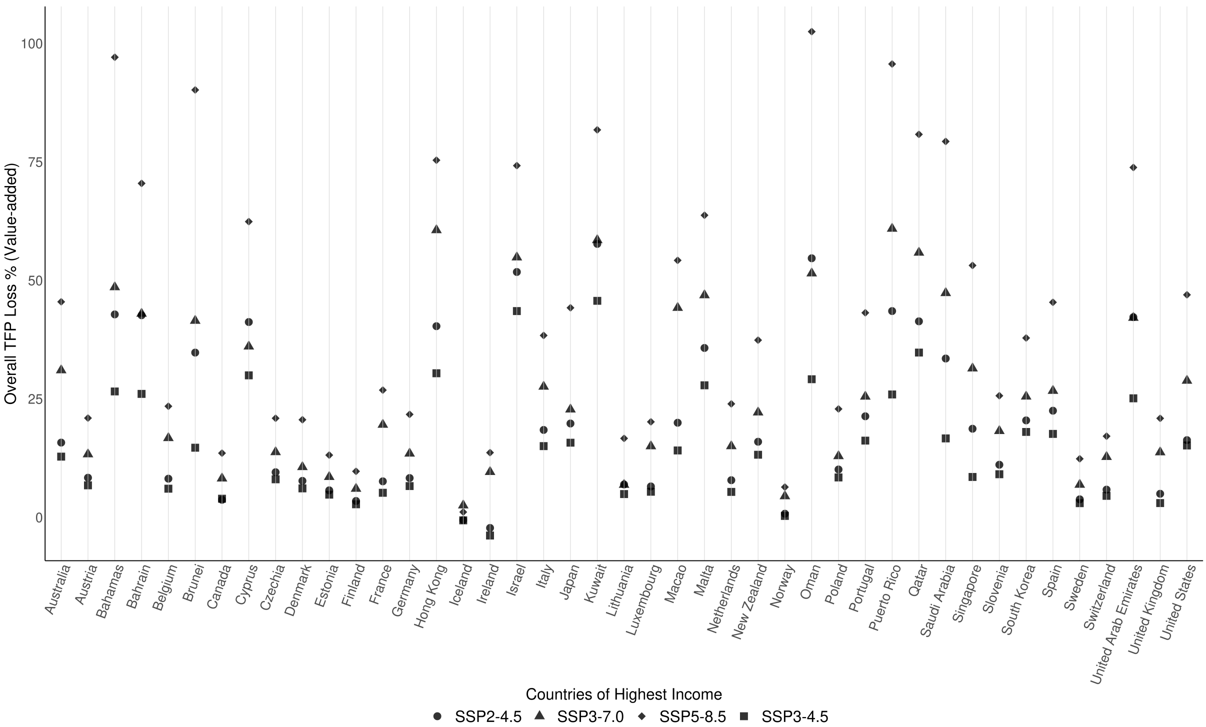

D Additional Tables for Regressions in Section 6

This appendix reports the estimates in Section 6, corresponding to Figures 6b and 6a.

Table D.2: Relative Firm Size and Firm MRPK

	(1)	(2)
< -5°C	0.00056**	0.00046*
	(0.00027)	(0.00027)
$-5 \sim 0$°C	0.00019	0.00012
	(0.00016)	(0.00015)
$0 \sim 5$°C	0.00015	0.00010
	(0.00013)	(0.00013)
$5 \sim 10$°C	0.00005	0.00001
	(0.00014)	(0.00013)
$15 \sim 20$°C	0.00004	0.00002
	(0.00011)	(0.00011)
$20 \sim 25$°C	-0.00016	-0.00024
	(0.00016)	(0.00016)
$25 \sim 30$°C	-0.00019	-0.00028
	(0.00024)	(0.00024)
> 30°C	-0.00119***	-0.00133***
	(0.00045)	(0.00044)
< -5°C × Relative Size		0.00089***
		(0.00019)
$-5 \sim 0$°C × Relative Size		0.00077***
		(0.00024)
$0 \sim 5$°C × Relative Size		0.00062***
		(0.00022)
$5 \sim 10$°C × Relative Size		0.00041
		(0.00027)
$15 \sim 20$°C × Relative Size		0.00021***
		(0.00008)
$20 \sim 25$°C × Relative Size		0.00092***
		(0.00017)
$25 \sim 30$°C × Relative Size		0.00098***
		(0.00031)
> 30°C × Relative Size		0.00105**
		(0.00049)
Control: Relative Size	Yes	Yes
Firm FE	Yes	Yes
Country-Sector-Year FE	Yes	Yes
Observations	73350226	73350226
R^2	0.880	0.880

Notes: Standard errors in parentheses. We cluster standard errors at the region level (NUTS3 level for European countries, province level for China, and first-level administrative divisions for India). The dependent variables are the log MRPK. These results are obtained by estimating Equation 31. Column 2 presents results that interact with relative firm size, $\text{Relative Size}_{it}^{r,s} := \log K_{it}^{s,r} - \overline{\log K_{it}}^{s,r}$, which is standardized over the entire sample.

* $p < 0.10$, ** $p < 0.05$, *** $p < 0.01$

Table D.3: AC Installation and Firm MRPK

	(1)	(2)	(3)	(4)
$< 10°C$	0.00156	0.00124	0.00083	0.00178
	(0.00105)	(0.00101)	(0.00268)	(0.00202)
$10 \sim 15°C$	0.00032	0.00075	-0.00064	0.00131*
	(0.00051)	(0.00051)	(0.00085)	(0.00075)
$20 \sim 25°C$	-0.00037	-0.00015	-0.00226***	-0.00175***
	(0.00027)	(0.00024)	(0.00080)	(0.00061)
$25 \sim 30°C$	-0.00060*	-0.00035	-0.00286***	-0.00245***
	(0.00031)	(0.00028)	(0.00083)	(0.00065)
$> 30°C$	-0.00068*	-0.00044	-0.00249**	-0.00224***
	(0.00040)	(0.00035)	(0.00099)	(0.00075)
$< 10°C \times$ AC Installation			0.00089	-0.00051
			(0.00305)	(0.00243)
$10 \sim 15°C \times$ AC Installation			0.00110	-0.00062
			(0.00095)	(0.00085)
$15 \sim 20°C \times$ AC Installation			0.00218***	0.00185***
			(0.00081)	(0.00062)
$20 \sim 25°C \times$ AC Installation			0.00259***	0.00240***
			(0.00087)	(0.00068)
$25 \sim 30°C \times$ AC Installation			0.00208**	0.00206***
			(0.00102)	(0.00077)
Control: lnK	No	Yes	No	Yes
Firm FE	Yes	Yes	Yes	Yes
Sector-Year FE	Yes	Yes	Yes	Yes
Observations	532,425	532,425	532,425	532,425
R^2	0.748	0.815	0.748	0.815

Notes: Standard errors in parentheses. We cluster standard errors at the districts level. The dependent variables are the log MRPK. These results are obtained by estimating Equation 31. Column 1 and 3 present results that do not include control variables $\log K$.
* $p < 0.10$, ** $p < 0.05$, *** $p < 0.01$

E Additional Derivations for Section 5

This appendix provides the derivations of the expressions and propositions featured in Section 5.

E.1 Proof of Lemma 1

Lemma 1. TFP Volatility, $\text{Var}(\hat{a}_{it} - \mathbb{E}_{t-1}[\hat{a}_{it}])$, and can be written as:

$$\text{Var}(\hat{a}_{it} - \mathbb{E}_{t-1}[\hat{a}_{it}]) = (T_t - T^*)^2\sigma^2_{\hat{\xi}} + \hat{\eta}_t^{T2}\sigma^2_{\hat{\beta}} + \sigma^2_{\hat{\varepsilon}}. \tag{51}$$

TFP volatility reaches its minimum when the temperature is at its optimum, $T_t = T^*$, and when there is no unexpected change in temperature, $\eta_t^T = 0$.
Proof. We can write a firm's (log) TFP, $\hat{a}_{it}$, as

$$\begin{aligned} \hat{a}_{it} &= \hat{\beta}_{it}(T_t - T^*) + \hat{z}_{it} \\ &= \left(\hat{\beta}_i + \hat{\xi}_{it} + \mathcal{O}_t\right)(T_t - T^*) + \rho_z \hat{z}_{it-1} + \hat{\varepsilon}_{it}. \end{aligned} \tag{52}$$

where $\mathcal{O}_t$ is defined as

$$\mathcal{O}_t = c(T_t - T^*), \quad \text{with } c = \frac{(\sigma^2_{\hat{\beta}} + \sigma^2_{\hat{\xi}})\sigma}{2}.$$

hen the expected TFP, $\mathbb{E}_{t-1}[\hat{a}_{it}]$, can be expressed as

$$\begin{aligned} \mathbb{E}_{t-1}[\hat{a}_{it}] &= \hat{\beta}_i \mathbb{E}_{t-1}[T_t - T^*] + \mathbb{E}_{t-1}[\hat{\xi}_{it}(T_t - T^*)] + \mathbb{E}_{t-1}[\mathcal{O}_t(T_t - T^*)] + \rho_z \hat{z}_{it-1} \\ &= \hat{\beta}_i \mathbb{E}_{t-1}[T_t - T^*] + c\mathbb{E}_{t-1}[(T_t - T^*)^2] + \rho_z \hat{z}_{it-1} \end{aligned} \tag{53}$$

where we have used that $\mathbb{E}_{t-1}[\hat{\xi}_{it}(T_t - T^*)] = \mathbb{E}_{t-1}[\hat{\xi}_{it}]\mathbb{E}_{t-1}[(T_t - T^*)] = 0$. Using Equations 52 and 53, we can write the forecast error of a firm's TFP as

$$\hat{a}_{it} - \mathbb{E}_{t-1}[\hat{a}_{it}] = \underbrace{\hat{\beta}_i \hat{\eta}_t^T + c\left((T_t - T^*)^2 - \mathbb{E}_{t-1}\left[(T_t - T^*)^2\right]\right)}_{\text{from Temperature FE}} + \underbrace{\hat{\xi}_{it}(T_t - T^*)}_{\text{from Sensitivity FE}} + \hat{\varepsilon}_{it}, \tag{54}$$

where the first term stems from the firm's forecast error on temperature, the second term represents the firm's unexpected sensitivity shock, and the third term represents the firm's idiosyncratic productivity.

We define TFP Volatility, $\text{Var}(\hat{a}_{it} - \mathbb{E}_{t-1}[\hat{a}_{it}])$, to be the cross-sectional variance of the TFP forecast error across firms. Taking the variance of 54 across i yields

$$\text{Var}(\hat{a}_{it} - \mathbb{E}_{t-1}[\hat{a}_{it}]) = (T_t - T^*)^2\sigma^2_{\hat{\xi}} + {\eta_t^T}^2\sigma^2_{\hat{\beta}} + \sigma^2_{\hat{\varepsilon}}. \tag{55}$$

We thus obtain Equation 51 in the text. ■

E.2 Solving the Model

This appendix provides additional derivations for solving the model in Section 5. Specifically, we will derive the optimal capital investment policy function in Equation 25.

Flexible Input Choice and Profits. Optimal choice of flexible inputs is made after capital inputs are allocated and all shocks are realized. The static input choice solves

$$\max_{N_{it}} P_{it}Y_{it} - W_t N_{it},$$

where $P_{it}Y_{it} = \hat{A}_{it}K_{it}^{\alpha_K} N_{it}^{\alpha_N}$. Taking the first-order condition of N_{it} gives

$$N_{it} = \left(\frac{W_t}{\hat{A}_{it}\alpha_N K_{it}^{\alpha_K}} \right)^{\frac{1}{\alpha_N - 1}}. \tag{56}$$

Plugging in the equilibrium wage, $W_t = \overline{W}\exp\left(\chi(T_t - T^*)\right)$, into this equation yields the optimal labor choice

$$N_{it} = \left(\frac{\overline{W}\exp\left(\chi(T_t - T^*)\right)}{\hat{A}_{it}\alpha_N K_{it}^{\alpha_k}} \right)^{\frac{1}{\alpha_N - 1}}. \tag{57}$$

Also, notice that $W_t N_{it} = \alpha_N P_{it} Y_{it}$, so the firm's profits can be written as

$$\begin{aligned} \Pi_{it} &= P_{it}Y_{it} - W_t N_{it} \\ &= (1-\alpha_N)\hat{A}_{it}K_{it}^{\alpha_K} N_{it}^{\alpha_N}, \end{aligned} \tag{58}$$

Plugging in the expression of optimal labor, we obtain

$$\Pi_{it} = G\exp\left(\chi(T_t - T^*)\right)^{-\frac{\alpha_N}{1-\alpha_N}} \hat{A}_{it}^{\frac{1}{1-\alpha_N}} K_{it}^{\alpha_K \frac{1}{1-\alpha_N}}, \tag{59}$$

where $G = (1-\alpha_N)\overline{W}^{-\frac{\alpha_N}{1-\alpha_N}} \alpha_N^{\frac{\alpha_N}{1-\alpha_N}}$. To simplify notations, we define a firm's *profitability*, A_{it}, as

$$A_{it} = \exp\left(\chi(T_t - T^*)\right)^{-\frac{\alpha_N}{1-\alpha_N}} \hat{A}_{it}^{\frac{1}{1-\alpha_N}} = \exp\left(\beta_{it}(T_t - T^*) + z_{it}\right),$$

where $z_{it} = \frac{1}{1-\alpha_N}\hat{z}_{it}$, and $\beta_{it} = \frac{\hat{\beta}_{it} - \chi\alpha_N}{1-\alpha_N}$ is the firm's profitability sensitivity to temperature. Therefore, we can write a firm's revenue function as

$$\Pi_{it} = G\exp\left(\beta_{it}(T_t - T^*) + z_{it}\right) K_{it}^{\alpha} := G A_{it} K_{it}^{\alpha},$$

where $\alpha = \frac{\alpha_K}{1-\alpha_N}$ is the curvature of profits. This is Equation 23 in the main text.

Dynamic Capital Investment. We now characterize the firm's investment problem. The firm's dynamic capital investment problem takes the form

$$\begin{aligned} V\left(T_t, Z_{it}, K_{it}\right) = \max_{K_{it+1}} \quad & G\exp\left(\beta_{it}(T_t - T^*) + z_{it}\right) K_{it}^{\alpha} - K_{it+1} + (1-\delta)K_{it} \\ & + \frac{1}{1+r}\mathbb{E}_t\left[V\left(T_{t+1}, Z_{it+1}, K_{it+1}\right)\right]. \end{aligned} \tag{60}$$

Combining the first order condition and the envelope condition associated with Equation 60 gives the Euler equation

$$1 = \underbrace{\frac{1}{1+r}}_{\text{Discount Factor}} \left(\underbrace{\alpha G K_{it+1}^{\alpha-1} \mathbb{E}_t \left[\exp\left(z_{it+1} + \beta_{it+1}(T_{t+1} - T^*)\right)\right]}_{\text{Expected Value of Marginal Profits of Capital}} + \underbrace{(1-\delta)}_{\substack{\text{Value of} \\ \text{Undepreciated Capital}}} \right). \tag{61}$$

We then rearrange the Euler equation to get the expression for optimal capital investment

$$\begin{aligned} K_{it+1}^{1-\alpha} &= \frac{\alpha G}{r+\delta} \mathbb{E}_t \left[\exp\left(a_{it+1}\right)\right] \\ &= \frac{\alpha G}{r+\delta} \mathbb{E}_t \left[\exp\left(\frac{\hat{\beta}_i + \hat{\xi}_{it+1} + \mathcal{O}_{t+1} - \chi \alpha_N}{1-\alpha_N} (T_{t+1} - T^*) \right) \right]. \end{aligned} \tag{62}$$

Notice that a first-order approximation of a non-linear function $f(\hat{\xi}_{it+1}, T_{t+1} - T^*)$ around $(\mathbb{E}_t[\hat{\xi}_{it}], \mathbb{E}_t[T_t - T^*])$, we get:

$$\begin{aligned} f(\hat{\xi}_{it+1}, T_{t+1} - T^*) \approx & f(\mathbb{E}_t[\hat{\xi}_{it+1}], \mathbb{E}_t[T_{t+1} - T^*]) \\ & + \left. \frac{\partial f(\hat{\xi}_{it+1}, T_{t+1} - T^*)}{\partial (T_{t+1} - T^*)} \right|_{(\mathbb{E}_t[\hat{\xi}_{it+1}], \mathbb{E}_t[T_{t+1} - T^*])} (T_{t+1} - \mathbb{E}_t[T_{t+1}]) \\ & + \left. \frac{\partial f(\hat{\xi}_{it+1}, T_{t+1} - T^*)}{\partial \hat{\xi}_{it+1}} \right|_{(\mathbb{E}_t[\hat{\xi}_{it+1}], \mathbb{E}_t[T_{t+1} - T^*])} (\hat{\xi}_{it+1} - \mathbb{E}_t[\hat{\xi}_{it+1}]). \end{aligned} \tag{63}$$

Applying expectation on both sides of this equation yields

$$\mathbb{E}_t \left[f(\hat{\xi}_{it+1}, T_{t+1} - T^*) \right] \approx f(\mathbb{E}_t \hat{\xi}_{it+1}, \mathbb{E}_t[T_{t+1} - T^*]). \tag{64}$$

Under this first-order approximation, the optimal investment in 62 becomes

$$K_{it+1}^{1-\alpha} \approx \frac{\alpha G}{r+\delta} \exp\left(\frac{\hat{\beta}_i + \mathbb{E}_t \hat{\xi}_{it+1} + \mathbb{E}_t \mathcal{O}_{t+1} - \chi \alpha_N}{1-\alpha_N} \mathbb{E}_t[T_{t+1} - T^*] + \frac{\mathbb{E}_t[\hat{z}_{it}]}{1-\alpha_N} \right).$$

Taking logs on both sides yields the policy function

$$k_{it+1} = \frac{1}{1-\alpha} \left(\frac{\hat{\beta}_i + \mathbb{E}_t \hat{\xi}_{it+1} + \mathbb{E}_t \mathcal{O}_{t+1} - \chi \alpha_N}{1-\alpha_N} \mathbb{E}_t[T_{t+1} - T^*] + \frac{\mathbb{E}_t[\hat{z}_{it}]}{1-\alpha_N} \right) + k_0. \tag{65}$$

where $k_0 = \frac{1}{1-\alpha} \left(\log \left[\frac{\alpha G}{r+\delta} \right] \right)$. Therefore, Firm i's investment, relative to the average firm in the economy at date $t+1$, would be:

$$k_{it+1} - \overline{k_{it+1}} = \frac{1}{1-\alpha} \left(\frac{\mathbb{E}_t[\hat{z}_{it+1}]}{1-\alpha_N} + \frac{(\hat{\beta}_i - \overline{\hat{\beta}_i})}{1-\alpha_N} \mathbb{E}_t[(T_{t+1} - T^*)] \right).$$

which is Equation 26 in the main text.

To gain some intuitions, using $\mathbb{E}_t[\mathcal{O}_{t+1}(T_{t+1} - T^*)] = \mathbb{E}_t[\mathcal{O}_{t+1}]\mathbb{E}_t[(T_{t+1} - T^*)] + c\sigma_\eta^2$, we can also write Equation 65 as

$$
\begin{aligned}
k_{it+1} =& \frac{1}{1-\alpha}\mathbb{E}_t[a_{it}] + k_0'. \\
=& \frac{1}{1-\alpha}\left(\frac{1}{1-\alpha_N}\mathbb{E}_t[\hat{a}_{it+1}] - \frac{\alpha_N}{1-\alpha_N}\mathbb{E}_t[w_{t+1} - \overline{w}]\right) + k_0' \\
=& \frac{1}{1-\alpha}\left(\frac{1}{1-\alpha_N}(\mathbb{E}_t[\hat{z}_{it+1}] + \mathbb{E}_t[\hat{\beta}_{it+1}(T_{t+1} - T^*)]) - \frac{\alpha_N\chi}{1-\alpha_N}\mathbb{E}_t[T_{t+1} - T^*]\right) + k_0',
\end{aligned}
\tag{66}
$$

where $k_0' = \frac{1}{1-\alpha}\left(\log\left[\frac{\alpha G}{r+\delta}\right] - \frac{c\sigma_\eta^2}{1-\alpha_N}\right)$. The derivations illustrate the following logic: investment is proportional to the expected profitability of capital, which is increasing in expected (revenue) productivity and decreasing in expected wages. These are, in turn, dependent on the firm's expectation of future temperature sensitivity and future temperature.

E.3 Proof of Proposition 3

Proposition 3 Firms with higher unexpected changes in productivity exhibit higher MRPK relative to the average level:

$$
mrpk_{it} - \overline{mrpk_{it}} = \frac{1}{1-\alpha_N}\left\{ \underbrace{(\hat{\beta}_i - \overline{\hat{\beta}_i})\eta_t^T}_{\substack{\text{Unexpected}\\\text{Temperature Shock}\\\text{on Productivity}}} + \underbrace{\hat{\xi}_{it}(T_t - T^*)}_{\substack{\text{Unexpected}\\\text{Damage}\\\text{Sensitivity}}} + \hat{\varepsilon}_{it} \right\},
\tag{67}
$$

where the relative MRPK of heat-averse firms ($\hat{\beta}_i < \overline{\hat{\beta}_i}$) will decrease with a positive temperature shock η_t^T; while the relative MRPK of heat-loving firms ($\hat{\beta}_i > \overline{\hat{\beta}_i}$) will increase with a positive temperature shock.

Proof. Recall that $P_{it}Y_{it} = \hat{A}_{it}K_{it}^{\alpha_K}N_{it}^{\alpha_N}$ and therefore a firm's MRPK can be written as

$$
\text{MRPK}_{it} = \frac{\partial P_{it}Y_{it}}{\partial K_{it}} = \alpha_K\frac{P_{it}Y_{it}}{K_{it}}.
\tag{68}
$$

Note that since $\alpha_K = \frac{\sigma-1}{\sigma}\hat{\alpha}_K$, this definition of MRPK is consistent with the definition in our accounting framework (see Equation 6). Using 58, we can write revenue as

$$
\begin{aligned}
P_{it}Y_{it} = \frac{\Pi_{it}}{1-\alpha_N} &= \frac{GA_{it}K_{it}^{\alpha}}{1-\alpha_N} \\
&= \overline{G}A_{it}K_{it}^{\alpha},
\end{aligned}
$$

where $\overline{G} = \frac{G}{1-\alpha_N}$. Plugging this expression in 68 and taking logs to both sides, we obtain

$$
mrpk_{it} = a_{it} + (\alpha - 1)k_{it} + \log(\alpha_K\bar{G}).
\tag{69}
$$

Plugging in the optimal investment policy k_{it} from 66 into this expression yields

$$\begin{aligned}
mrpk_{it} =& (a_{it} - \mathbb{E}_{it-1}[a_{it}]) + \log(r+\delta) + \frac{c\sigma_\eta^2}{1-\alpha_N} \\
=& \frac{1}{1-\alpha_N}\left\{ (\hat{a}_{it} - \mathbb{E}_{it-1}[\hat{a}_{it}]) - \chi\alpha_N(T_t - \mathbb{E}_{t-1}[T_t]) \right\} + \log(r+\delta) + \frac{c\sigma_\eta^2}{1-\alpha_N} \\
=& \frac{1}{1-\alpha_N}\left(\underbrace{\hat{\beta}_i\eta_t^T}_{\substack{\text{Unexpected}\\ \text{T Shock}\\ \text{on Productivity}}} + \underbrace{\hat{\xi}_{it}(T_t - T^*)}_{\substack{\text{Unexpected}\\ \text{Damage}\\ \text{Sensitivity}}} - \underbrace{\chi\alpha_N\eta_t^T}_{\substack{\text{Unexpected}\\ \text{T Shock}\\ \text{on Wage}}} + \hat{\varepsilon}_{it} \right\} + \log(r+\delta) \\
&+ \frac{(\mathcal{O}_t(T_t - T^*) - \mathbb{E}_{t-1}[\mathcal{O}_t]\mathbb{E}_{t-1}[T_t - T^*])}{1-\alpha_N}.
\end{aligned} \tag{70}$$

which made clear that MRPK is just the user cost $r+\delta$ in the absence of any forecast error.

To calculate the average mrpk across all firms in a given year $\overline{mrpk_{it}}$, we notice that variables without i subscript will remain the same. And thus, when calculating the difference between $mrpk_{it}$ and $\overline{mrpk_{it}}$, those terms will be canceled out. Knowing this, we achieve the following

$$mrpk_{it} - \overline{mrpk_{it}} = \frac{1}{1-\alpha_N}\left\{ (\hat{\beta}_i - \overline{\hat{\beta}_i})\eta_t^T + \hat{\xi}_{it}(T_t - T^*) + \hat{\varepsilon}_{it} \right\},$$

where $\overline{\hat{\xi}_{it}} = 0$.

■

E.4 Proof of Proposition 4

Proposition 4 Within a region-sector pair $n = (r,s)$, the $mrpk$ dispersion across firms is increasing in TFP Volatility, $\text{Var}(\hat{a}_{nit} - \mathbb{E}_{t-1}[\hat{a}_{nit}])$, and can be decomposed into:

$$\begin{aligned}
\sigma^2_{mrpk,(r,s),t} &= \left(\frac{1}{1-\alpha_N}\right)^2 \text{Var}(\hat{a}_{nit} - \mathbb{E}_{t-1}[\hat{a}_{nit}]) \\
&= \left(\frac{1}{1-\alpha_N}\right)^2 \left[\underbrace{(T_{r,t} - T^*)^2\sigma^2_{\xi,(r,s)}}_{\substack{\text{Damage Volatility}\\ \text{(Level Effect)}}} + \underbrace{{\eta^T_{r,t}}^2\sigma^2_{\beta,(r,s)}}_{\substack{\text{Climate Uncertainty}\\ \text{(Shock Effect)}}} + \sigma^2_{\varepsilon,(r,s)} \right]
\end{aligned} \tag{71}$$

Within $n = (r,s)$, $mrpk$ dispersion is increasing in:

(1) squared deviation from optimal temperature, $(T_{r,t+1} - T^*)^2$,

(2) squared (unexpected) temperature shocks ${\eta^T_{r,t}}^2$.

Proof. From the proof above for Proposition 3, we know that

$$mrpk_{it} = \frac{1}{1-\alpha_N}\left(\hat{a}_{it} - \mathbb{E}_{it-1}[\hat{a}_{it}]\right) + \text{constant terms}$$

We can then compute the variance and obtain the following equation:

$$\begin{aligned}\sigma^2_{mrpk,(r,s),t} &= \left(\frac{1}{1-\alpha_N}\right)^2 \mathrm{Var}(\hat{a}_{nit} - \mathbb{E}_{t-1}[\hat{a}_{nit}]) \\ &= \left(\frac{1}{1-\alpha_N}\right)^2 \Bigg[\underbrace{(T_{r,t}-T^*)^2\sigma^2_{\xi,(r,s)}}_{\substack{\text{Damage Uncertainty}\\ \text{Channel}}} + \underbrace{{\eta^T_{r,t}}^2\sigma^2_{\beta,(r,s)}}_{\substack{\text{Climate Uncertainty}\\ \text{Channel}}} + \sigma^2_{\varepsilon,(r,s)} \Bigg]. \end{aligned} \tag{72}$$

Note that we have obtained $\mathrm{Var}(\hat{a}_{it} - \mathbb{E}_{t-1}[\hat{a}_{it}]) = (T_t - T^*)^2\sigma^2_{\hat{\xi}} + {\eta^T_t}^2\sigma^2_{\hat{\beta}} + \sigma^2_{\hat{\varepsilon}}$ from Equation 55.
■

E.5 Derivation of TFP Loss from Misallocation

This appendix provides the derivation for Equation 30. We now aggregate firm-level production and productivity to the aggregate region-sector level. Labor market clearing implies

$$\begin{aligned} N_t = \int N_{it} di &= \int \left(\frac{\hat{A}_{it}\alpha_N K^{\alpha_k}_{it}}{\overline{W}exp(\chi(T_t - T^*)}\right)^{\frac{1}{1-\alpha_N}} di \\ &= \left(\frac{\alpha_N}{\overline{W}\exp(\chi(T_t - T^*)}\right)^{\frac{1}{1-\alpha_N}} \int \left(\hat{A}_{it}K^{\alpha_k}_{it}\right)^{\frac{1}{1-\alpha_N}} di. \end{aligned}$$

Then we solve for $MRPK_{it}$ through the revenue function.

$$\begin{aligned} P_{it}Y_{it} &= \hat{A}_{it}K^{\alpha_K}_{it}N^{\alpha_N}_{it} \\ &= \hat{A}_{it}K^{\alpha_K}_{it}\left(\frac{\overline{W}\exp\left(\chi(T_t - T^*)\right)}{\hat{A}_{it}\alpha_N K^{\alpha_k}_{it}}\right)^{\frac{\alpha_N}{\alpha_N - 1}}. \end{aligned}$$

Note that from the labor market clearing condition, we can get the following equation

$$\left(\frac{\overline{W}\exp(\chi(T_t - T^*))}{\alpha_N}\right)^{\frac{1}{\alpha_N - 1}} = \frac{N_t}{\int \left(\hat{A}_{it}K^{\alpha_K}_{it}\right)^{\frac{1}{1-\alpha_N}} di}.$$

We plug this back into the revenue function and get

$$\begin{aligned} P_{it}Y_{it} &= \hat{A}_{it}K^{\alpha_K}_{it}(\hat{A}_{it}K^{\alpha_K}_{it})^{\frac{\alpha_N}{1-\alpha_N}}\left(\frac{N_t}{\int \left(\hat{A}_{it}K^{\alpha_K}_{it}\right)^{\frac{1}{1-\alpha_N}} di}\right)^{\alpha_N} \\ &= \left(\hat{A}_{it}K^{\alpha_K}_{it}\right)^{\frac{1}{1-\alpha_N}} \cdot \left(\frac{N_t}{\int \left(\hat{A}_{it}K^{\alpha_K}_{it}\right)^{\frac{1}{1-\alpha_N}} di}\right)^{\alpha_N} \end{aligned} \tag{73}$$

From this, we can solve for $MRPK_{it}$. Note that $MRPK_{it} = \alpha_K \frac{P_{it}Y_{it}}{K_{it}} = \alpha_K \frac{\hat{A}_{it}K_{it}^{\alpha_K}N_{it}^{\alpha_N}}{K_{it}}$.[49] Plugging in the expression of revenue function, we get

$$MRPK_{it} = \alpha_K \hat{A}_{it}^{\frac{1}{1-\alpha_N}} K_{it}^{\theta-1} \cdot \left(\frac{N_t}{\int \left(\hat{A}_{it} K_{it}^{\alpha_K} \right)^{\frac{1}{1-\alpha_N}} di} \right)^{\alpha_N},$$

where $\theta = \frac{\alpha_K}{1-\alpha_N}$. Next we rearrange terms to find expressions for K_{it}

$$K_{it} = \left(\frac{\alpha_K \hat{A}_{it}^{\frac{1}{1-\alpha_N}}}{MRPK_{it}} \right)^{\frac{1}{1-\theta}} \cdot \left(\frac{N_t}{\int \left(\hat{A}_{it} K_{it}^{\alpha_K} \right)^{\frac{1}{1-\alpha_N}} di} \right)^{\frac{\alpha_N}{1-\theta}}$$

We now use the capital market clearing condition

$$\begin{aligned} K_t &= \int K_{it} di \\ &= \alpha_K^{\frac{1}{1-\theta}} \cdot \left(\frac{N_t}{\int \left(\hat{A}_{it} K_{it}^{\alpha_K} \right)^{\frac{1}{1-\alpha_N}} di} \right)^{\frac{\alpha_N}{1-\theta}} \int \left(\frac{\hat{A}_{it}^{\frac{1}{1-\alpha_N}}}{MRPK_{it}} \right)^{\frac{1}{1-\theta}} di \end{aligned}$$

Rearrange terms we can have

$$\left(\frac{N_t}{\int \left(\hat{A}_{it} K_{it}^{\alpha_K} \right)^{\frac{1}{1-\alpha_N}} di} \right)^{\frac{\alpha_N}{1-\theta}} = \frac{K_t}{\alpha_K^{\frac{1}{1-\theta}} \int \left(\frac{\hat{A}_{it}^{\frac{1}{1-\alpha_N}}}{MRPK_{it}} \right)^{\frac{1}{1-\theta}} di}$$

We can plug this equation to the expression for K_{it}

$$\begin{aligned} K_{it} &= \left(\frac{\alpha_K \hat{A}_{it}^{\frac{1}{1-\alpha_N}}}{MRPK_{it}} \right)^{\frac{1}{1-\theta}} \cdot \frac{K_t}{\alpha_K^{\frac{1}{1-\theta}} \int \left(\frac{\hat{A}_{it}^{\frac{1}{1-\alpha_N}}}{MRPK_{it}} \right)^{\frac{1}{1-\theta}} di} \\ &= \frac{\hat{A}_{it}^{\frac{1}{1-\alpha_N}\frac{1}{1-\theta}} MRPK_{it}^{\frac{-1}{1-\theta}}}{\int \hat{A}_{it}^{\frac{1}{1-\alpha_N}\frac{1}{1-\theta}} MRPK_{it}^{\frac{-1}{1-\theta}} di} K_t \end{aligned}$$

49. Note that it's also fine to use the derivative definition of MRPK. This term will cancel out later.

We now have solved for N_{it}, K_{it} all in terms of $MRPK_{it}$ and aggregate variables N_t and K_t. We plug N_{it}, K_{it} back into Equation 73 and get

$$P_{it}Y_{it} = \left(\hat{A}_{it}K_{it}^{\alpha_K}\right)^{\frac{1}{1-\alpha_N}} \cdot \left(\frac{N_t}{\int \left(\hat{A}_{it}K_{it}^{\alpha_K}\right)^{\frac{1}{1-\alpha_N}} di}\right)^{\alpha_N}$$

$$= \frac{\hat{A}_{it}^{\frac{1}{1-\alpha_N}\frac{1}{1-\theta}} MRPK_{it}^{\frac{-\theta}{1-\theta}}}{\left(\int \hat{A}_{it}^{\frac{1}{1-\alpha_N}\frac{1}{1-\theta}} MRPK_{it}^{\frac{-\theta}{1-\theta}} di\right)^{\alpha_N} \left(\int \hat{A}_{it}^{\frac{1}{1-\alpha_N}\frac{1}{1-\theta}} MRPK_{it}^{\frac{-1}{1-\theta}} di\right)^{\alpha_K}} K_t^{\alpha_K} N_t^{\alpha_N}$$

Using $P_{it}Y_{it} = B_{it}^{\frac{1}{\sigma}} Y_{it}^{\frac{\sigma-1}{\sigma}}$, we can write aggregate output as

$$\begin{aligned} Y_t &= \left(\int B_{it}^{\frac{1}{\sigma}} Y_{it}^{\frac{\sigma-1}{\sigma}} di\right)^{\frac{\sigma}{\sigma-1}} = \left(\int P_{it}Y_{it} di\right)^{\frac{\sigma}{\sigma-1}} \\ &= \left[\frac{\int \hat{A}_{it}^{\frac{1}{1-\alpha_N}\frac{1}{1-\theta}} MRPK_{it}^{\frac{-\theta}{1-\theta}} di}{\left(\int \hat{A}_{it}^{\frac{1}{1-\alpha_N}\frac{1}{1-\theta}} MRPK_{it}^{\frac{-\theta}{1-\theta}} di\right)^{\alpha_N} \left(\int \hat{A}_{it}^{\frac{1}{1-\alpha_N}\frac{1}{1-\theta}} MRPK_{it}^{\frac{-1}{1-\theta}} di\right)^{\alpha_K}}\right]^{\frac{\sigma}{\sigma-1}} K_t^{\alpha_K \frac{\sigma}{\sigma-1}} N_t^{\alpha_N \frac{\sigma}{\sigma-1}} \\ &= \tilde{A}_t^{\frac{\sigma}{\sigma-1}} K_t^{\tilde{\alpha}_K} N_t^{\tilde{\alpha}_N}, \end{aligned} \tag{74}$$

where we define $\tilde{A}_t := \frac{\left(\int \hat{A}_{it}^{\frac{1}{1-\alpha_N}\frac{1}{1-\theta}} MRPK_{it}^{\frac{-\theta}{1-\theta}} di\right)^{1-\alpha_N}}{\left(\int \hat{A}_{it}^{\frac{1}{1-\alpha_N}\frac{1}{1-\theta}} MRPK_{it}^{\frac{-1}{1-\theta}} di\right)^{\alpha_K}}$. We take logs to $\tilde{A}_t$ and get

$$\tilde{a}_t = (1-\alpha_N)\left[\log\left(\int \mathring{A}_{it}^{\frac{1}{1-\theta}} MRPK_{it}^{-\frac{\theta}{1-\theta}}\right) - \theta \log\left(\int \mathring{A}_{it}^{\frac{1}{1-\theta}} MRPK_{it}^{-\frac{1}{1-\theta}}\right)\right],$$

where $\mathring{A}_{it} = \hat{A}_{it}^{\frac{1}{1-\alpha_N}}$. Now, assuming log-normality, the first term is equal to

$$\begin{aligned} \log\left(\int \mathring{A}_{it}^{\frac{1}{1-\theta}} MRPK_{it}^{-\frac{\theta}{1-\theta}}\right) &= \frac{1}{1-\theta}\overline{\mathring{a}_{it}} - \frac{\theta}{1-\theta}\overline{mrpk_{it}} \\ &+ \frac{1}{2}\left(\frac{1}{1-\theta}\right)^2 \sigma_{\mathring{a},t}^2 + \frac{1}{2}\left(\frac{\theta}{1-\theta}\right)^2 \sigma_{mrpk,t}^2 - \frac{\theta}{(1-\theta)^2}\sigma_{mrpk,\mathring{a},t} \end{aligned}$$

The second term is equal to

$$\begin{aligned} \theta \log\left(\int \mathring{A}_{it}^{\frac{1}{1-\theta}} MRPK_{it}^{-\frac{1}{1-\theta}}\right) &= \frac{\theta}{1-\theta}\overline{\mathring{a}_{it}} - \frac{\theta}{1-\theta}\overline{mrpk_{it}} \\ &+ \frac{1}{2}\theta\left(\frac{1}{1-\theta}\right)^2 \sigma_{\mathring{a},t}^2 + \frac{1}{2}\theta\left(\frac{1}{1-\theta}\right)^2 \sigma_{mrpk,t}^2 - \frac{\theta}{(1-\theta)^2}\sigma_{mrpk,\mathring{a},t} \end{aligned}$$

Combining them together, we have the following equation for aggregate productivity

$$\tilde{a}_t = (1-\alpha_N)\left[\overline{\mathring{a}_t} + \frac{1}{2}\frac{1}{1-\theta}\sigma_{\mathring{a},t}^2 - \frac{1}{2}\frac{\theta}{1-\theta}\sigma_{mrpk,t}^2\right]$$

Using Equation 74, we write the log aggregate output as

$$\begin{aligned}
y_t &= \frac{\sigma}{\sigma-1}\tilde{a}_t + \tilde{\alpha}_K k_t + \tilde{\alpha}_N n_t \\
&= \frac{\sigma}{\sigma-1}\left(1-\alpha_N\right)\left[\overline{\mathring{a}_t} + \frac{1}{2}\frac{1}{1-\theta}\sigma^2_{\mathring{a},t} - \frac{1}{2}\frac{\theta}{1-\theta}\sigma^2_{mrpk,t}\right] + \tilde{\alpha}_K k_t + \tilde{\alpha}_N n_t \\
&= a_t + \tilde{\alpha}_K k_t + \tilde{\alpha}_N n_t,
\end{aligned}$$

where the total factor productivity is defined as

$$\begin{aligned}
a_t =& \frac{\sigma}{\sigma-1}\left(1-\alpha_N\right)\left[\overline{\mathring{a}_{it}} + \frac{1}{2}\frac{1}{1-\alpha}\sigma^2_{\mathring{a},t} - \frac{1}{2}\frac{\alpha}{1-\alpha}\sigma^2_{mrpk,t}\right] \\
=& \frac{\sigma}{\sigma-1}\overline{\hat{a}_{it}} + \frac{1}{2}\frac{\sigma}{\sigma-1}\frac{1}{\left(1-\alpha\right)\left(1-\alpha_N\right)}\sigma^2_{\hat{a},t} \\
& - \frac{1}{2}\frac{\sigma}{\sigma-1}\frac{\alpha_K}{1-\alpha}\sigma^2_{mrpk,t}
\end{aligned}$$

Finally, we plug in the definition for $\overline{\hat{a}_{it}}$ and $\sigma^2_{\hat{a},t}$, and we can write the TFP as

$$\begin{aligned}
a_{nt} =& \frac{\sigma}{\sigma-1}\left[\overline{\hat{\beta}_i}(T_t-T^*) + c(T_t-T^*)^2\right] \\
& + \frac{\sigma}{2}\frac{\sigma}{\sigma-1}\left[\left(\sigma^2_{\hat{\beta}} + \sigma^2_{\hat{\xi}}\right)(T_t-T^*)^2 + \frac{\sigma^2_{\hat{\varepsilon}}}{1-\rho_z^2}\right] \\
& - \frac{\tilde{\alpha}_K + \tilde{\alpha}_K^2(\sigma-1)}{2}\left(\frac{1}{1-\alpha_N}\right)^2\left[(T_t-T^*)^2\sigma^2_{\hat{\xi}} + \eta_t^{T2}\sigma^2_{\hat{\beta}} + \sigma^2_{\hat{\varepsilon}}\right]
\end{aligned} \tag{75}$$

Under the parametrization that $c = -\frac{\sigma}{2}\left(\sigma^2_{\hat{\beta}} + \sigma^2_{\hat{\xi}}\right)$, we will have

$$\begin{aligned}
a_t =& a_t^* - \text{Misallocation Loss}_t \\
=& \frac{\sigma}{\sigma-1}\left[\overline{\hat{\beta}_i}(T_t-T^*)\right] + \frac{\sigma}{2}\frac{\sigma}{\sigma-1}\left[\frac{\sigma^2_{\hat{\varepsilon}}}{1-\rho_z^2}\right] \\
& - \frac{\tilde{\alpha}_K + \tilde{\alpha}_K^2(\sigma-1)}{2}\left(\frac{1}{1-\alpha_N}\right)^2\left[(T_t-T^*)^2\sigma^2_{\hat{\xi}} + \eta_t^{T2}\sigma^2_{\hat{\beta}} + \sigma^2_{\hat{\varepsilon}}\right]
\end{aligned} \tag{76}$$

E.6 General Solution of the Firm's Investment Problem

This Appendix outlines the general solution of the firm's investment problem without using the first-order approximation method in Section 5. We will discuss why our first-order approximation is valid for both the theoretical analysis and the empirical identification of key model parameters.

We rearrange the Euler equation in equation 24 to get the expression for optimal capital

$$\begin{aligned}
K_{it}^{1-\alpha} =& \frac{\alpha G}{r+\delta}\mathbb{E}_{t-1}\left[\exp\left(a_{it}\right)\right] \\
=& \frac{\alpha G}{r+\delta}\frac{1}{\sqrt{d}} e^{\left(\frac{\frac{(\hat{\beta}_i-\chi\alpha_N)}{(1-\alpha_N)}\mathbb{E}_{t-1}[(T_t-T^*)]+\frac{1}{2}\frac{(\hat{\beta}_i-\chi\alpha_N)^2\sigma_\eta^2}{(1-\alpha_N)^2}+\frac{c}{(1-\alpha_N)}(\mathbb{E}_{t-1}[(T_t-T^*)])^2+\frac{1}{2}\frac{\sigma_{\hat{\xi}}^2}{(1-\alpha_N)^2}(\mathbb{E}_{t-1}[(T_t-T^*)])^2}{d}\right)} \\
&\cdot e^{\left(\frac{\rho_z \hat{z}_{it-1}}{1-\alpha_N}+\frac{\sigma_{\hat{\varepsilon}}^2}{2(1-\alpha_N)^2}\right)}
\end{aligned} \tag{77}$$

where $d = 1-2\frac{c\sigma_\eta^2}{1-\alpha_N} - \frac{\sigma_\eta^2\sigma_{\hat{\xi}}^2}{(1-\alpha_N)^2}$. Notice that the risk-adjusted terms are small (as shown by our estimation), so empirically we have that $d \approx 1$.

Taking logs on both sides yields the investment decision:

$$\begin{aligned}
k_{it} =& \frac{1}{(1-\alpha)d}\Bigg(\frac{(\hat{\beta}_i-\chi\alpha_N)}{(1-\alpha_N)}\mathbb{E}_{t-1}[(T_t-T^*)] + \frac{c}{(1-\alpha_N)}(\mathbb{E}_{t-1}[(T_t-T^*)])^2 + \frac{1}{2}\frac{\sigma_{\hat{\xi}}^2}{(1-\alpha_N)^2}(\mathbb{E}_{t-1}[(T_t-T^*)])^2 \\
&+ \frac{1}{2}\frac{(\hat{\beta}_i-\chi\alpha_N)^2\sigma_\eta^2}{(1-\alpha_N)^2}\Bigg) + \frac{1}{1-\alpha}\big(\rho_z z_{it-1} + \frac{1}{2}\sigma_\varepsilon^2\big) + \frac{1}{1-\alpha}\log\Big(\frac{\alpha G}{(r+\delta)\sqrt{d}}\Big) \\
=& \frac{1}{(1-\alpha)d}\Bigg(\mathbb{E}_{t-1}[a_{it}-z_{it}] - \frac{c\sigma_\eta^2}{1-\alpha_N} + \frac{1}{2}\frac{\sigma_{\hat{\xi}}^2}{(1-\alpha_N)^2}(\mathbb{E}_{t-1}[(T_t-T^*)])^2 + \frac{1}{2}\frac{(\hat{\beta}_i-\chi\alpha_N)^2\sigma_\eta^2}{(1-\alpha_N)^2}\Bigg) \\
&+ \frac{1}{1-\alpha}\big(\rho_z z_{it-1} + \frac{1}{2}\sigma_\varepsilon^2\big) + \frac{1}{1-\alpha}\log\Big(\frac{\alpha G}{(r+\delta)\sqrt{d}}\Big).
\end{aligned} \tag{78}$$

The $mrpk$ of a firm can be then expressed as:

$$\begin{aligned}
mrpk_{it} =& \beta_i\Big(\frac{d-1}{d}(T_t-T^*) + \frac{1}{d}(T_t-\mathbb{E}[T_t])\Big) + \frac{1}{2}\frac{\beta_i^2\sigma_\eta^2}{d} + \xi_{it}(T_t-T^*) + \varepsilon_{it} \\
&+ \frac{(\mathcal{O}_t(T_t-T^*) - \mathbb{E}_{t-1}[\mathcal{O}_t]\mathbb{E}_{t-1}[T_t-T^*])}{1-\alpha_N} \\
&+ \left(\frac{1}{2}\frac{\sigma_\xi^2}{d}(\mathbb{E}_{t-1}[(T_t-T^*)])^2\right) \\
&- \frac{1}{2}\sigma_\varepsilon^2 + \log\Big(\frac{\alpha G}{(r+\delta)\sqrt{d}}\Big).
\end{aligned} \tag{79}$$

We now take variance of both sides of the $mrpk$ expression and use the fact that for a standard normal variable $x \sim \mathcal{N}(\mu, \sigma^2)$, $\text{Var}(Ax+Bx^2) = (A+2B\mu)^2\sigma^2 + 2\mu^2\sigma^4$. A few lines of algebra yields:

$$
\begin{aligned}
\sigma^2_{mrpk,t} =& \Big(\frac{d-1}{d}(T_t - T^*) + \frac{1}{d}(T_t - \mathbb{E}[T_t]) + \frac{\sigma^2_\eta \bar{\beta}}{d}\Big)^2 \sigma^2_\beta + 2\bar{\beta}^2\sigma^4_\beta + (T_t - T^*)^2\sigma^2_\xi + \sigma^2_\varepsilon \\
=& \frac{(d-1)^2}{d^2}\sigma^2_\beta\,(T_t - T^*)^2 + \frac{1}{d^2}\sigma^2_\beta\,(T_t - \mathbb{E}\,[T_t])^2 + \sigma^2_\xi (T_t - T^*)^2 + 2\frac{d-1}{d^2}\sigma^2_\beta\,(T_t - T^*)\,(T_t - \mathbb{E}\,[T_t]) \\
&+ 2\frac{(d-1)\sigma^2_\eta\sigma^2_\beta\bar{\beta}}{d^2}\,(T_t - T^*) + 2\frac{\sigma^2_\eta\sigma^2_\beta\bar{\beta}}{d^2}\,(T_t - \mathbb{E}\,[T_t]) + \frac{\left(\sigma^2_\eta\bar{\beta}\right)^2\sigma^2_\beta}{d^2} + 2\bar{\beta}^2\sigma^4_\beta + \sigma^2_\varepsilon
\end{aligned}
$$

Lastly, notice that since $d \approx 1$, as our empirical results suggest, the above expression can be approximated as:

$$
\begin{aligned}
\sigma^2_{mrpk,t} \approx& \frac{1}{(1-\alpha_N)^2}\Bigg(\sigma^2_{\hat{\beta}}\eta^{T^2}_t + \sigma^2_{\hat{\xi}}(T_t - T^*)^2 + \sigma^2_{\hat{\varepsilon}} \\
&+ 2\frac{\sigma^2_{\eta^T}\sigma^2_{\hat{\beta}}(\bar{\hat{\beta}} - \chi\alpha_N)}{(1-\alpha_N)}\eta^T_t + \frac{\bar{\hat{\beta}}^2\sigma^2_{\hat{\beta}}\sigma^4_{\eta^T}}{(1-\alpha_N)^2} + 2\frac{(\bar{\hat{\beta}} - \chi\alpha_N)^2\sigma^4_{\hat{\beta}}}{(1-\alpha_N)^4}\Bigg)
\end{aligned}
$$

where we have used that $\sigma^2_\beta = \frac{\sigma^2_{\hat{\beta}}}{(1-\alpha_N)^2}$, $\sigma^2_\xi = \frac{\sigma^2_{\hat{\xi}}}{(1-\alpha_N)^2}$. Notice that apart from the risk-adjusted terms in the second line, the first line of this equation yields exactly Equation 29 in the main text.

We now discuss in detail why the risk-adjusted terms in the second line do not affect our analysis. First, regarding the identification of $\sigma^2_{\hat{\beta}}$ and $\sigma^2_{\hat{\xi}}$ in the regression specification of Equation 35, the linear term $\frac{\sigma^2_{\eta^T}\sigma^2_{\hat{\beta}}(\bar{\hat{\beta}}-\chi\alpha_N)}{(1-\alpha_N)}\eta^T_t$ does not affect the identification of $\sigma^2_{\hat{\beta}}$, given that $\eta^T_t \sim N(0, \sigma^2_{\eta^T})$. Even if we use the monthly aggregated index, $\text{MSFE}_{\text{annual},r,t} = \sum_{m=1}^{12} \eta^{T\ 2}_{m,t}$, as an empirical counterpart for $\eta^{T^2}_t$, the forecast error of any month remains uncorrelated with $\text{MSFE}_{\text{annual},r,t}$ as long as $\eta^T_{m,t} \sim N(0, \Sigma_{\eta^T_m\eta^T_m})$.

Second, regarding the analysis of the computed average misallocation, the linear term $\frac{\sigma^2_{\eta^T}\sigma^2_{\hat{\beta}}(\bar{\hat{\beta}}-\chi\alpha_N)}{(1-\alpha_N)}\eta^T_t$ has a mean of zero and does not affect the average misallocation around year τ, $\mathbb{E}_t[\sigma^2_{mrpk,t+\tau} \mid \bar{T}', \sigma'^2_{\eta^T}]$, given the temperature distribution or forecastability $(\bar{T}', \sigma'^2_{\eta^T})$. The constant term $\frac{\sigma^4_{\eta^T}\bar{\hat{\beta}}^2\sigma^2_{\hat{\beta}}}{(1-\alpha_N)^2}$ is small as it is of the fourth order in σ_{η^T}. If we are interested in analyzing a positive change in $\sigma^2_{\eta^T}$, ignoring this term would only lead to an underestimate of the welfare loss associated with MRPK dispersion; similarly, for a negative change in $\sigma^2_{\eta^T}$ (i.e., a decrease in forecast error), ignoring this term would lead to an underestimate of the benefits. Thus, we will always capture a conservative lower bound. Therefore, we conclude that the first-order approximation approach in the main text is valid for the purpose of analysis.